APPENDIX 2.4.12C TABLE OF CONTENTS

APPENDIX 2.4.12C LIST OF TABLES

APPENDIX 2.4.12C LIST OF FIGURES

APPENDIX 2.4.12C LIST OF FIGURES (CONTINUED)

Appendix 2.4.12C
Groundwater Flow Model for the Clinch River Nuclear Site

2.4.12C Groundwater Flow Model for the Clinch River Nuclear Site

2.4.12C.1 Objective and Scope

The Clinch River Nuclear (CRN) Site groundwater flow model for the Tennessee Valley Authority (TVA) CRN Site, Roane County, Tennessee is prepared to evaluate groundwater levels during the operation of small modular reactors (SMRs) constructed at the site. The primary objective of the groundwater model is to assess the post-construction maximum groundwater levels for future SMR power blocks.

The scope of work for the groundwater flow model included the following:

- Developing a conceptual hydrogeologic model
- Developing a numerical groundwater flow model
- Developing a pre-construction site model to simulate maximum water level at and around the future SMR power blocks and compare against the observed maximum water level
- Performing a sensitivity analysis to document the effects of parameter uncertainty
- Performing predictive post-construction simulations to determine maximum groundwater levels at and around the future SMR power blocks
- Performing a sensitivity analysis to document the effects of uncertainty in predictive simulations
- Documenting modeling results

2.4.12C.2 Regional Geology and Hydrogeology

2.4.12C.2.1 Regional Geologic Setting

The CRN Site is located as shown in Figure 2.4.12C-1. The site is located near the western boundary of the Valley and Ridge Physiographic Province, which is characterized by folded and faulted geologic units of Paleozoic age, that produce a series of valleys and ridges. This province extends south to Georgia and Alabama and north to Pennsylvania and New Jersey.

In eastern Tennessee, the processes of folding, faulting, and erosion have resulted in a series of northeast trending ridges and valleys. As described by Lloyd and Lyke (Reference 2.4.12C-14), “compressive forces from the southeast have caused these rocks to yield, first by folding and subsequently by repeated breaking along a series of thrust faults.” This successive faulting has resulted in several outcropping units in the area that occur in parallel belts aligned roughly with the topography. The folding/faulting process has produced a repeated sequence of outcropping units. Major units present in the area include, from younger to older, the Chickamauga Group, the Knox Group, the Conasauga Group, and the Rome Formation. All are composed primarily of Ordovician and Cambrian carbonate rocks. The dip of these formations is to the southeast. In nearby Melton Valley and within the Oak Ridge Reservation (ORR), east of the CRN Site, Tucci (Reference 2.4.12C-35) reports that rock units generally strike between 50 and 60 degrees northeast, while dips vary with proximity to faults. Dips in Melton Valley are gentle (10 to 20 degrees) and become steeper close to faults (45 to 90 degrees) (Reference 2.4.12C-35).

2.4.12C.2.2 Regional Hydrogeologic Setting

The primary aquifers in the Valley and Ridge Province in eastern Tennessee are the carbonate rocks that underlie the majority of the province and include the Knox Group in eastern Tennessee. Of particular hydrogeologic interest in the vicinity of the CRN Site are the Chickamauga Group and the Knox Group (Reference 2.4.12C-24).

Secondary porosity, in the form of bedding planes, fractures, and solution openings, comprise the primary flow pathways in the Valley and Ridge Province, as most of the rock material in the province has a low primary porosity and a low permeability matrix. The overlying regolith layers are composed of clayey soils and saprolite. Typical conceptual hydrogeologic cross-sections consist of a stormflow zone near ground surface, a less permeable unsaturated zone, and an underlying saturated zone consisting of fractured bedrock with fracture density decreasing with depth (Reference 2.4.12C-17). Solomon et al. (Reference 2.4.12C-33) divided the subsurface flow system in both the Knox aquifer and in the ORR aquitards into: 1) the stormflow zone; 2) the vadose (unsaturated) zone; and 3) the saturated zone, which is subdivided into the water table interval, the intermediate interval, the deep interval, and the aquiclude (Figure 2.4.12C-2). These hydrologic subsystems are defined on the basis of water flux, which decreases with depth; the largest flux is associated with the stormflow zone and the lowest with the aquiclude (Reference 2.4.12C-10).

The stormflow zone, which is typically 3 to 6 feet (ft) thick on the ORR, conducts approximately 90 percent of the subsurface flow. This is a highly transmissive zone; infiltration tests indicate that this zone is as much as 1000 times more permeable than the underlying vadose zone (Reference 2.4.12C-6). During rain events, the stormflow zone partially or completely saturates and transmits water laterally to the surface water system. However, during significant rain events, the stormflow zone can be completely saturated, in which case overland flow occurs (Reference 2.4.12C-10). At the CRN Site the stormflow zone may be absent or significantly disturbed as a result of previous site work (excavation and fill) associated with the Clinch River Breeder Reactor Project (CRBRP). This land disturbance affected the stormflow zone at the CRN Site, and it is likely to have been replaced by the fill materials encountered in the more recently drilled CRN geologic borings.

The vadose zone encompasses the regolith, is comprised mostly of clays and silts derived from weathering of bedrock materials, and can have significant storage capacity. The thickness of the vadose zone varies between approximately 3 and 50 ft at the ORR. Recharge through the vadose zone is episodic and occurs along discrete permeable features (macropores) that may become saturated during rain events, even though surrounding micropores remain unsaturated and contain trapped air (Reference 2.4.12C-10). In between rain events, recharge rates decrease significantly. The flow paths in the vadose zone are toward the underlying saturated zone.

The saturated zone includes connected open fractures below the base of the vadose zone. Most of the water in this zone is transmitted through a narrow interval of approximately 3 to 15 ft in thickness. The water table generally occurs near the interface between the regolith and underlying bedrock. In the intermediate interval of the saturated zone, groundwater movement occurs primarily in fractures that are poorly connected in three dimensions (Reference 2.4.12C-10). The dominant fracture orientation through which groundwater flow occurs is primarily along bedding plane strike and strike-parallel fractures. These fractures have better interconnection and are more permeable than the dip-parallel fractures. Flow paths follow the valleys towards the crosscutting tributary streams (References 2.4.12C-17; 2.4.12C-10; 2.4.12C-33).

Groundwater flow is generally from recharge areas at high elevation (ridges) to local streams and rivers at lower elevations. The repeating geological sequences described above along with the regional stream network create a series of adjacent, isolated, shallow groundwater flow systems (Reference 2.4.12C-14). Many of the carbonate-rock aquifers are directly connected to surface water such as rivers and lakes. Other types of rocks can yield large quantities of water to wells where the rocks are fractured, contain solution openings, or are hydraulically connected to a source of recharge (Reference 2.4.12C-14).

Long-term average annual precipitation is approximately 50 in. in the vicinity of the CRN Site, with an estimated long-term average runoff of 25 to 30 in. (Reference 2.4.12C-14). Precipitation that percolates downward becomes groundwater recharge to the shallow aquifers; a small portion enters the deep aquifers.

Groundwater on the ORR occurs in the unsaturated zone as transient, shallow subsurface stormflow as well as within the deeper saturated zone as summarized by Parr and Hughes (Reference 2.4.12C-23). An unsaturated zone of variable thickness separates the stormflow zone and water table. Adjacent to surface water features or in valley floors, the water table is found at shallow depths where the stormflow and unsaturated zones are indistinguishable. Along the ridge tops or near high topographic areas, the unsaturated zone is thick, and the water table often lies at considerable depths (greater than approximately 50 ft).

Recharge to the groundwater system is reported to be strongly seasonal at the ORR. The amount of water that recharges the saturated zone is highly variable depending on the shallow soil characteristics, permeability and degree of regolith fracturing beneath the soil, and the presence of dolines (sinkholes) and paved or covered areas. Higher recharge is expected in areas of karst hydrogeology such as the Knox aquifer. In the ORR aquitards, groundwater is considered to be transmitted through fractures (Reference 2.4.12C-23). Where the fractures in the shallow bedrock are dominant, they behave as porous media flow.

The hydrogeologic conditions at the CRN Site are similar to the ORR with the exception of land disturbance areas resulting from earlier site work performed for the CRBRP where fill material is present.

2.4.12C.3 Site-Specific Information

CRN site-specific information was obtained primarily from the site subsurface investigation program conducted between July 2013 and March 2014, documented in Reference 2.4.12C-1. Previous site CRBRP subsurface investigation data (Reference 2.4.12C-24) were also reviewed; the geologic and hydrogeologic data were similar to that of the CRN Site subsurface investigation. The site subsurface investigation indicates that the lithologic units at the CRN Site are generally composed of man-made fill materials, residual soil, weathered bedrock, fractured bedrock, and competent bedrock. The thickness of the fill materials varies spatially at the site from less than 1 ft to approximately 50 ft (Reference 2.4.12C-1). Thickness of residual soil varies from 0 to approximately 50 ft. Weathered bedrock units also vary spatially from 0 to approximately 21 ft in thickness.

The weathered bedrock unit acts as a water table aquifer where the majority of groundwater flow is suspected to occur along the strike of the bedding plane. The fractured rock units below the weathered bedrock unit can also transmit a significant amount of water; the thickness of the heavily fractured bedrock unit at the CRN Site varies from a few feet to approximately 50 ft. Figure 2.4.12C-3 shows the frequency distribution of open fractures with elevation as identified from boring acoustic televiewer logs (Reference 2.4.12C-1). The dominant groundwater flow is through the fractures at the site and is approximately bounded within the upper 100 ft of subsurface material below ground surface (bgs).

Open fractures identified from geologic core borings, caliper logs, and acoustic televiewer logs guided the placement of site observation well screens (Reference 2.4.12C-1). The frequency of open fractures decreases with depth. Wells with a screened zone placed at shallower depth (i.e., the upper or U series wells) intersected a higher density of open fractures than wells screened at deeper depths. Table 2.4.12C-1 presents the construction information for the site observation wells installed along with the geologic formation in which the wells are screened. The location of the site observation wells is shown in Figure 2.4.12C-4. Well installation depths were less than

310 ft bgs. The supplemental pumping and observation wells used for the aquifer pumping test (Figure 2.4.12C-4) were not monitored on a long-term basis.

Groundwater recharge to the regolith and underlying bedrock is mainly through infiltration of precipitation at the land surface at the CRN Site. Infiltrating water collects in the regolith (and where present, fill material) and recharges the underlying bedrock fracture system. Joints, weathered zones, dissolution openings, zones of brittle fractures in bedrock, and combinations of these features also can store a substantial quantity of water.

2.4.12C.3.1 Groundwater Level Measurements

Groundwater level measurements were taken from 34 groundwater observation wells of which 6 locations consisted of 3-well clusters, and 8 locations consisted of 2-well clusters. The locations of the wells are shown in Figure 2.4.12C-4. The footprints and dimensions of the reactor area location shown in Figure 2.4.12C-4 are a generic representation of an SMR that could be constructed within the power block area at the CRN Site.

Table 2.4.12C-1 presents the construction information for the observation wells. Wells are identified with a suffix of either U, L, or D. U represents the upper series of wells, which are the shallower wells, predominantly screened within the weathered bedrock and generally within 80 ft of ground surface. L represents the lower series of wells, generally screened to a depth of approximately 150 ft bgs but do vary from location to location. Similarly, D represents the deeper wells that are generally screened at depth intervals varying from 200 to 250 ft bgs with a few of the wells as deep as 310 ft bgs. The wells were specifically screened within zones that contain the maximum fracture density as identified from geologic core logs and acoustic televiewer logs.

Table 2.4.12C-2 includes manual water level data for all 34 wells (generally collected every month). Pressure transducers were installed in 13 wells. Water level data were recorded every 30 minutes by the pressure transducers (real-time continuous monitoring of water levels) (Reference 2.4.12C-1).

2.4.12C.3.2 Groundwater Level and Hydraulic Gradient Analysis

A summary of the groundwater level and hydraulic gradient analysis, based on water level data between September 24, 2013 to March 16, 2014, is provided below:

- Groundwater flow occurs primarily in the interface zone between regolith and bedrock. Flow primarily occurs along the strike of the bedding planes. Figure 2.4.12C-5 shows the equipotential contours and groundwater flow directions (assumes no vertical gradient) for the maximum water level observed in each well cluster (regardless of depth) for January 13, 2014.

- Based on the potentiometric surface maps, groundwater flow is toward the Clinch River arm of the Watts Bar Reservoir, primarily in the northeasterly and southwesterly direction. This indicates groundwater flow from beneath the upland area (center of the CRN peninsula) toward the Clinch River arm of the Watts Bar Reservoir.

- The maximum water level elevation measured during the monitoring period (September 24, 2013 to March 16, 2014) in the general area of the future SMR power block area was 800.3 ft North American Vertical Datum of 1988 (NAVD88) at observation well OW-202U.

- Horizontal hydraulic gradients range from 0.02 to 0.12 ft/ft.

- Vertical hydraulic gradients at the site indicate potential for downward movement at most well pair locations. The average downward vertical hydraulic gradient ranged from 0.01 to 0.24 ft/ft for all the wells; however, the OW-429U/L well pair showed a vertical hydraulic gradient greater than 1. Well pairs OW-409 U/L, OW-415 U/L, OW-417 U/L, and OW-423 U/L/D exhibit an upward vertical gradient, ranging between -0.05 and -0.71ft/ft.

- All observation wells respond quickly to precipitation events. The U-series wells show faster and higher magnitude response to precipitation than the L- and D-series wells.

- The surface water stage in the Clinch River arm of the Watts Bar Reservoir is less than the groundwater levels observed in the observation wells. Based on the daily stage variations in the tail water of the Melton Hill Dam (sometimes greater than a foot) and precipitation events, it is not conclusive whether the Clinch River arm of the Watts Bar Reservoir stage influences the groundwater elevations at the CRN Site.

2.4.12C.3.3 Packer Test Analysis

Packer tests were conducted and analyzed in selected geologic core holes (Figure 2.4.12C-6). The following summarizes the results of the analysis performed:

- Transmissivity estimates range from 0.3 to 40 ft^2/day with a geometric mean of 3.4 ft^2/day;

- Hydraulic conductivity estimates, based on a test interval of 7.5 ft, range from 0.04 to 5 ft/day with a geometric mean of 0.5 ft/day.

- The average and geometric mean transmissivity values for the Knox Group were 4.6 ft^2/day and 3.2 ft^2/day, respectively.

- The average and geometric mean transmissivity values for the Chickamauga Group were 7.8 ft^2/day and 3.5 ft^2/day, respectively.

- In general transmissivity values decreased with elevation (Figure 2.4.12C-7). In some geologic units (e.g., Fleanor), the trend is apparent; however, in some other geologic units it was not apparent (Figure 2.4.12C-7).

2.4.12C.3.4 Slug Test Analysis

Slug tests were conducted in the site observation wells (Figure 2.4.12C-4). Graphical representation of the slug test analysis is shown in Figures 2.4.12C-8 through 2.4.12C-10. The following is a summary of the slug test analysis results:

- Hydraulic conductivity values generally decrease with depth (Figure 2.4.12C-9);

- The range of hydraulic conductivity values varies by 4 orders-of-magnitude, with the maximum value in excess of 10 ft/day and a minimum value of 0.001 ft/day (Table 2.4.12C-3);

- Figure 2.4.12C-10 shows the variability of hydraulic conductivity values in different geologic units. Except for the Fleanor Shale Member of the Lincolnshire Formation, all geologic units have a large variability of hydraulic conductivity values, ranging from 2 to 4 orders-of-magnitude. The greatest variability is observed in the Newala Formation of the Knox Group.

2.4.12C.3.5 Aquifer Pumping Test Analysis

An aquifer pumping test was conducted in the vicinity of OW-423 U/L/D well series and included 7 supplemental wells (Figure 2.4.12C-4). Transmissivity, storage coefficient, and hydraulic conductivity values were estimated from the pumping and recovery plots of the pumping test observation wells using the Hantush-Jacob solution for a leaky aquifer with partial penetration and no aquitard storage. A summary of the results of this analysis is as follows:

Transmissivity (ft^2/d): 7 – 410

Storage Coefficient (dimensionless): 2.7×10^{-4} – 4.8×10^{-2}

(A lower value of storage coefficient of 8.9×10^{-10} was reported for the pumping period of one of the observation wells (Table 2.4.12C-4); however, for the same well in the recovery period, for which the derivative data contained less noise, a value of 8.1×10^{-3} was reported. Therefore, the value derived from the pumping period is considered to be unreliable.)

Hydraulic Conductivity (ft/d): 0.06 – 2.6

Table 2.4.12C-4, presents the hydrogeologic parameters estimated from a subset of the observation wells during the pumping test. The saturated thickness of the aquifer and the anisotropy ratio (ratio of vertical hydraulic conductivity to horizontal hydraulic conductivity) values used to determine the hydraulic conductivities and storage coefficients from the pumping test were 155 ft and 0.1, respectively. The results of the pumping test indicate that horizontally anisotropic conditions are present, with the highest transmissivity and hydraulic conductivity found in observation wells oriented along the strike of the bedding planes, N52°E.

2.4.12C.3.6 Hydrogeologic Data—Literature Information

A large amount of hydrogeologic data exists for the ORR. Figure 2.4.12C-11 shows the hydraulic conductivity distribution with depth below ground for the Rome Formation, Knox Group, Conasauga Group, and the Chickamauga Group for the ORR area based on slug, packer, and aquifer pumping tests. The Knox Group and the Chickamauga Group are the representative hydrogeologic formations at the CRN Site. The Knox Group is a sequence of rocks that mainly corresponds to the Knox Dolomite with several beds of limestone. The Chickamauga Group consists of silty and clayey limestones and limy siltstones. The composition and texture of the rock vary with location. A high degree of fracturing and jointing is characteristic of this rock unit. Hydraulic conductivity values obtained from slug and packer tests in fractured and jointed carbonate aquifers, such as in the CRN Site and ORR, are likely to be scale dependent, with pumping tests providing more representative regional values (Reference 2.4.12C-28).

As part of the licensing activities for the CRBRP, a site subsurface investigation was performed and included 129 borings, 37 observation wells, 11 piezometers, and 117 bedrock packer tests. The investigation also included collection of groundwater level data from site wells and a survey of local groundwater users (Reference 2.4.12C-24). The CRBRP subsurface investigation (Reference 2.4.12C-24) identified four bedrock joint set orientations at the site:

- N52°E 37°SE
- N52°E 58°NW
- N25°W 80°SW
- N65°W 75°NE

The predominant joint set is oriented N52°E 37°SE, which corresponds with the bedding plane partings in bedrock. The N52°E 58°NW joint set has a joint spacing of between 1 and 6 ft (Reference 2.4.12C-24).

CRBRP packer testing, which utilized larger test intervals than that performed for the CRN Site subsurface investigation, derived hydraulic conductivity values similar to those determined at the ORR. Both sets of results indicate a decreasing trend in hydraulic conductivity at depths greater than approximately 100 ft bgs.

CRBRP on-site observation water level measurements indicated up to 20 ft fluctuation in water levels. Maximum water levels were observed in January and February, and minimum water levels were observed in October and November. Movement of groundwater is described as generally from topographically high areas to topographic lows; however, this pattern is modulated by the extent of weathering in the bedrock. Ultimately, the Clinch River acts as a sink for site groundwater flow. The investigation concluded that major ridges on the site may be regarded as approximate locations of groundwater divides (Reference 2.4.12C-24).

2.4.12C.3.7 Recharge Data – Literature Information

Groundwater response as a result of precipitation at the CRN Site is generally more rapid in the shallow wells than in the deeper wells. Much of the precipitation moves through the shallow zone (at the ORR it is referred to as the stormflow zone; however, in the case of the CRN Site, the stormflow zone is very likely to be disturbed due to previous CRBRP Site preparation activities). The shallow zone is considered to be only a few inches to a few feet above the vadose zone. As the shallow zone saturates with precipitation, a portion percolates downward through the unsaturated regolith (soils and shallow fractured bedrock interface) and exposed bedrock units (Reference 2.4.12C-16). The precipitation that enters the stormflow zone is above the water table, and generally does not recharge the underlying saturated groundwater system (Reference 2.4.12C-16). The stormflow zone at the CRN Site is equivalent to the fill materials and some portion of the saprolitic soil at the site (which is a result of CRBRP disturbance). The vadose zone is classified as most of the unsaturated soil above the fractured bedrock at the CRN Site.

Precipitation amounts reported for Oak Ridge, Tennessee by Oak Ridge National Laboratory (ORNL) (Reference 2.4.12C-22) are as follows:

- Average annual precipitation (1981-2010 period of record) = 50.91 in.
- 2013 annual precipitation = 67.37 in.
- Maximum annual precipitation (1948-2013 period of record) = 76.33 in.

Most of the literature on recharge is from the many studies conducted at the ORR, which has similar climate and geology as that at the CRN Site. A summary of this literature is as follows:

- Bailey and Lee (Reference 2.4.12C-3) applied a hydrograph-separation technique to estimate recharge to Poplar Creek, which is approximately 3 miles north of the CRN Site, resulting in recharge estimates of 15, 20, and 12 percent of annual precipitation, respectively, for a typical year (1984), wet year (1973), and dry year (1985). This results in recharge estimates of 6 to 15 in./yr.

- Bailey (Reference 2.4.12C-2) investigated the distribution of recharge in a cross-sectional, finite-difference model of the waste burial grounds at the ORR. Based on this model, most of the recharge occurs on the ridges of Pine Ridge (approximately two miles north of the future SMR power block area) and Chestnut Ridge (approximately one mile north of the future SMR power block area). For Pine Ridge and Chestnut Ridge, recharge was estimated to be 25

in./yr and 20 in./yr, respectively. The overall average recharge for the model domain was about 14 in./yr. The thicker regolith on the ridges retains water that slowly recharges the underlying formations as compared to the valleys where the regolith is much thinner (Reference 2.4.12C-3).

- Tucci (Reference 2.4.12C-34) calibrated a three-dimensional, finite-difference model for the Melton Valley at the ORR with an aerial distribution of recharge rate of 3.2 in./yr.
- Tucci (Reference 2.4.12C-35) estimated recharge from a two-dimensional, profile model for Melton Valley at the ORR to be between 2.1 and 4.7 in./yr.

2.4.12C.4 Conceptual Site Model and Assumptions

Two major hydrostratigraphic units are identified at the CRN Site: the Chickamauga Group and the Knox Group. The Chickamauga Group is in most part identified as an aquitard and the Knox Group is identified as an aquifer (Reference 2.4.12C-33). The Chickamauga Group of rocks outcrops along the southern part of the Clinch River peninsula at the CRN Site (most of the footprint of the power block area lies within the Chickamauga Group of rocks). The Knox Group lies below the Chickamauga Group and outcrops at the northern extremity of the power block area at the CRN Site. The Chickamauga Group and the Knox Group are separated by an unconformity and the various geologic bedding units within the two groups strike approximately at N52°E and dip at 33°SE. The Chickamauga Group at the CRN Site is comprised of interbedded siltstone and limestone and is comprised of the following geologic formations, from older to younger: Blackford, Eidson, Fleanor, Rockdell, Benbolt, Bowen, Witten, and Moccasin (Reference 2.4.12C-10). The Knox Group is primarily composed of dolomite where groundwater flow occurs through solution conduits. The Knox Group at the CRN Site consists of the Newala Formation.

The Clinch River arm of the Watts Bar Reservoir surrounding the CRN peninsula (east, west, and south) is the main discharge point for the active groundwater flow system and is considered to be the hydrologic boundary (Reference 2.4.12C-24). The higher portion of Chestnut Ridge (which is nearly one mile north of the power block area) is a major topographic divide between Bear Creek Valley to the northwest and the peninsula formed by the Clinch River arm of the Watts Bar Reservoir (Reference 2.4.12C-24). The summit of the Chestnut Ridge has an elevation greater than 1100 ft above sea level and is more than 300 ft above the elevation of the plant grade. Because of this difference in elevation and because the upper portion of the ridge is nearly one mile from the power block area, it is unlikely that changes in groundwater levels at or near the Chestnut Ridge could affect groundwater levels at the CRN Site.

Groundwater recharge is derived primarily from precipitation, although periodic recharge from the Clinch River arm of the Watts Bar Reservoir during high stages of the Reservoir may also be occurring, but this is not considered to represent a significant part of the recharge to the aquifer. Recharge is most effective in those areas where the overburden soils are thin and permeable. Recharge may also occur through sinkholes (if present) that penetrate relatively thick and impervious formations (Reference 2.4.12C-24).

Based on evaluation of the site geologic cores, geophysical logs, and the geotechnical and hydrogeologic investigations, the following can be concluded with regards to the site hydrogeologic conceptual model:

1. Man-made fill materials are ubiquitous and more prominent in the proposed power block area and also west of the proposed power block area. The fill materials identified from the CRN Site subsurface investigations (Reference 2.4.12C-1) are likely to be from the excavation work undertaken for the defunct CRBRP (Reference 2.4.12C-24). Site conditions reflect the

state of excavation and partial backfilling when the CRBRP was discontinued in the 1980s. Thickness of the fill materials range from non-existent to approximately 51 ft (Reference 2.4.12C-1).

2. The fill materials are underlain by unconsolidated residual soil materials of silt and clay, which vary in thickness from non-existent to approximately 50 ft (Reference 2.4.12C-1).

3. The residual soil materials are underlain by weathered and heavily fractured bedrock, which varies in thickness from non-existent to approximately 21 ft. The weathered bedrock unit acts as a transmissive unit with dominant groundwater flow along the strike of the bedding planes. The water table is typically in the interface of the weathered bedrock unit and in the residual soil (Reference 2.4.12C-1).

4. Below the weathered zone is the competent bedrock unit with the frequency of fractures and joints progressively decreasing with depth (Figure 2.4.12C-3). The bedrock units have a bedding plane strike of approximately N52°E and dip to the southeast at an average angle of approximately 33 degrees. The recent CRN Site subsurface investigation indicates a primary discontinuity set oriented at a strike of N60°E and dip of 59°NW and a secondary set oriented N60°E and dip of 38°SE. The strike and dip of the rocks underlying the site is approximately N51° to N53°E and 32° to 36°SE, respectively, as calculated using the top of the Fleanor Member and the top of the Rockdell Formation. This may vary slightly across the site as a result of localized deformation.

5. The fill, residual soil, and weathered bedrock units (regolith) along with the shallower depths of the competent bedrock units act as a porous medium (Figures 2.4.12C-12, Sheets 1–11). The shear zone depicted on Figures 2.4.12C-12, Sheets 6 to 10, represents a laterally continuous interval of calcite-filled and cemented fractures in the lower Eidson. As these fractures are completely healed, they do not represent a zone of secondary porosity that would be conducive to preferential groundwater flow. Webster and Bradley (Reference 2.4.12C-37) state that groundwater flow in the regolith is characteristic of both porous media as well as fracture controlled flow at the nearby ORNL Site.

6. The groundwater flow at the CRN Site can be characterized as fractured porous media within the shallower regions (less than 100 ft bgs) of the competent bedrock due to the dominance of fractures. This results in a porous media flow; however, flow in the deeper regions of the competent bedrock units are purely fracture flow as groundwater flow occurs only through some of the fractures and negligible flow through the rock matrix. As the groundwater flow through the fractured porous media is mainly through fractures, it is conceptually understood that most of the water contained within this domain is stored in the rock matrix. Although deeper regions in the bedrock might contain higher hydraulic conductivity zones at a particular location, on a regional scale these zones are only connected through the shallow zones. As a result, when the water table drops these fractures remain saturated but are no longer connected regionally, and flow through these fractures decreases significantly (References 2.4.12C-17 and 2.4.12C-18).

7. The hydraulic properties at the site are spatially variable as is the groundwater flow rate. The hydraulic properties are also anisotropic with groundwater flow dominating along the strike of the bedding planes (References 2.4.12C-17, 2.4.12C-18, 2.4.12C-19, and 2.4.12C-35). The groundwater flow velocity is highly transmissive through the fractures; however, the number of fractures in comparison to the total volume of the aquifer is small; therefore, the average volumetric flow rate through the aquifer is low. Weathering of the bedrock unit can increase the porosity, hydraulic conductivity, and matrix diffusion coefficient.

8. Groundwater heads from the majority of the onsite well clusters show significant vertical variation, and this implies poor vertical connection of fractures. Conversely, in some of the well clusters the vertical variations of the hydraulic heads are minimal, which is attributed to a localized strong vertical interconnection of fractures.

9. Moore (Reference 2.4.12C-20) stated the following based on conditions observed at the ORR area within fractured limestone and siltstone: 1) most of the groundwater flow occurs in a thin layer near the water table, 2) transmissivity changes with time, and 3) about 90 percent of the groundwater flow occurs in only 10 percent of the area, and the locations of the most permeable flow paths are unknown. As indicated in Reference 2.4.12C-35 only about 1 percent of the total groundwater flow occurs below 200 ft of ground surface at the nearby ORNL.

10. Several investigators have reported that the hydraulic conductivity is greatest in a direction parallel to strike in the ORR area (References 2.4.12C-7, 2.4.12C-27, 2.4.12C-32, 2.4.12C-34, and 2.4.12C-38).

11. Tucci (Reference 2.4.12C-35) states that the hydraulic conductivity is greatest within the upper 50 ft bgs and tends to decrease with increasing depth at the Melton Valley, ORNL. Slug test analysis at the CRN Site tends to show a decreasing trend in hydraulic conductivity with depth. Similarly, packer tests conducted in the geotechnical boreholes (Reference 2.4.12C-1) show a general decrease in hydraulic conductivity with depth.

12. The CRN Site is surrounded by the Clinch River arm of the Watts Bar Reservoir on three sides and by Chestnut Ridge to the north (trending southwest to northeast) approximately 1 mile from the proposed power block area. The surface elevation of Chestnut Ridge and at the power block area is approximately 1100 ft NAVD88 to approximately 800 ft NAVD88, respectively. The dominant rock type at Chestnut Ridge is the Knox Group, which has similar strike and dip trends as the Chickamauga Group at the power block area. Based on a difference of approximately 300 ft of surface elevation between Chestnut Ridge and the immediate vicinity of the power block area, it is anticipated that the groundwater head elevations at the power block area are lower than those at Chestnut Ridge. This difference is likely to cause groundwater flow perpendicular to the strike (along down dip direction). However, the flow in the down dip direction from Chestnut Ridge is likely to be deeper at the CRN Site (as the bedrock dip varies from approximately 30 to 35 degrees) with most of the flow occurring parallel to the strike (i.e., along the bedding planes as the path of the least resistance).

13. The surface water elevation of the Clinch River arm of the Watts Bar Reservoir is maintained by the tail water of the Melton Hill Dam located approximately 4.5 miles from the CRN Site. The reservoir stage varied from 742.74 to 735.42 ft NAVD88 (7.32 ft) during the monitoring period (September 1, 2013 to March 31, 2014). The average reservoir stage for the monitoring period was 738.88 ft NAVD88.

14. The changes in the reservoir stage levels were not conclusively discernible within the CRN Site observation wells water levels. It does not appear that groundwater levels at the CRN Site are influenced by changes in reservoir stage, at least over the range of stages observed.

15. Groundwater levels respond rapidly to precipitation events; in some wells the water level response was more than 5 ft. Maximum observed water levels in some of the CRN Site wells were only a few feet below ground surface after significant precipitation events. As the groundwater levels at the CRN Site are dictated by the amount and duration of precipitation, it can be assumed that the recharge rates associated with large precipitation events that cause significant increase in the water levels in the wells are much greater than the annual

recharge rates that appear in the literature for the ORR, where the objective of the groundwater modeling is to determine average groundwater elevations (References 2.4.12C-16, 2.4.12C-34, and 2.4.12C-35). Any attempt to replicate the maximum groundwater elevations at the CRN Site would include higher recharge rates than the average annual values used in most of the modeling studies in similar geologic settings, such as at the ORR.

16. Horizontal hydraulic gradients are more dominant along northeast and southwest direction (i.e., towards the Clinch River arm of the Watts Bar Reservoir from the proposed power block area). The vertical hydraulic gradient beneath the power block area is generally downward and changes to an upward hydraulic gradient near the Clinch River arm of the Watts Bar Reservoir.

17. Based on recovery plots of pumping test data at the CRN Site, the log derivative plot versus the log of the recovery time shows a typical leaky aquifer model response, similar to that depicted in Figure 2e of Renard et al. (Reference 2.4.12C-26). This behavior is consistent with a single porosity aquifer model for the site.

The following assumptions are used based on the hydrogeological understanding of the site:

- Assumption: The groundwater model is developed as porous medium flow.

  Rationale: A basic assumption of the groundwater model is that the fracture and solution zones within the regolith as well as within the shallow bedrock are extensive in both area and depth and can be simulated as a porous medium flow (References 2.4.12C-3, 2.4.12C-34, and 2.4.12C-35).

- Assumption: A two-dimensional, profile model can be used to determine the maximum groundwater level.

  Rationale: Groundwater flow is dominant along the strike of the bedding planes of the power block area and allows simulation of the maximum water levels at the power block area. Two-dimensional, vertical, profile modeling was also employed for flow and contaminant transport modeling at a proposed low-level radioactive waste disposal site on the ORR (Reference 2.4.12C-13).

- Assumption: The groundwater model in the vertical domain can be limited to less than 200 ft bgs.

  Rationale: Tucci (Reference 2.4.12C-35) estimated that 97 percent of groundwater flow occurs within 100 ft of the ground surface with about one percent of flow occurring at depths below 200 ft for the ORR area. The hydrogeology at the ORR is similar to that at the CRN Site and thus the vertical depth of the groundwater model was limited to less than 200 ft.

- Assumption: The model domain is limited to the geographic limits of the Clinch River arm of the Watts Bar Reservoir at the CRN Site.

  Rationale: Studies performed for the ORR Melton Valley offsite monitoring system (Reference 2.4.12C-5), which is located approximately 2 miles east of the CRN Site, investigated the groundwater flow relationship with the Clinch River arm of the Watts Bar Reservoir. A hydrologic cross-section presents a section through the river showing the groundwater head distribution and the Clinch River arm of the Watts Bar Reservoir acting as a hydrologic sink (Reference 2.4.12C-5). This head distribution suggests the Clinch River

arm of the Watts Bar Reservoir also acts as a hydrologic sink for the surrounding groundwater system.

- Assumption: The Clinch River arm of the Watts Bar Reservoir is assigned a constant head boundary.

  Rationale: As the reservoir stage is artificially maintained and the groundwater level influence relative to changes in river stage is insignificant, the Clinch River arm of the Watts Bar Reservoir acts as a constant head boundary. The Clinch River arm of the Watts Bar Reservoir was assigned a constant head of 740.63 ft NAVD88, similar to the value assigned by Tucci (Reference 2.4.12C-35), which was 741 ft National Geodetic Vertical Datum of 1929 (NGVD29). The Clinch River arm of the Watts Bar Reservoir at the site is the tail water value of the Melton Hill dam and is regulated and generally fluctuates a few feet above and below the 741 ft NGVD29 (Reference 2.4.12C-24).

- Assumption: The groundwater model is simulated as a steady-state model.

  Rationale: The objective of the groundwater model is to determine the maximum groundwater heads under post-construction conditions at the power block area. This is achieved by simulating steady-state conditions using recharge rates that produce the maximum water level. This is a conservative assumption for estimating the maximum water level at and around the power blocks. A transient model using time-dependent recharge would provide groundwater heads that vary temporally, encompassing both high as well as low groundwater heads. As the main objective of the model is to predict the maximum water level, this is achieved using a steady-state model.

- Assumption: Hydraulic conductivity within a model layer and recharge distribution are assumed to be uniformly distributed.

  Rationale: Although the subsurface hydrogeology is heterogeneous at the CRN Site, no attempt is made to calibrate the groundwater model by spatially prescribing hydraulic conductivities or recharge rates to match the groundwater heads. It should be noted that a calibrated model that fits the observed field data (in this case groundwater heads) may not be unique (i.e., different parameter sets can calibrate the same model). An emphasis was placed to assign hydraulic conductivities that can be uniformly represented within each of the model layers based on site-specific and literature data for similar hydrostratigraphy and, at the same time, can meet the objective of the groundwater model.

2.4.12C.5 Numerical Model

Figure 2.4.12C-13 presents a conceptual site layout which is a composite that represents the bounding area for the different potential SMR technologies. Geotechnical borings (referred to as MPs) are concentrated within the power block area and centered near borings MP-101 and MP-202 (Figure 2.4.12C-13). Based on geology observed in the geotechnical borings, most of the footprint of the power block area lies within the Chickamauga Group of rocks (interbedded siltstone and limestone), whereas the Knox Group (comprised mostly of dolomite) outcrops in the northern extremities of the power block area as indicated on Figure 2.4.12C-13. Within the power block area, the Knox is significantly deeper. For example, at the MP-202 and MP-101 locations, it is encountered at a depth of approximately 450 and 1000 ft bgs, respectively, while at MP-423 and MP-426 the Knox is first encountered at a depth of approximately 30 to 50 ft bgs.

Two, two-dimensional, vertical profile, groundwater models (profile models) were developed along the strike of the bedding planes (approximately N52°E) for the CRN Site. Figure 2.4.12C-13 shows the plan view of the profile models. Profile A intersects and lies close to

the MP-202 series of geotechnical borings, representing the northern portion of the power block area, while Profile C (Profile B is not used) intersects the MP-101 series of geotechnical borings and represents the southern portion of the power block area (Figure 2.4.12C-13). Both profiles fall along a three-cluster groundwater monitoring well series (OW-202 U/L/D and OW-101 U/L/D) at the power block area. The geologic formations present along the two profiles are different; Profile A mostly intersects the Fleanor Shale Member of the Lincolnshire Formation, while Profile C mostly intersects the Benbolt Formation. The hydraulic conductivity distribution along these lines, determined from the slug and packer tests, is also different (Table 2.4.12C-6). The combination of a concentration of geotechnical borings in two different clusters (within the footprint of the power block area) and the difference in hydraulic conductivity values led to the need to create two profile models to adequately represent the power block area.

The objective of the groundwater modeling is to determine maximum groundwater heads at and near the power block area under post-construction conditions. The profile models described above are based on the conceptual hydrogeological model for the CRN Site. The intent of the groundwater model is not to exactly duplicate the subsurface geology, but to approximate the site conceptual model, such that the numerical model represents current conditions and conservatively estimates future groundwater flow conditions at the site. It is well understood that there is significant uncertainty in the thickness and hydrogeologic properties of the geologic formations in between the investigation boreholes as a result of subsurface heterogeneity. However, reproduction of this heterogeneity is not an objective of the groundwater model. The groundwater model is intended to be a simplistic representation of the subsurface conditions that is capable of providing credible maximum groundwater heads to reproduce the maximum observed groundwater heads at the CRN Site. The pre-construction or ambient groundwater model can then be modified to represent post-construction conditions and meet the objectives of the groundwater model stated above. The profile models are used to provide conservative estimates of the maximum groundwater heads below safety-related structures. This is achieved through a steady-state groundwater model rather than a transient model to meet the objectives of this modeling task.

The groundwater model was developed using the pre- and post-processor groundwater modeling software, Groundwater Vistas, Version 6.07, Build 10. The numerical code used to simulate the profile models is MODFLOW-SURFACT, Version 3.0, as implemented in Groundwater Vistas (Reference 2.4.12C-11).

2.4.12C.5.1 Model Grid

Both profile models include a total of 7 model layers. The table below provides details on the grid dimensions and associated information.

Grid Information	Profile A	Profile C
Grid Dimension	Along Rows = 50 ft Along Columns = 50 ft	Along Rows = 50 ft Along Columns = 50 ft
Number of rows and columns	Rows = 1 Columns = 99	Rows = 1 Columns = 87
Number of layers	7	7
Grid Rotation	37 degrees, i.e. oriented to N53°E	37 degrees, i.e. oriented to N53°E

2.4.12C.5.2 Model Layers

Model layers thicknesses for the vertical profiles (Profiles A and C) were based on the CRN Site subsurface investigation geotechnical boring logs (Reference 2.4.12C-1). Geotechnical boring logs that either intersected or were near the vertical profile were used to determine the thickness of the fill, soil, weathered zone, and competent bedrock materials. The surface elevations assigned to each of the vertical profiles were determined from site LiDAR (Light Detection and Ranging) data. The bottom elevation for both vertical profiles was assigned a value of 657 ft NAVD88, which serves as a no-flow boundary. The active bottom layer was assigned a value of 658 ft NAVD88, which was based on the frequency distribution of open fractures decreasing significantly below this elevation (Figure 2.4.12C-3). This depth is also below the Plant Parameter Envelope (PPE) SMR maximum foundation embedment depth and bounds the post-construction depths of excavation for the SMRs, minimizing any significant alteration of the model layers from the pre-construction model to the post-construction model.

Table 2.4.12C-5 provides detailed information on the thickness of the layers in each of the pre-construction profile models. Layers 1, 2, and 3 are assigned as fill, soil, and weathered rock, respectively, based on geotechnical core logs (Reference 2.4.12C-1). Layers 4 and 5 are assigned to the competent bedrock, each with a thickness 15 ft. Layer 6 is also the competent bedrock with a bottom elevation set at 658 ft NAVD88. Layer 7 is the basal no-flow layer with a thickness of 1 ft, with its bottom elevation set at 657 ft NAVD88. The competent rock type encountered along Profile A is predominantly the Fleanor Shale Member of the Lincolnshire Formation and a portion of the Eidson Member of the Lincolnshire Formation. The competent rock formation encountered along Profile C is the Benbolt Formation. The bathymetry of the Clinch River arm of the Watts Bar Reservoir along the two profiles varies from 720 ft NAVD88 at the river centerline to 735 ft NAVD88 at the river edges. These elevations fall within the range observed during the subsurface investigations for the CRBRP in the 1980s. The sediment comprising the river bed was assigned a uniform value of 5 ft. These values are approximate values based on geologic sampling within the Clinch River arm of the Watts Bar Reservoir performed for the CRBRP subsurface investigations (Reference 2.4.12C-25).

2.4.12C.5.3 Boundary Conditions

The Clinch River arm of the Watts Bar Reservoir was assigned as a constant-head boundary in both profile models. The Clinch River arm of the Watts Bar Reservoir is regulated by the tail water of the Melton Hill Dam (located approximately 5 miles to the east of the CRN Site) and by the head water of the Watts Bar Dam in the Tennessee River (located approximately 50 miles to the west of the CRN Site). The average value of the Clinch River arm of the Watts Bar Reservoir stage at the CRN Site is 740.63 ft NAVD88, based on an average tail water elevation of 741 ft NGVD29 in Tucci (Reference 2.4.12C-35). During the September 1, 2013 to March 31, 2014 monitoring period, the tail water stage of the Melton Hill Dam varied from 742.74 to 735.42 ft NAVD88. The average stage value of 740.63 ft NAVD88 reported in the literature (Reference 2.4.12C-35) is within the range measured during the monitoring period. As the long-term fluctuations in the river stage are not significant, it is reasonable to represent this boundary as a constant head. This approach of assigning a constant-head boundary condition to the Clinch River arm of the Watts Bar Reservoir has been applied to other models in the region (Reference 2.4.12C-35).

A no-flow boundary condition is applied below an elevation of 658 ft NAVD88 in the two profile models. This is justified based on the conceptual understanding that most of the flow occurs within the first 100 ft of the subsurface and that the fracture density decreases significantly with depth below an elevation of 658 ft NAVD88 (Figure 2.4.12C-3). A no-flow boundary is also assigned along the centerline of the river. This is based on the rationale that the river acts as a groundwater sink (from either side of the river) and that the majority of the groundwater discharge

to the river occurs at shallow depths; deeper groundwater flow below the river is considered minimal as the rock is more competent (with significantly less fracturing) at an elevation of approximately 700 ft NGVD29 (Reference 2.4.12C-25). Figures 2.4.12C-14 to 2.4.12C-15 show the boundary conditions in the two profile models.

2.4.12C.5.4 Numerical Code

MODFLOW-SURFACT Version 3.0, as implemented in Groundwater Vistas, was used to simulate the two profile models.

MODFLOW-SURFACT is a fully integrated flow and transport code, based on the U.S. Geological Survey (USGS) groundwater modeling software, MODFLOW (Reference 2.4.12C-15) and developed by Hydrogeologic, Inc. (Reference 2.4.12C-11). As stated in the software user manual (Reference 2.4.12C-11), MODFLOW-SURFACT contains additional modules to MODFLOW that improve on its robustness and increase its physical simulation capabilities, refining MODFLOW's treatment of complex saturated and unsaturated subsurface flow analysis and contaminant fate and transport calculations while maintaining the comprehensive, well-established simulation framework of MODFLOW.

MODFLOW-SURFACT consists of subroutines or modules that complement or supplement MODFLOW, and it is generally compatible with pre-existing MODFLOW packages. The MODFLOW-SURFACT modules are, in general, separated into two categories: 1) flow packages, referred to as SURF packages, which are used to compute groundwater flow fields and hydraulic head values and 2) transport packages, referred to as ACT packages, which are used for the computation of contaminant migration. The MODFLOW-SURFACT packages that were used are: BCF4, RSF4, ATO4, and PCG5.

BCF4 Package: This is the new block-centered flow (BCF) package that replaces the earlier BCF packages of MODFLOW. This package incorporates a variably saturated simulation option with pseudo-soil water retention functions to enable robust simulations of desaturation/re-saturation cases.

PCG5 Package: This is a preconditioned conjugate gradient solver that is faster than the standard MODFLOW solvers. The solver contains the Newton-Raphson Linearization option with backtracking that enhances the robustness of the numerical solutions for unconfined and/or unsaturated solutions.

ATO4 Package: This is an adaptive time-stepping and output control package. The adaptive time-stepping scheme selects a time-step size depending on the anticipated nonlinearities of the system for a given calculation. If the anticipated nonlinearities are not significant, a larger time-step size is selected to aggressively move forward with the simulation. If the anticipated nonlinearities are severe, a smaller time-step size is selected to ensure convergence for that time step. In the event that the solution fails to converge for a given time step, the time-step size is further reduced, and the solution is repeated (Reference 2.4.12C-11).

RSF4 Package: This is a recharge-seepage package. Unlike the original MODFLOW recharge package (RCH1), the RSF4 package allows supplied recharge into the groundwater system if the water table is below a user prescribed pool (ponding) elevation. Normally the ponding elevation is the ground surface. If the water elevation reaches the pool elevation, the simulation allows only as much recharge to occur to maintain the prescribed pool conditions. The remaining recharge is not accepted into the simulated domain (Reference 2.4.12C-11). However, in the case of the RCH1 package it is incapable of handling such a situation and recharge continues to occur even though the groundwater has reached the ground surface. For the CRN Site groundwater model, the pool elevation is the ground surface.

2.4.12C.5.5 Hydrogeologic Parameters

Initial hydraulic conductivity values for the profile models are shown in Table 2.4.12C-6. Profiles A and C parallel the Fleanor Shale Member of the Lincolnshire Formation and the Benbolt Formation, respectively. Hydraulic conductivity values for Layers 1 and 2 are based on published literature for the infiltration studies conducted in ORNL's Melton Valley, for forested soils, where the saturated hydraulic conductivity values are assumed to be equal to the infiltration rates (Reference 2.4.12C-16). The hydraulic conductivity for Layers 3 to 6 are based on site-specific slug test results. Layers, 3, 4, 5, and 6 hydraulic conductivity values are based on maximum, 75th percentile, median, and 25th percentile hydraulic conductivity values, respectively, obtained for the Fleanor Shale Member of the Lincolnshire Formation and the Benbolt Formation. These values are comparable to the values obtained from the borehole packer tests and also within an order of magnitude of the hydraulic conductivity values derived from pumping tests (Table 2.4.12C-4). The rationale for using the maximum, 75th percentile, median, and 25th percentile hydraulic conductivity values as described above is based on the premise that the greatest values are within the shallower layers for each of the formations, which then decrease with depth.

An anisotropy ratio of 10:1 for horizontal to vertical hydraulic conductivity was assumed for the model. This ratio is consistent with the value used in the profile model applied in the Melton Valley (Reference 2.4.12C-35).

An initial recharge rate of 15.3 in./yr was applied uniformly across the two profile models. This estimate was based on 20 percent of the maximum annual precipitation of 76.33 in. measured at Oak Ridge, Tennessee, from 1948 to 2013 (Reference 2.4.12C-22). The value of 20 percent comes from the estimate provided by Bailey and Lee (Reference 2.4.12C-3) for a wet period in 1973 based on the hydrograph-separation technique at Poplar Creek, which is approximately 3 miles north of the CRN Site. The choice of the wettest year on record is intended to provide a conservative estimate of the groundwater heads in the power block area. Since the groundwater levels at the CRN Site are the direct result of precipitation events, recharge is a sensitive parameter in the groundwater models.

2.4.12C.6 Groundwater Model Calibration

Groundwater model calibration was conducted by approximately matching the maximum measured groundwater levels in the power block area by adjusting the hydraulic conductivity values and recharge estimates. Individual model layers are homogeneous and anisotropic (i.e., the ratio of the horizontal to vertical hydraulic conductivity is not same) with uniform recharge applied across the entire profile model. No attempt is made to create zones of hydraulic conductivities and recharge to match the maximum measured water levels to the simulated levels. Creating zones of hydraulic conductivity and recharge could provide a better match between measured heads and simulated heads; however, this does not mean the zones of hydraulic conductivity and recharge for the model would represent a unique solution. Calibration was conducted through a trial-and-error approach by adjusting hydraulic conductivities for model layers and recharge rates, and comparing simulated heads against measured heads across the profile models. A series of model runs were conducted by increasing and decreasing the hydraulic conductivity for each layer relative to those in model Run 1 (Table 2.4.12C-7), determining the simulated heads, and comparing them against the measured heads (Table 2.4.12C-8). Calibration of the model was achieved when the residual in the power block area (i.e., measured head minus simulated head) is either close to zero or negative. A negative residual indicates that the simulated head is greater than the measured head, indicating a conservative simulated value relative to the observed maximum water level under the power block area.

The response of the profile models to adjustments in recharge, hydraulic conductivities of the layers, anisotropy ratio (ratio of horizontal to vertical hydraulic conductivities), and the constant head at the Clinch River arm of the Watts Bar Reservoir was evaluated through a series of model runs. Table 2.4.12C-7 provides an explanation of each of the model runs. Recharge was adjusted in Run 2 and Run 3 to 50 percent and 5 percent, respectively, of the maximum annual precipitation of 76.33 in. Hydraulic conductivities in each of the model layers were increased and decreased by an order-of-magnitude from the initial hydraulic conductivity values as stated in Table 2.4.12C-6. The anisotropy ratio was varied between 1:1 to 100:1 for Runs 16 and 17, respectively. The constant head in Clinch River arm of the Watts Bar Reservoir (740.63 ft NAVD88) was varied by increasing and decreasing this value by 4 ft in Runs 19 and 20. The variation of constant head by 4 ft is within the range of change in the tail water at the Melton Hill Dam, which approximates the Clinch River arm of the Watts Bar Reservoir stage at the CRN Site.

The head residuals along with root mean square error (RMSE) are indicators of how well the model replicates the observed head measurements. The RMSE is calculated as follows:

$$\boldsymbol{RMSE} = \sqrt{\sum_{i=1}^{N} \frac{\left(h_i^m - h_i^s\right)^2}{N}}$$

Where:

N is the number of measured values from the observation wells (Profiles A and C have 7 and 2 observation wells, respectively);

h_i^m is the measured water level in ft NAVD88; and

h_i^s is the simulated water level in ft NAVD88.

Figures 2.4.12C-16 and 2.4.12C-17 shows the RMSE for the model runs as well as the residuals (for observation wells OW-202U and OW-101U) for the two profile models (Profiles A and C). A significant change in the RMSE and/or the residuals indicates a sensitive parameter. The sensitivity of the parameters is discussed below with respect to each of the two profile models.

2.4.12C.6.1 Profile Models

2.4.12C.6.1.1 Profile A

Based on Figure 2.4.12C-16 for Profile A model, a decrease of recharge to 5 percent of the precipitation (Run 3) results in a lower RMSE and a significant positive residual for OW-202U. However, increasing the recharge to 50 percent of precipitation (Run 2) did not result in any significant change in RMSE and residuals from the initial starting recharge value of 20 percent of the precipitation. This is because the starting recharge of 20 percent of the maximum precipitation already results in high simulated heads and any further increase in recharge does not have any appreciable impact on the heads because excess recharge is lost as seepage or overland flow. Decreasing recharge to 5 percent of precipitation results in a significant change in RMSE and residuals. The value of the starting recharge of 20 percent of the maximum annual precipitation of 76.33 in. may represent the upper end of the recharge estimate for the CRN Site. The other sensitive parameters that have a significant effect on the RMSE of the model are the hydraulic conductivity of Layer 2 (Run 6) and the anisotropy ratio (Run 16). Increasing the hydraulic conductivity of Layer 2 by an order of magnitude resulted in a decrease of RMSE as well as the residual for OW-202U. Using an anisotropy ratio to 1:1 has a similar effect. Sensitivity to the stage of the Clinch River arm of the Watts Bar Reservoir was evaluated by increasing (Run 19) and decreasing (Run 20) the constant head by 4 ft. These changes did not produce any

appreciable change in RMSE and residuals (Table 2.4.12C-8). This indicates that changes in water levels in the Clinch River arm of the Watts Bar Reservoir at the CRN Site do not likely result in any significant impact on the groundwater heads at and around the power block area.

2.4.12C.6.1.2 Profile C

A series of runs were conducted using the profile model for Profile C by: varying the hydraulic conductivity of each layer by an order of magnitude; increasing and decreasing recharge to 50 percent and 5 percent of maximum recorded precipitation; increasing and decreasing the anisotropy by an order of magnitude; and increasing and decreasing the constant head of the Clinch River arm of the Watts Bar Reservoir by 4 ft (Table 2.4.12C-7). Based on the RMSE values and residuals as shown in Figure 2.4.12C-17, the most sensitive parameters are: a) hydraulic conductivity of Layer 2 in Run 7; b) hydraulic conductivity of Layer 6 in Run 14; and c) anisotropy ratio to 100:1 in Run 17. Increasing recharge to 50 percent of precipitation did not result in any appreciable change in RMSE or residuals when compared to Run 1 (Figure 2.4.12C-17). Whereas lowering the recharge to 5 percent of precipitation lowers RMSE and the residuals (Table 2.4.12C-8). This behavior is similar to the sensitivity model runs for Profile A. Increasing the hydraulic conductivity of Layer 1 by an order-of-magnitude resulted in similar RMSE and slightly lower residuals as in Run 3 (Figure 2.4.12C-17). This is a result of greater flow through Layer 1 and less flow into the layers below it. Increasing the hydraulic conductivity of Layer 6 by an order-of-magnitude resulted in more flow through this layer, which lowers the RMSE and decreases the residuals (Figure 2.4.12C-17). Increasing or decreasing the constant head of the Clinch River arm of the Watts Bar Reservoir results in no appreciable change in the RMSE or residuals. This is similar to the model runs conducted for Profile A. The model simulations have shown that groundwater heads are more sensitive to some parameters than others and at the same time the same set of parameters results in similar groundwater heads and RMSE.

The results describe above further indicates that it is possible to calibrate a model (by lowering RMSE and residuals close to zero) using different parameter sets; however, the parameters might not be indicative of unique sets of parameters that govern the site hydrogeology, and the values are likely to deviate from the measured site values (e.g., slug, packer, and pumping tests results).

2.4.12C.6.1.3 Calibrated Model Runs

Using the initial hydraulic conductivities as described in Table 2.4.12C-6 and a recharge estimate of 20 percent of the maximum annual precipitation of 76.33 in., the simulated heads were greater than the maximum measured heads in all of the CRN observation wells, except for OW-202U (Table 2.4.12C-8). The rationale for the choice of 20 percent recharge of the maximum recorded annual precipitation is provided in Subsection 2.4.12C.3.7, *Recharge Data – Literature Information*. Decreasing the initial hydraulic conductivities in Layers 5 and 6 by an order of magnitude in the Profile A model results in simulated heads in OW-202U that approximate the measured heads (Run 18 in Table 2.4.12C-8). The hydraulic conductivity values in Profile A of 0.1 ft/day and 0.041 ft/day for Layers 5 and 6, respectively, were within the range of hydraulic conductivity values determined from the slug and the packer tests. It is to be noted that the residuals (i.e., simulated heads minus measured heads) in Run 1 (Profile C) and Run 18 (Profile A) are negative, which means the simulated heads are higher than the measured heads. However, the simulated heads for the shallow U-series observation wells at OW-202U and OW-101U are comparable to the maximum measured water levels. Although the residuals are high in the observation wells at greater distances from the modeled power block area, this has little to no effect on the maximum simulated water levels at the modeled power block area; therefore, no attempt is made to decrease the residuals by further improvement of the calibration. The groundwater flow directions in the profile models (Figures 2.4.12C-18 and 2.4.12C-19) show

upward flows near the river (depicted by blue arrows) and downward flow at the center of the power block area (depicted by red arrows), which is in general agreement with the vertical hydraulic gradients determined for the site observation wells.

Decreasing the hydraulic conductivity of Layer 2 by an order-of-magnitude from the initial value (Table 2.4.12C-6) in Profile C results in lower RMSE and lower residuals in well OW-101U; however, the residuals in OW-202U increased (indicating a lower simulated head than the measured head) from the initial model Run 1. In order to maintain consistency of hydraulic conductivity in Layer 2 across the two models, the initial hydraulic conductivity as stated in Table 2.4.12C-6 was chosen for the calibrated runs. This resulted in higher negative residuals (simulated heads greater than the measured heads) at the power block area and provided conservative estimates of maximum simulated heads. The measured heads, simulated heads, and residuals for each of the model runs are provided in Table 2.4.12C-8. Thus, Run 18 for Profile A and Run 1 for Profile C are considered the calibrated model simulations (Table 2.4.12C-8 and Figures 2.4.12C-16 to 2.4.12C-19). A combination of model runs with different recharge and hydraulic conductivities could have produced a lower RMSE and residuals; however, this may not have been a unique set of parameters and thus may not have produced values that are representative of the site conditions.

The profile models were based on the knowledge of the site-specific hydraulic conductivity distribution and recharge values as based on studies in similar hydrogeologic settings close to the CRN Site. The hydraulic conductivity distribution is representative of the geologic formations and does not represent the complex heterogeneity within each formation at the CRN Site. The calibrated groundwater models are thus a simplistic representation of the subsurface and the post-construction simulations should be used with the understanding that the predictions may not precisely mimic future groundwater conditions. However, the groundwater heads obtained from the post-construction simulations are likely to approximate or be higher than the actual post-construction heads.

2.4.12C.6.2 Groundwater Budget

Table 2.4.12C-9 shows the groundwater budget estimate from the two profile models (Run 18 for Profile A and Run 1 for Profile C). As apparent, the shallower layers (1 to 4) show more flow than the deeper layers (Table 2.4.12C-10). This is consistent with the site conceptual understanding, where more flow occurs through the regolith and the shallow fractured bedrock and decreases significantly below a depth of 150 ft bgs. Based on a groundwater budget analysis, the net recharge rates (i.e., recharge in minus recharge out) for Profiles A and C were 21.4 percent and 21 percent, respectively, of the input recharge. The remainder of the recharge is lost as runoff by overland flow when the groundwater elevation reaches the land surface elevation (although runoff by overland flow is not simulated explicitly in the model). Groundwater seepage occurs in low lying areas at the CRN Site when intense precipitation occurs at the site and when groundwater elevations are close to the land surface. During the SMR site subsurface field investigation, seepage was observed in some outcrops in the low lying CRBRP disturbed area. The model is very sensitive to recharge and a small increase in recharge results in an increase in groundwater levels. A similar observation was made on the hydrographs of the site observation wells, where a few inches of precipitation caused the groundwater levels to increase appreciably in the observation wells.

The Clinch River arm of the Watts Bar Reservoir in the model is depicted as a constant head and the contributions to the constant head immediately below (Layers 2 to 6) the Clinch River for the Profiles A and C, amount to 28 percent and 25 percent, respectively. While the contributions to the constant head from the immediate vicinity (which is Layer 1) of the Clinch River for the Profiles A and C are approximately 72 percent and 75 percent, respectively.

2.4.12C.6.3 Alternate Conceptual Model

Three alternate conceptual models were considered in order to address the high residuals for the model runs in Table 2.4.12C-8. One of the alternate conceptual models includes a preferential flow zone in Layer 3, representing a highly fractured zone in the Chickamauga Group and solution cavities that are prevalent within the Knox Group. The second alternate conceptual model included spatially variable recharge rates at the CRN Site, and the third includes uniform recharge rate.

2.4.12C.6.3.1 Preferential Flow Zone: Layer 3

The preferential flow zone was included in Layer 3, which is the highly fractured and weathered portion of the bedrock through which most of the subsurface flow occurs at the site. Similar zones at ORNL have been reported to conduct significant flow (References 2.4.12C-3 and 2.4.12C-20). Run 8 in Table 2.4.12C-7 uses an order-of-magnitude increase in the hydraulic conductivity of Layer 3, and Table 2.4.12C-8 shows the associated residuals for Run 8. Although hydraulic conductivities for Layer 3 in Profiles A and C are 22 ft/day and 2.9 ft/day, respectively, these values could be significantly larger for a highly preferential flow zone layer. Sen (Reference 2.4.12C-31) states that dissolution of limestone may create a network of open fractures with hydraulic conductivities in the range of 330 to 33,000 ft/day. Thus, a value of hydraulic conductivity of 3300 ft/day was assigned for Layer 3 uniformly (anisotropy ratio is 1:1) for both profile models. The choice of 3300 ft/day is at mid-range described in Sen (Reference 2.4.12C-31). Run 21 in Table 2.4.12C-7 provides explanation of the model simulations, and Table 2.4.12C-8 provides the residuals for the simulations. Figures 2.4.12C-16 and 2.4.12C-17 show the trend of the RMSE and the residuals in selected wells OW-202U and OW-101U as compared to all other simulations. The results show that representing Layer 3 as a preferential flow zone did not result in decrease of the residuals.

2.4.12C.6.3.2 Variable Recharge Rates

The second alternate conceptual model considers spatially-variable recharge rates. For simplicity it was assumed that recharge is uniform across the site (simulation conducted in model Runs 1 to 21); however, recharge may be spatially variable at the CRN Site as has been documented at ORNL (References 2.4.12C-2, 2.4.12C-3, and 2.4.12C-17). Modeling studies conducted at the ORNL by USGS and U.S. Department of Energy used recharge that varied from 1 to 8 in./yr (References 2.4.12C-16, 2.4.12C-34, and 2.4.12C-35).

Run 22 includes variable recharge rates, varying from 0 to 8.76 in./yr in the profile models. Two zones of recharge were depicted in the profile models, which provide a lower RMSE and residuals compared to the model Runs 1 to 21 (Table 2.4.12C-8 and Figures 2.4.12C-16 and 2.4.12C-17). Figure 2.4.12C-20 presents the recharge zones and head distribution in the Profiles A and C, respectively. The green zone is 0 in./yr, and the white zone is 8.76 in./yr (Figure 2.4.12C-20). The delineation of the recharge zone is arbitrary; however, the distribution was also based on site-specific observations during the subsurface investigation at the CRN Site. The response of the groundwater heads due to precipitation at the proposed power block area was rapid and thus a recharge of 8.76 in./year was assigned to this area. Further away from the power block area, the recharge may be less and thus a low recharge was provided (in this case recharge of zero). Although the residuals did decrease slightly, this alternative conceptual model is not conservative in terms of predicting the maximum water levels. Thus, a third alternate conceptual model was investigated by assuming uniform recharge within the model domain as is described in Subsection 2.4.12C.6.3.3.

2.4.12C.6.3.3 Uniform Recharge Rate

A uniform recharge of 8.76 in./yr was assigned in both profile models in Run 23 (Table 2.4.12C-7 provides explanation of the simulation and Table 2.4.12C-8 provides observed, simulated, and residual values). The simulated groundwater heads are close to the land surface (Figures 2.4.12C-21 and 2.4.12C-22). The residuals were negative, indicating that the simulated heads are greater than the maximum observed heads. Although the residuals were greater, this alternative conceptual model run provided a conservative estimate in terms of the maximum water level for a predictive simulation.

The recharge rate of 8.76 in./yr is slightly higher than the maximum reported literature value of 8 in./yr from the modeling studies undertaken at the ORR. The use of a higher recharge rate of 8.76 in./yr for the predictive simulation would provide a conservative estimate in regards to the maximum water level at and near the proposed power block area. The uniform recharge simulation of 8.76 in./yr is therefore adopted as the base case model simulation for the post-construction simulations for Profiles A and C (Figures 2.4.12C-21 and 2.4.12C-22).

2.4.12C.7 Post-Construction Modeling

Post-construction modeling is referred to here as the response of groundwater levels to the inclusion of general representative structures (such as radwaste building, nuclear reactor building, auxiliary building, and turbine building) in the profile models. Although the groundwater model is developed for an Early Site Permit Application (ESPA), which is independent of specific SMR technologies, the representative embedment of structures is a generalization of the type of structures that are typical of a nuclear power plant. The PPE provides an approximate maximum foundation embedment depth for the SMR technologies selected for the ESPA evaluation.

2.4.12C.7.1 Modifications to Pre-Construction Models

The general structure of the profile models along with hydraulic conductivity distributions for subsurface layers remained the same as the pre-construction model; however, some nominal changes were made to include representative structures (Figures 2.4.12C-23 and 2.4.12C-24). The following describes the changes to the pre-construction models to develop the post-construction profile models:

- An extra subsurface model layer was added below the bottom of the conceptualized SMR nuclear reactor (Layer 7) to determine the maximum head imposed at the base of the reactor foundation embedment depth and SMR structure. The hydraulic conductivity for this layer remained the same as in the pre-construction model for the same depth. Figures 2.4.12C-23 and 2.4.12C-24 shows the hydraulic conductivity distributions for the layers in the post-construction models for Profiles A and C.

- Surface grade elevations across the two profile models were based on the PPE with maximum foundation embedment depth of approximately 140 ft below grade. Additionally, a shallow SMR foundation embedment depth was also included (in a separate model configuration) at approximately 50 ft below grade (top of the competent rock) in order to represent a technology requiring a shallow foundation embedment depth. These two different excavation depths provide the bounding foundation embedment depths for the different SMR technologies. The width of the power block in the profile models approximates the width of the power block area in the site layout drawing (shown in Figure 1.2-2). The grade elevations are approximate and may change when a specific technology is selected for the Combined License Application (COLA).

- Granular backfill material was included in areas where the surface elevation of the pre-construction model was raised to accommodate the post-construction model grade. The grade elevation of the power block area corresponds to an elevation of 821 ft NAVD88. The power block area is assumed to include: a) radwaste building with foundation embedment elevation selected at 818 ft NAVD88; b) reactor building foundation embedment elevation selected at approximately 681 ft NAVD88 for the deepest SMR technology and at approximately 770 ft NAVD88 for the shallowest SMR technology; and c) auxiliary building elevation selected at 748 ft NAVD88 for the deepest SMR technology and at about 770 ft NAVD88 for the shallowest SMR technology. The embedment depth of the turbine building was assumed to be at an elevation of 814 ft NAVD88, which is 6 ft below grade. The assumption of the embedment depth of the turbine building is based on the approximation of a shallow depth of embedment. The turbine building depth is independent of the different SMR technologies. The inclusion of the radwaste, turbine, and auxiliary buildings, which are not part of the PPE, provides a representation of the type of buildings that are likely to be constructed for a nuclear power plant; these buildings do not have any appreciable impact on the outcome of the hydraulic heads. Embedded structures in the profile models are represented by no-flow cells.

In summary:

1. The hydraulic conductivity of the granular backfill material is assumed to be representative of clean sand with a value of 10^{-2} cm/s (28.35 ft/day) (Reference 2.4.12C-8). The value of hydraulic conductivity is assumed to be uniform (i.e., homogeneous) and represents fill adjacent in and outside of the power block area.

2. Recharge is assumed to be 8.76 in./yr, based on an alternative conceptual model for the pre-construction model runs, except in the power block area and part of the turbine area, which are assumed to be impervious.

2.4.12C.7.2 Results

The objective of the groundwater modeling as outlined in Subsection 2.4.12C.1 is to determine post-construction maximum groundwater head in the power block area.

The maximum allowable head at the foundation embedment depth of the reactor building is based on the requirements of a specific nuclear technology. However, as the present groundwater modeling post-construction analysis is independent of any technology, and site-specific grade elevations (i.e., beyond the immediate vicinity of the power block area) are not finalized, the groundwater heads reported here are preliminary until a technology is selected and site-specific grade elevations are established in the COLA.

The hydraulic conductivity of the site granular backfill as well as amount of post-construction recharge to the subsurface are the dominant factors controlling the hydraulic heads in the power block area. Two sensitivity runs were conducted by varying the hydraulic conductivity of the granular backfill by an order of magnitude larger and smaller than the base value of 10^{-2} cm/s (28.35 ft/day). A value of granular backfill of 10^{-3} cm/s (2.835 ft/day) typically represents a highly compacted backfill; whereas, a value of 10^{-1} cm/s (283.5 ft/day) represents an uncompacted granular backfill material.

Tables 2.4.12C-11 and 2.4.12C-12 depict the simulated groundwater heads beneath the reactor and the auxiliary building as well as adjacent to the reactor building. Figures 2.4.12C-25 and 2.4.12C-26 show the locations of the simulated groundwater heads in the profile section with deep and shallow foundation embedment, as presented in Tables 2.4.12C-11 and 2.4.12C-12. Figures 2.4.12C-27 to 2.4.12C-29 show hydraulic head distribution in the Profile A model for the

deep and shallow foundation embedment, with hydraulic conductivity of the granular backfill materials of 10^{-2} cm/s (28.35 ft/day), 10^{-3} cm/s (2.835 ft/day), and 10^{-1} cm/s (283.5 ft/day), respectively. Similarly, Figures 2.4.12C-30 to 2.4.12C-32 show hydraulic head distribution in the Profile C model for the deep and shallow foundation embedment, with hydraulic conductivity of the granular backfill material of 10^{-2} cm/s (28.35 ft/day), 10^{-3} cm/s (2.835 ft/day), and 10^{-1} cm/s (283.5 ft/day), respectively.

Simulated groundwater heads are typically lower in Profile A than compared to Profile C. This is a result of a combination of more granular backfill in the area of the previous CRBRP excavation area and higher hydraulic conductivity values in the Fleanor Shale Member of the Lincolnshire Formation (Profile A) than in the Benbolt Formation (Profile C). The variability of the depth and location of the granular backfill also results in variable groundwater heads underneath the structures. Variation of granular backfill hydraulic conductivity values by an order of magnitude did not result in a significant change in groundwater head elevations underneath the structures, although there was slight difference in the groundwater head elevations. Lower groundwater heads were observed underneath the structures with higher granular backfill hydraulic conductivity. A higher granular backfill hydraulic conductivity value of 10^{-1} cm/s (283.5 ft/day) results in lower groundwater heads below the shallow SMR foundation embedment than deep SMR foundation embedment depth. The difference is more apparent in Profile C than Profile A (Tables 2.4.12C-11 and 2.4.12C-12).

2.4.12C.8 Conclusions

The following are concluded from the groundwater modeling results:

- Pre-construction groundwater model simulated heads closely matched the observed maximum groundwater heads at observation wells near the proposed location of the SMRs for this modeling exercise.

- Groundwater heads are sensitive to recharge in the groundwater model, similar to observed water level response due to precipitation during the subsurface investigations at the CRN Site. Higher recharge translates to higher water levels. A uniform recharge of 8.76 in./yr in the two profile models results in water levels close to the land surface at the power block area. This provides a conservative estimate with respect to the maximum water levels under predictive model simulations.

- Higher hydraulic conductivity of the granular backfill results in decreases in the simulated groundwater heads surrounding the shallow and deep structures.

- Maximum simulated groundwater heads surrounding the shallow and deep structures varies between the profile models (Profiles A and C). The simulated groundwater heads were slightly lower in Profile A than in Profile C. This is due to the presence of more granular backfill and a higher hydraulic conductivity of the geologic formation in Profile A than in Profile C.

- Simulated groundwater heads underneath the structures in deep foundations varied between 802.3 to 810.9 ft NAVD88 for Profile A and 807.3 to 816.1 ft NAVD88 for Profile C using the highest hydraulic conductivity granular backfill.

2.4.12C.9 References

2.4.12C-1. AMEC Environmental and Infrastructure, Inc., *Geotechnical Exploration and Testing, Clinch River Construction Permit Application, Roane County, Tennessee, Data Report,* Rev. 4, October 2014.

2.4.12C-2. Bailey, Z.C., *Preliminary evaluation of ground-water flow in Bear Creek Valley, the Oak Ridge Reservation, Tennessee*, U.S. Geological Survey (USGS), Water-Resources Investigations Report 88-4010, p.12.

2.4.12C-3. Bailey, Z.C., and R.W. Lee, *Hydrogeology and Geochemistry in Bear Creek and Union Valleys, Near Oak Ridge, Tennessee,* USGS, Water-Resources Investigations Report 90-4008, pp. 1–72.

2.4.12C-4. Bechtel Jacobs (Bechtel Jacobs Company LLC), *Field Summary Report for Drilling and Installation of the Melton Valley Offsite Monitoring Wells, September 2009 to August 2010*, prepared for the U.S. Department of Energy (DOE) Office of Environmental Management under contract DE-AC05-98OR22700, BJC/OR-3483, September 2010.

2.4.12C-5. Bechtel Jacobs (Bechtel Jacobs Company LLC), Melton Valley Exit Pathway and Offsite Groundwater Monitoring Results: July 2012–March 2011, prepared for DOE Office of Environmental Management under contract DE-AC05-98OR22700, June 2011.

2.4.12C-6. Bonine, T.M., and R.H. Ketelle, ORNL Groundwater Protection Plan Description, prepared by the Oak Ridge National Laboratory, Oak Ridge, Tennessee 37831-6285, managed by UT-Batelle, LLC for DOE under contract DE-AC05-000R22725.

2.4.12C-7. Davis, B.C., J.W. Boegly, Jr., E.R. Rothschild, B.P. Spaulding, N.D. Vaughan, C.S. Haase, D.D. Huff, S.Y. Lee, B.C. Walls, J.D. Newbold, and E.D. Smith, *Site characterization techniques used at a low-level waste shallow land burial field demonstration facility*, DOE, Oak Ridge National Laboratory (Report) ORNL/TM-9146, Environmental Sciences Division Publication No. 2306, p. 173.

2.4.12C-8. Freeze, R.A., and J.A. Cherry, *Groundwater*, Prentice-Hall, Inc., Englewood Cliffs, New Jersey 07632, ISBN: 0-13-365312-9, pp. 1–589, 1979.

2.4.12C-9. Golder Associates, Inc., *Contaminant Transport Model Validation, Geohydrologic Site Characterization, and Groundwater Flow Computer Model Application*, ORNL/Sub/88-SA706/5/V1, prepared for Oak Ridge National Laboratory for DOE under contract DE-AC05-84OR21400, September 1988.

2.4.12C-10. Hatcher, Jr., R.D., P.J. Lemiszki, R.B. Dreier, R.H. Ketelle, R.R. Lee, D.A. Lietzke, W.M. McMaster, J.L. Foreman, and S.Y. Lee, *Status Report on the Geology of the Oak Ridge Reservation*, prepared by the Oak Ridge National Laboratory and managed by Martin Marietta Energy Systems, Inc. for DOE under contract DE-AC05-84OR21400, pp. 1–294.

2.4.12C-11. Hydrogeologic, Inc., *MODFLOW-SURFACT Software (Ver. 3.0) Documentation*, file includes Overview, Vol. 1 and Vol. 2, 1996.

2.4.12C-12. Jacobs EM Team (Garrett Weiss), *Task Order 125–Documentation Regarding Slug Test Data and Analysis, White Wing Scrap Yard and East Bear Creek Valley Sites Task 35H83125,* JE/OR/97-01839, Memorandum to Steve Lampkins, September 29, 1997.

2.4.12C-13. Lee, R.R., R.H. Ketelle, J.M. Bownds, and T.A. Rizk, *Aquifer Analysis and Modeling in a Fractured Heterogeneous Medium*, Vol. 30, No. 4, Ground Water, July–August, 1992.

2.4.12C-14. Lloyd, O.B., and W.L. Lyke, *Ground Water Atlas of the United States*: *Segment 10, Illinois, Indiana, Kentucky, Ohio, Tennessee,* USGS Hydrological Atlas 730-K, p. 30, 1995.

2.4.12C-15. McDonald, M.G., and A.W. Harbaugh, *A modular three-dimensional finite difference groundwater flow model*, USGS Techniques of Water-Resources Investigations, Book 6, Chap. A1, 1988.

2.4.12C-16. Moore, G.K., *Concepts of groundwater occurrence and flow near Oak Ridge National Laboratory, Tennessee*, DOE, Oak Ridge National Laboratory (Report) ORNL/TM-10969, Environmental Sciences Division Publication No. 3218, p. 96, 1988.

2.4.12C-17. Moore, G.K., *Hydrograph Analysis in a Fractured Rock Terrane Near Oak Ridge, Tennessee*, prepared for DOE, Office of Environmental Restoration and Waste Management under budget and reporting code EW 20, Oak Ridge National Laboratory, Oak Ridge, Tennessee, under contract DE-AC05-84OR21400, 1991.

2.4.12C-18. Moore, G.K., *Hydrograph Analysis in a fractured rock terrane,* Ground Water, Vol. 30, No. 3, pp. 390–395, 1992.

2.4.12C-19. Moore, G.K., *Supplement to a hydrologic framework for the Oak Ridge Reservation, Oak Ridge, Tennessee, With a Summary of ground-water modeling by L.E. Toran*, Oak Ridge National Laboratory, Oak Ridge, Tennessee, ORNL/TM-12191, 1992.

2.4.12C-20. Moore, G.K., *Quantification of Ground-Water Flow in Fractured Rock, Oak Ridge, Tennessee*, Vol. 35, No. 3, Ground Water, May–June, 1997.

2.4.12C-21. Moore, G.K., and S.C. Young, *Identification of Groundwater-Producing Fractures by Using an Electromagnetic Borehole Flowmeter in Monitoring Wells on the Oak Ridge Reservation, Oak Ridge, Tennessee*, ORNL/ER–91, prepared for DOE Office of Environmental Restoration and Waste Management under contract DE-AC05-840R21400, Oak Ridge National Laboratory Environmental Sciences Division, March 1992.

2.4.12C-22. Oak Ridge National Laboratory, *Precipitation Data for Oak Ridge, Tennessee*, Oak Ridge Reservation Meteorology, Climate Data, Normals, and Extremes. Available at http://web.ornl.gov/~das/web/Normals/30YRNorm.pdf, accessed on October 29, 2014.

2.4.12C-23. Parr, P.D., and J.F. Hughes, *Oak Ridge Reservation Physical Characteristics and Natural Resources*, prepared for DOE by Oak Ridge National Laboratory, managed by UT-Battelle, LLC, Oak Ridge, Tennessee, under contract DE-AC05-00OR22725, October 2006.

2.4.12C-24. Project Management Corporation, *Clinch River Breeder Reactor Project, Preliminary Safety Analysis Report,* Vol. 2, Amdt. 68, May 1982.

2.4.12C-25. Project Management Corporation, *Clinch River Breeder Reactor Plant, Environmental Report,* Vol. 5, Document Control No. 885, 1982.

2.4.12C-26. Renard, P., D. Glenz, and M. Mejias, *Understanding Diagnostic Plots for Well-Test Interpretation*, Hydrogeology Journal, DOI 10.1007/s10040-008-0392-0, 2008.

2.4.12C-27. Rothschild, E.R., D.D. Huff, C.S. Haase, R.B. Clapp, B.P. Spalding, C.D. Farmer, and N.D. Farrow, *Geohydrologic characterization of proposed solid waste storage area (SWSA) 7*, Oak Ridge National Laboratory (Report) ORNL/TM-9314, Environmental Sciences Division Publication No. 2380, p. 262, 1984.

2.4.12C-28. Rovey, C.W., and D. Cherkauer, *Scale Dependency of Hydraulic Conductivity Measurement*, Ground Water, Vol. 33, No. 5, pp. 769–780, 1995.

2.4.12C-29. SAIC, *Decision Document for Performing a Long-Term Pumping Test at the S-3 Site, Oak Ridge Y-12 Plant, Oak Ridge, Tennessee,* Y/ER-210, prepared for DOE Office of Environmental Restoration and Waste Management under contract DE-AC05-84OR21400, February 1995.

2.4.12C-30. SAIC, Science Applications International Corporation, *East End VOC Plume Pump and Tracer Test Technical Memorandum,* BJC/OR-103, prepared for DOE Office of Environmental Management under contract DE-AC05-98OR22700, August 1998.

2.4.12C-31. Sen, Zakai, *Applied Hydrogeology for Scientists and Engineers*, ISBN 1-56670-091-4, 1995.

2.4.12C-32. Smith, E.D., and N.D. Vaughan, *Aquifer test analysis in nonradial flow regimes: A case study,* Groundwater, Vol. 23, No. 2, March–April, pp. 167–175, 1985.

2.4.12C-33. Solomon, D.K., G.K. Moore, L.E. Toran, R.B. Drier, and W.M. McMaster, *Status Report, A Hydrologic Framework for the Oak Ridge Reservation*, prepared for the Energy Systems Groundwater Program Office, prepared by the Oak Ridge National Laboratory, Oak Ridge, Tennessee 37831, managed by Martin Marietta Energy Systems Inc., for DOE under contract DE-AC05-84OR21400, 1992.

2.4.12C-34. Tucci, P., *Ground-Water Flow in Melton Valley, Oak Ridge Reservation, Roane County, Tennessee—Preliminary Model Analysis*, USGS, Water-Resources Investigations Report 85-4221, pp. 1–21, 1986.

2.4.12C-35. Tucci, P., *Hydrology of Melton Valley at Oak Ridge National Laboratory, Tennessee*, USGS, Water-Resources Investigations Report 92-4131, 1992.

2.4.12C-36. URS|CH2M Oak Ridge LLC, Final Zone 1 *Remedial Investigation and Feasibility Study for East Tennessee Technology Park, Oak Ridge, Tennessee,* prepared for DOE Office of Environmental Management under contract DE-SC-0004645, March 2012.

2.4.12C-37. Webster, D.A., and M.W. Bradley, *Hydrology of the Melton Valley radioactive-waste burial grounds at Oak Ridge National Laboratory, Tennessee*, USGS Open-File Report 87-686, p. 115, 1988.

2.4.12C-38. Webster, D.A., *A review of hydrologic and geologic conditions related to the radioactive solid-waste burial grounds at Oak Ridge National Laboratory, Tennessee*, USGS Open-File Report 76-727, p. 85.

Table 2.4.12C-1 (Sheet 1 of 2)
Construction Information for the Observation Wells

Observation Well	Formation	Ground Surface Elevation (ft NAVD88)	Top of Casing Elevation (ft NAVD88)	State Plane Coordinates		Diameter (inches)	Well Casing Schedule	Elevation Filter Pack		Elevation Well Screen		Well Depth (ftbgs)
				Northing (feet)	Easting (feet)			Top (ft NAVD88)	Bottom (ft NAVD88)	Top (ft NAVD88)	Bottom (ft NAVD88)	
OW-101U	Benbolt	800.58	803.72	570235.5	2448339.3	2	40	779.2	750.6	774.6	754.6	50.00
OW-101L	Rockdell	800.66	803.48	570262.0	2448370.8	2	80	667.1	639.7	662.7	642.7	161.00
OW-101D	Rockdell	800.65	803.57	570274.9	2448386.4	2	80	574.9	539.2	570.2	550.2	261.50
OW-202U	Fleanor	811.83	815.38	570946.0	2448081.1	2	40	800.7	772.8	796.1	776.1	39.00
OW-202L	Fleanor	811.97	815.05	570934.2	2448064.9	2	80	665.0	639.0	661.5	641.5	173.00
OW-202D	Eidson	812.10	815.00	570909.7	2448033.7	2	80	539.1	509.1	535.7	515.7	303.00
OW-401U	Newala	817.39	820.48	571967.9	2447619.9	2	40	806.9	779.9	802.2	782.2	37.50
OW-401L	Newala	817.22	820.57	571973.8	2447628.0	2	80	686.4	657.9	682.0	662.0	159.30
OW-401D	Newala	818.17	821.28	571941.2	2447589.7	2	80	596.3	566.5	591.6	571.6	251.70
OW-409U	Rockdell	806.91	809.70	570557.1	2448130.3	2	40	754.5	728.9	752.0	732.0	78.00
OW-409L	Rockdell	806.67	809.51	570570.8	2448143.3	2	40	720.1	694.7	717.6	697.6	112.00
OW-415U	Bowen/Benbolt	784.13	787.22	569590.2	2448180.2	2	40	760.0	733.0	756.0	736.0	51.10
OW-415L	Benbolt	783.65	786.75	569564.4	2448148.1	2	80	631.8	606.3	628.8	608.8	177.40
OW-416U	Rockdell	809.54	812.82	569990.0	2447535.9	2	40	737.7	712.0	734.1	714.1	97.50
OW-416L	Rockdell	809.43	812.73	569965.2	2447504.9	2	40	701.8	676.4	698.8	678.8	133.00
OW-417U	Fleanor	772.20	775.03	569927.1	2446646.9	2	40	725.4	699.1	722.1	702.1	73.10
OW-417L	Fleanor	772.65	775.71	569903.0	2446614.6	2	40	681.2	654.7	677.7	657.7	118.00
OW-418U	Eidson	810.01	812.94	570526.8	2447065.0	2	40	719.9	702.0	715.0	705.0	108.00
OW-418L	Blackford	811.44	814.41	570506.0	2447038.8	2	80	677.8	651.4	674.6	654.6	160.00
OW-419U	Newala	799.98	803.13	571283.4	2446716.1	2	40	745.6	720.4	742.8	722.8	79.60
OW-419L	Newala	799.75	802.72	571257.7	2446683.4	2	40	698.8	673.3	695.3	675.3	126.50
OW-420U	Newala	802.85	805.70	572009.6	2446886.0	2	40	781.7	754.4	776.9	756.9	48.50
OW-420L	Newala	803.07	806.15	572021.1	2446902.0	2	40	675.7	650.7	672.2	652.2	152.40
OW-421U	Blackford	805.36	808.27	570557.7	2446471.7	2	40	754.0	727.4	750.4	730.4	78.00
OW-421L	Blackford/Newala	804.78	807.81	570544.2	2446455.6	2	40	703.8	676.8	700.0	680.0	128.00
OW-421D	Newala	802.49	805.20	570520.1	2446424.4	2	80	629.7	604.5	626.8	606.8	198.00
OW-423U	Eidson	797.41	800.21	571494.1	2448309.5	2	40	758.3	732.4	755.2	735.2	65.00
OW-423L	Blackford	798.02	801.13	571481.6	2448293.2	2	80	661.4	635.0	658.4	638.4	163.00
OW-423D	Blackford	799.89	802.86	571457.9	2448262.0	2	80	555.7	526.9	551.8	531.8	273.00
OW-428U	Rockdell	804.33	807.78	570781.4	2448710.6	2	40	769.9	741.3	763.9	743.9	63.00

Table 2.4.12C-1 (Sheet 2 of 2)
Construction Information for the Observation Wells

Observation Well	Formation	Ground Surface Elevation (ft NAVD88)	Top of Casing Elevation (ft NAVD88)	State Plane Coordinates		Diameter (inches)	Well Casing Schedule	Elevation Filter Pack		Elevation Well Screen		Well Depth (ftbgs)
				Northing (feet)	Easting (feet)			Top (ft NAVD88)	Bottom (ft NAVD88)	Top (ft NAVD88)	Bottom (ft NAVD88)	
OW-428L	Rockdell	803.86	807.06	570767.9	2448696.6	2	40	693.7	665.9	688.7	668.7	138.00
OW-428D	Rockdell	803.73	807.03	570741.9	2448666.5	2	80	618.5	590.7	613.5	593.5	213.00
OW-429U	Benbolt	796.21	799.17	569989.1	2448606.2	2	40	764.4	736.2	759.4	739.4	60.00
OW-429L	Benbolt	796.26	799.49	569965.3	2448576.5	2	80	656.2	628.3	651.2	631.2	168.00

Source: Reference 2.4.12C-1

Notes:
ftbgs = feet below ground surface
NAVD88 = North American Vertical Datum of 1988

Table 2.4.12C-2
Monthly Manual Groundwater Elevation Data

Wells	24-Sep-13	26-Oct-13	23-Nov-13	20-Dec-13	13-Jan-14	18-Feb-14	16-Mar-14
OW-101U	790.71	782.73	783.95	790.65	795.74	791.86	785.52
OW-101L	768.33	756.89	762.05	768.74	771.52	768.70	766.01
OW-101D	743.45	741.33	739.25	741.05	745.15	741.50	739.22
OW-202U	798.65	788.51	797.43	798.10	799.47	798.84	795.76
OW-202L	766.92	762.86	705.78	773.58	776.79	772.85	771.33
OW-202D	759.34	755.67	755.05	762.41	764.04	761.97	760.31
OW-401U	810.96	809.94	809.63	810.63	811.60	810.86	810.41
OW-401L	783.49	778.67	780.61	787.29	795.55	788.69	785.22
OW-401D	781.67	777.33	780.49	781.23	794.33	791.44	787.87
OW-409U	744.72	740.84	739.10	741.99	756.04	743.63	738.31
OW-409L	771.91	760.40	768.26	773.06	777.13	774.07	769.68
OW-415U	758.80	755.21	756.38	764.40	767.22	763.22	760.06
OW-415L	763.83	765.40	766.13	770.87	NM	769.68	767.15
OW-416U	741.44	739.89	737.22	738.50	742.62	739.24	736.64
OW-416L	741.48	739.92	737.29	738.56	742.60	739.30	736.75
OW-417U	746.97	745.93	744.30	747.39	749.18	747.71	746.82
OW-417L	750.41	749.15	747.77	750.11	752.28	751.87	751.44
OW-418U	750.96	749.38	747.17	754.59	757.14	755.36	754.81
OW-418L	748.21	744.96	742.98	752.07	753.03	751.43	749.21
OW-419U	757.40	748.62	751.16	759.76	763.71	758.78	755.60
OW-419L	756.40	748.72	751.07	758.77	761.86	758.00	755.12
OW-420U	758.87	Dry	758.61	758.88	759.04	759.13	758.33
OW-420L	742.13	741.01	736.59	739.99	745.43	741.77	739.83
OW-421U	753.23	754.12	754.15	754.45	754.55	754.45	754.51
OW-421L	709.27	747.92	688.34	749.45	750.43	750.26	750.11
OW-421D	629.04	733.19	743.40	745.20	719.16	744.70	745.90
OW-423U	761.43	758.49	758.68	760.92	762.28	761.51	761.17
OW-423L	771.60	763.72	763.36	774.24	776.65	775.23	774.00
OW-423D	775.52	772.06	772.70	782.42	784.91	782.40	780.98
OW-428U	NA	NA	773.13	785.43	791.44	788.43	785.08
OW-428L	NA	NA	782.21	778.42	789.46	790.14	790.74
OW-428D	NA	NA	761.53	779.64	NM	797.23	795.07
OW-429U	NA	NA	762.10	768.22	768.20	766.89	766.17
OW-429L	NA	NA	638.49	641.29	639.49	642.72	644.89

Notes:

All values are in ft NAVD88

NA: Wells OW-428U/L/D and OW-429U/L were not installed.

NM: Water levels not measured.

Dry: Water level is below bottom of well.

(yellow)	Well was being sampled.
(pink)	Well still recovering after water quality sampling.
(green)	Water recovering after well development.
(lavender)	Maximum water levels for each well.

Table 2.4.12C-3
Slug Test Statistics – Hydraulic Conductivity

Category	All Tests	Retained Tests			
		All	U Wells	L Wells	D Wells
Number of Tests	53	47	20	22	5
Average (ft/day)	1.1	1.2	1.7	1.1	0.06
Geometric Mean (ft/day)	0.11	0.16	0.20	0.15	0.046
Max (ft/day)	13	13	13	7.6	0.13
Min (ft/day)	5.5×10^{-4}	5.5×10^{-4}	1.6×10^{-3}	5.5×10^{-4}	1.6×10^{-2}

Table 2.4.12C-4
Results From the Pumping Test

Well Name	Screened Interval (ftbgs)	Transmissivity Pumping Period (ft^2/d) T_p	Transmissivity Recovery Period (ft^2/d) T_r	Storage Coefficient Pumping Period (dimensionless)	Storage Coefficient Recovery Period (dimensionless)	Hydraulic Conductivity $(T_p+T_r)/2/155$ ft (ft/d)
PT-OW-U1	41.8 – 61.8	10.6	7	5.37×10^{-4}	1.30×10^{-3}	0.06
PT-OW-L1	139.7 – 159.7	129.3	128.7	3.10×10^{-3}	4.0×10^{-3}	0.8
PT-OW-U2	42 – 62	28.4	22.2	4.83×10^{-2}	1.60×10^{-2}	0.2
PT-OW-L2	139.8 – 159.8	28.1	30.3	2.28×10^{-3}	3.10×10^{-3}	0.2
PT-OW-L3	140.5 – 160.5	11.8	8.0	2.73×10^{-4}	2.90×10^{-4}	0.06
OW-423L	139.6 – 159.6	410.1	391.1	8.91×10^{-10}	8.10×10^{-3}	2.6

Table 2.4.12C-5
Thickness of the Profile Model Layers

Profiles	Geotechnical Core Logs[c]	Average Thickness of Fill (ft) = Model Layer 1[b]	Average Thickness of Soil (ft) = Model Layer 2	Average Thickness of Weathered Rock (ft) = Model Layer 3	Average Thickness of Model Layer 4 (ft)	Average Thickness of Model Layer 5 (ft)	Average Thickness of Model Layer 6 (ft)	Average Thickness of Model Layer 7 (ft)[d]
Profile A[a]	MP-205, MP-201, MP-202, MP-217, MP-220, and MP-423	9.2	11.3	6.0	15.0	15.0	Varies between 9.7 to 121	1
Profile C	MP-101, MP-120, and MP-422	6.0	9.6	2.7	15.0	15.0	Varies between 13.7 to 127.4	1

Notes:
(a) MP-417 and MP-418A lies along transect of Profile A; however, the average fill and the soil thickness are 21.75 ft and 35.75 ft, respectively. To prevent sudden change in model layer thickness in the general area of MP-417 and MP-418A, adjustment of the layer thickness was not made in this location.
(b) Layer 1 represented the thickness of the sediments underneath the Clinch River. A uniform thickness of 5 ft was assigned for the two profiles.
(c) Reference 2.4.12C-1.
(d) Layer 7 in the numerical model represents the no flow layer.

Table 2.4.12C-6
Initial Hydraulic Conductivity Values Used in the Profile Models

Model Layers	Hydraulic Conductivity (ft/day)		Source of Hydraulic Conductivity Values		Type of Material
	Profile A	Profile C	Profile A	Profile C	
Layer 1	6.6	6.6	Average infiltration rate studies on forested soils at ORNL (Reference 2.4.12C-16, page 36)		Represents the fill material.
Layer 2	9.84E-3	9.84E-3	Geometric mean of infiltration rate in vadose zone soil at ORNL (Reference 2.4.12C-16, page 41)		Represents the soil material (part of the vadose zone).
Layer 3	2.2	0.29	Maximum hydraulic conductivity value determined from slug test of Fleanor Formation	Maximum hydraulic conductivity value determined from slug test of Benbolt Formation	Represents the shallow heavily weathered rock.
Layer 4	1.8	0.11	The 75th percentile hydraulic conductivity value determined from slug test of Fleanor Formation	The 75th percentile hydraulic conductivity value determined from slug test of Benbolt Formation	Represents fractured but competent bedrock.
Layer 5	1	0.051	Median hydraulic conductivity value determined from slug test of Fleanor Formation	Median hydraulic conductivity value determined from slug test of Benbolt Formation	Represents fractured but competent bedrock.
Layer 6	0.41	0.037	The 25th percentile hydraulic conductivity value determined from slug test of Fleanor Formation	The 25th percentile hydraulic conductivity value determined from slug test of Benbolt Formation	Represents fractured but competent bedrock.

Table 2.4.12C-7 (Sheet 1 of 2)
Explanation of the Model Runs

Model Runs	Summary
Run 1	Includes hydraulic parameters as defined in Table 2.4.12C-6 for initial hydraulic conductivity values for Profiles A and C, with uniform recharge of 15.3 in./yr. Anisotropy ratio for horizontal hydraulic conductivity to vertical hydraulic conductivity is 10:1.
Run 2	Includes hydraulic parameters as defined in Table 2.4.12C-6 for initial hydraulic conductivity values for Profiles A and C, with uniform recharge of 38.17 in./yr. Anisotropy ratio for horizontal hydraulic conductivity to vertical hydraulic conductivity is 10:1.
Run 3	Includes hydraulic parameters as defined in Table 2.4.12C-6 for initial hydraulic conductivity values for Profiles A and C, with uniform recharge of 3.82 in./yr. Anisotropy ratio for horizontal hydraulic conductivity to vertical hydraulic conductivity is 10:1.
Run 4	Includes hydraulic parameters as defined in Table 2.4.12C-6 for initial hydraulic conductivity values for Profiles A and C, with uniform recharge of 15.3 in./yr. Except for Layer 1, where the hydraulic conductivity was increased by an order-of-magnitude to 66 ft/day. Anisotropy ratio for horizontal hydraulic conductivity to vertical hydraulic conductivity is 10:1.
Run 5	Includes hydraulic parameters as defined in Table 2.4.12C-6 for initial hydraulic conductivity values for Profiles A and C, with uniform recharge of 15.3 in./yr. Except for Layer 1, where the hydraulic conductivity was decreased by an order-of-magnitude to 0.66 ft/day. Anisotropy ratio for horizontal hydraulic conductivity to vertical hydraulic conductivity is 10:1.
Run 6	Includes hydraulic parameters as defined in Table 2.4.12C-6 for initial hydraulic conductivity values for Profiles A and C, with uniform recharge of 15.3 in./yr. Except for Layer 2, where the hydraulic conductivity was increased by an order-of-magnitude to 9.84E-2 ft/day. Anisotropy ratio for horizontal hydraulic conductivity to vertical hydraulic conductivity is 10:1.
Run 7	Includes hydraulic parameters as defined in Table 2.4.12C-6 for initial hydraulic conductivity values for Profiles A and C, with uniform recharge of 15.3 in./yr. Except for Layer 2, where the hydraulic conductivity was decreased by an order-of-magnitude to 9.84E-4 ft/day. Anisotropy ratio for horizontal hydraulic conductivity to vertical hydraulic conductivity is 10:1.
Run 8	Includes hydraulic parameters as defined in Table 2.4.12C-6 for initial hydraulic conductivity values for Profiles A and C, with uniform recharge of 15.3 in./yr. Except for Layer 3, where the hydraulic conductivity was increased by an order-of-magnitude to 22 ft/day and 2.9 ft/day, for model Profiles A and C, respectively. Anisotropy ratio for horizontal hydraulic conductivity to vertical hydraulic conductivity is 10:1.
Run 9	Includes hydraulic parameters as defined in Table 2.4.12C-6 for initial hydraulic conductivity values for Profiles A and C, with uniform recharge of 15.3 in./yr. Except for Layer 3, where the hydraulic conductivity was decreased by an order-of-magnitude to 0.22 ft/day and 0.029 ft/day, for model Profiles A and C, respectively. Anisotropy ratio for horizontal hydraulic conductivity to vertical hydraulic conductivity is 10:1.
Run 10	Includes hydraulic parameters as defined in Table 2.4.12C-6 for initial hydraulic conductivity values for Profiles A and C, with uniform recharge of 15.3 in./yr. Except for Layer 4, where the hydraulic conductivity was increased by an order-of-magnitude to 18 ft/day and 1.1 ft/day, for model Profiles A and C, respectively. Anisotropy ratio for horizontal hydraulic conductivity to vertical hydraulic conductivity is 10:1.
Run 11	Includes hydraulic parameters as defined in Table 2.4.12C-6 for initial hydraulic conductivity values for Profiles A and C, with uniform recharge of 15.3 in./yr. Except for Layer 4, where the hydraulic conductivity was decreased by an order-of-magnitude to 0.18 ft/day and 0.011 ft/day, for model Profiles A and C, respectively. Anisotropy ratio for horizontal hydraulic conductivity to vertical hydraulic conductivity is 10:1.

Table 2.4.12C-7 (Sheet 2 of 2)
Explanation of the Model Runs

Model Runs	Summary
Run 12	Includes hydraulic parameters as defined in Table 2.4.12C-6 for initial hydraulic conductivity values for Profiles A and C, with uniform recharge of 15.3 in./yr. Except for Layer 5, where the hydraulic conductivity was increased by an order-of-magnitude to 10 ft/day and 0.51 ft/day, for model Profiles A and C, respectively. Anisotropy ratio for horizontal hydraulic conductivity to vertical hydraulic conductivity is 10:1.
Run 13	Includes hydraulic parameters as defined in Table 2.4.12C-6 for initial hydraulic conductivity values for Profiles A and C, with uniform recharge of 15.3 in./yr. Except for Layer 5, where the hydraulic conductivity was decreased by an order-of-magnitude to 0.1 ft/day and 0.0051 ft/day, for model Profiles A and C, respectively. Anisotropy ratio for horizontal hydraulic conductivity to vertical hydraulic conductivity is 10:1.
Run 14	Includes hydraulic parameters as defined in Table 2.4.12C-6 for initial hydraulic conductivity values for Profiles A and C, with uniform recharge of 15.3 in./yr. Except for Layer 6, where the hydraulic conductivity was increased by an order-of-magnitude to 4.1 ft/day and 0.37 ft/day, for model Profiles A and C, respectively. Anisotropy ratio for horizontal hydraulic conductivity to vertical hydraulic conductivity is 10:1.
Run 15	Includes hydraulic parameters as defined in Table 2.4.12C-6 for initial hydraulic conductivity values for Profiles A and C, with uniform recharge of 15.3 in./yr. Except for Layer 6, where the hydraulic conductivity was decreased by an order-of-magnitude to 0.041 ft/day and 0.0037 ft/day, for model Profiles A and C, respectively. Anisotropy ratio for horizontal hydraulic conductivity to vertical hydraulic conductivity is 10:1.
Run 16	Includes hydraulic parameters as defined in Table 2.4.12C-6 for initial hydraulic conductivity values for Profiles A and C, with uniform recharge of 15.3 in./yr. Anisotropy ratio for horizontal hydraulic conductivity to vertical hydraulic conductivity is 1:1.
Run 17	Includes hydraulic parameters as defined in Table 2.4.12C-6 for initial hydraulic conductivity values for Profiles A and C, with uniform recharge of 15.3 in./yr. Anisotropy ratio for horizontal hydraulic conductivity to vertical hydraulic conductivity is 100:1.
Run 18	Includes hydraulic parameters as defined in Table 2.4.12C-6 for initial hydraulic conductivity values for Profile A (no simulation run conducted for Profile C), with uniform recharge of 15.3 in./yr. Only hydraulic conductivities of Layers 4, 5, and 6 were decreased by an order-of-magnitude to 0.18 ft/day, 0.1 ft/day, and 0.041 ft/day, respectively. Anisotropy ratio for horizontal hydraulic conductivity to vertical hydraulic conductivity is 10:1.
Run 19	Includes hydraulic parameters as defined in Table 2.4.12C-6 for initial hydraulic conductivity values for Profiles A and C, with uniform recharge of 15.3 in./yr. Constant head values for the Clinch River arm of the Watts Bar Reservoir was increased by 4 ft to 744.63 ft NAVD88. Anisotropy ratio for horizontal hydraulic conductivity to vertical hydraulic conductivity is 10:1.
Run 20	Includes hydraulic parameters as defined in Table 2.4.12C-6 for initial hydraulic conductivity values for Profiles A and C, with uniform recharge of 15.3 in./yr. Constant head values for the Clinch River arm of the Watts Bar Reservoir was decreased by 4 ft to 736.63 ft NAVD88. Anisotropy ratio for horizontal hydraulic conductivity to vertical hydraulic conductivity is 10:1.
Run 21	Includes hydraulic conductivity distribution for Profile A as similar to Run 18 and for Profile C is same as that of Run 1, respectively. However, Layer 3 in each of the Profiles A and C, was set at 3300 ft/day, with recharge of 15.3 in./yr. The anisotropy ratio (Kx: Kz) of Layer 3 is 1:1.
Run 22	Includes hydraulic conductivity distribution for Profile A as similar to Run 18 and for Profile C is same as that of Run 1, respectively. Recharge is variable from 0 in./yr to 8.76 in./yr in Profiles A and C.
Run 23	Includes hydraulic conductivity distribution for Profiles A and C similar to Run 22. Except, recharge is uniform in the two profile models to be 8.76 in./yr.

Table 2.4.12C-8 (Sheet 1 of 3)
Measured and Simulated Heads for the Two Profile Models

Model Runs	Profile A				Profile C			
	Wells	Measured Heads (ft NAVD88)	Simulated Heads (ft NAVD88)	Residuals (Measured Heads—Simulated Heads, ft)	Wells	Measured Heads (ft NAVD88)	Simulated Heads (ft NAVD88)	Residuals (Measured Heads—Simulated Heads, ft)
Run 1	OW-417U	749.18	775.24	-26.06	OW-415U	767.22	800.84	-33.62
	OW-417L	752.28	775.89	-23.61	OW-101U	795.74	802.04	-6.30
	OW-418U	757.14	780.39	-23.25				
	OW-418L	753.03	780.78	-27.75				
	OW-202U	799.47	791.41	8.06				
	OW-202L	776.79	790.50	-13.71				
	OW-423U	762.28	792.00	-29.72				
Run 2	OW-417U	749.18	776.21	-27.03	OW-415U	767.22	801.22	-34.00
	OW-417L	752.28	776.87	-24.59	OW-101U	795.74	802.39	-6.65
	OW-418U	757.14	781.39	-24.25				
	OW-418L	753.03	781.78	-28.75				
	OW-202U	799.47	792.28	7.19				
	OW-202L	776.79	791.38	-14.59				
	OW-423U	762.28	792.86	-30.58				
Run 3	OW-417U	749.18	768.15	-18.97	OW-415U	767.22	799.75	-32.53
	OW-417L	752.28	768.65	-16.37	OW-101U	795.74	801.52	-5.78
	OW-418U	757.14	772.41	-15.27				
	OW-418L	753.03	772.76	-19.73				
	OW-202U	799.47	779.20	20.27				
	OW-202L	776.79	778.53	-1.74				
	OW-423U	762.28	778.39	-16.11				
Run 4	OW-417U	749.18	773.36	-24.18	OW-415U	767.22	799.48	-32.26
	OW-417L	752.28	774.01	-21.73	OW-101U	795.74	801.43	-5.69
	OW-418U	757.14	778.54	-21.40				
	OW-418L	753.03	778.94	-25.91				
	OW-202U	799.47	788.92	10.55				
	OW-202L	776.79	788.08	-11.29				
	OW-423U	762.28	789.80	-27.52				
Run 5	OW-417U	749.18	777.35	-28.17	OW-415U	767.22	801.45	-34.23
	OW-417L	752.28	778.02	-25.74	OW-101U	795.74	802.79	-7.05
	OW-418U	757.14	782.53	-25.39				
	OW-418L	753.03	782.92	-29.89				
	OW-202U	799.47	793.18	6.29				
	OW-202L	776.79	792.30	-15.51				
	OW-423U	762.28	793.80	-31.52				
Run 6	OW-417U	749.18	766.09	-16.91	OW-415U	767.22	801.83	-34.61
	OW-417L	752.28	767.40	-15.12	OW-101U	795.74	801.14	-5.40
	OW-418U	757.14	774.72	-17.58				
	OW-418L	753.03	775.20	-22.17				
	OW-202U	799.47	792.69	6.78				
	OW-202L	776.79	790.41	-13.62				
	OW-423U	762.28	793.35	-31.07				
Run 7	OW-417U	749.18	780.35	-31.17	OW-415U	767.22	795.17	-27.95
	OW-417L	752.28	780.45	-28.17	OW-101U	795.74	798.96	-3.22
	OW-418U	757.14	781.16	-24.02				
	OW-418L	753.03	781.23	-28.20				
	OW-202U	799.47	783.09	16.38				
	OW-202L	776.79	782.94	-6.15				
	OW-423U	762.28	783.15	-20.87				
Run 8	OW-417U	749.18	776.43	-27.25	OW-415U	767.22	799.78	-32.56
	OW-417L	752.28	776.84	-24.56	OW-101U	795.74	802.45	-6.71
	OW-418U	757.14	781.04	-23.90				
	OW-418L	753.03	781.50	-28.47				
	OW-202U	799.47	788.98	10.49				
	OW-202L	776.79	788.46	-11.67				
	OW-423U	762.28	789.51	-27.23				
Run 9	OW-417U	749.18	775.09	-25.91	OW-415U	767.22	800.90	-33.68
	OW-417L	752.28	775.80	-23.52	OW-101U	795.74	801.97	-6.23
	OW-418U	757.14	780.34	-23.20				
	OW-418L	753.03	780.72	-27.69				
	OW-202U	799.47	791.89	7.58				
	OW-202L	776.79	790.89	-14.10				
	OW-423U	762.28	792.52	-30.24				

Table 2.4.12C-8 (Sheet 2 of 3)
Measured and Simulated Heads for the Two Profile Models

Model Runs	Profile A				Profile C			
	Wells	Measured Heads (ft NAVD88)	Simulated Heads (ft NAVD88)	Residuals (Measured Heads—Simulated Heads, ft)	Wells	Measured Heads (ft NAVD88)	Simulated Heads (ft NAVD88)	Residuals (Measured Heads—Simulated Heads, ft)
Run 10	OW-417U	749.18	779.96	-30.78	OW-415U	767.22	798.50	-31.28
	OW-417L	752.28	780.20	-27.92	OW-101U	795.74	802.09	-6.35
	OW-418U	757.14	781.92	-24.78				
	OW-418L	753.03	782.10	-29.07				
	OW-202U	799.47	786.89	12.58				
	OW-202L	776.79	786.54	-9.75				
	OW-423U	762.28	787.12	-24.84				
Run 11	OW-417U	749.18	774.37	-25.19	OW-415U	767.22	800.36	-33.14
	OW-417L	752.28	775.18	-22.90	OW-101U	795.74	801.99	-6.25
	OW-418U	757.14	780.46	-23.32				
	OW-418L	753.03	780.89	-27.86				
	OW-202U	799.47	793.05	6.42				
	OW-202L	776.79	791.71	-14.92				
	OW-423U	762.28	793.47	-31.19				
Run 12	OW-417U	749.18	778.02	-28.84	OW-415U	767.22	799.56	-32.34
	OW-417L	752.28	778.33	-26.05	OW-101U	795.74	802.13	-6.39
	OW-418U	757.14	780.43	-23.29				
	OW-418L	753.03	780.63	-27.60				
	OW-202U	799.47	786.19	13.28				
	OW-202L	776.79	785.72	-8.93				
	OW-423U	762.28	786.32	-24.04				
Run 13	OW-417U	749.18	774.93	-25.75	OW-415U	767.22	799.71	-32.49
	OW-417L	752.28	775.63	-23.35	OW-101U	795.74	801.82	-6.08
	OW-418U	757.14	780.39	-23.25				
	OW-418L	753.03	780.80	-27.77				
	OW-202U	799.47	792.94	6.53				
	OW-202L	776.79	791.47	-14.68				
	OW-423U	762.28	793.01	-30.73				
Run 14	OW-417U	749.18	778.92	-29.74	OW-415U	767.22	796.18	-28.96
	OW-417L	752.28	779.14	-26.86	OW-101U	795.74	799.69	-3.95
	OW-418U	757.14	780.51	-23.37				
	OW-418L	753.03	780.63	-27.60				
	OW-202U	799.47	784.53	14.94				
	OW-202L	776.79	784.00	-7.21				
	OW-423U	762.28	784.38	-22.10				
Run 15	OW-417U	749.18	773.74	-24.56	OW-415U	767.22	801.64	-34.42
	OW-417L	752.28	774.56	-22.28	OW-101U	795.74	801.86	-6.12
	OW-418U	757.14	780.57	-23.43				
	OW-418L	753.03	781.11	-28.08				
	OW-202U	799.47	794.71	4.76				
	OW-202L	776.79	793.62	-16.83				
	OW-423U	762.28	796.03	-33.75				
Run 16	OW-417U	749.18	766.12	-16.94	OW-415U	767.22	802.30	-35.08
	OW-417L	752.28	767.38	-15.10	OW-101U	795.74	800.91	-5.17
	OW-418U	757.14	775.30	-18.16				
	OW-418L	753.03	775.79	-22.76				
	OW-202U	799.47	791.41	8.06				
	OW-202L	776.79	790.47	-13.68				
	OW-423U	762.28	793.73	-31.45				
Run 17	OW-417U	749.18	780.56	-31.38	OW-415U	767.22	792.46	-25.24
	OW-417L	752.28	780.64	-28.36	OW-101U	795.74	798.88	-3.14
	OW-418U	757.14	781.19	-24.05				
	OW-418L	753.03	781.24	-28.21				
	OW-202U	799.47	783.55	15.92				
	OW-202L	776.79	782.64	-5.85				
	OW-423U	762.28	782.59	-20.31				
Run 18	OW-417U	749.18	770.31	-21.13	OW-415U	NC	NC	NC
	OW-417L	752.28	771.76	-19.48	OW-101U	NC	NC	NC
	OW-418U	757.14	782.53	-25.39				
	OW-418L	753.03	783.21	-30.18				
	OW-202U	799.47	800.53	-1.06				
	OW-202L	776.79	798.68	-21.89				
	OW-423U	762.28	804.07	-41.79				

Table 2.4.12C-8 (Sheet 3 of 3)
Measured and Simulated Heads for the Two Profile Models

Model Runs	Profile A				Profile C			
	Wells	Measured Heads (ft NAVD88)	Simulated Heads (ft NAVD88)	Residuals (Measured Heads—Simulated Heads, ft)	Wells	Measured Heads (ft NAVD88)	Simulated Heads (ft NAVD88)	Residuals (Measured Heads—Simulated Heads, ft)
Run 19	OW-417U	749.18	776.05	-26.87	OW-415U	767.22	800.86	-33.64
	OW-417L	752.28	776.67	-24.39	OW-101U	795.74	802.05	-6.31
	OW-418U	757.14	780.91	-23.77				
	OW-418L	753.03	781.29	-28.26				
	OW-202U	799.47	791.64	7.83				
	OW-202L	776.79	790.74	-13.95				
	OW-423U	762.28	792.25	-29.97				
Run 20	OW-417U	749.18	774.42	-25.24	OW-415U	767.22	800.82	-33.60
	OW-417L	752.28	775.10	-22.82	OW-101U	795.74	802.02	-6.28
	OW-418U	757.14	779.86	-22.72				
	OW-418L	753.03	780.28	-27.25				
	OW-202U	799.47	791.17	8.30				
	OW-202L	776.79	790.24	-13.45				
	OW-423U	762.28	791.73	-29.45				
Run 21	OW-417U	749.18	779.92	-30.74	OW-415U	767.22	791.23	-24.01
	OW-417L	752.28	780.21	-27.93	OW-101U	795.74	791.37	4.37
	OW-418U	757.14	784.55	-27.41				
	OW-418L	753.03	784.90	-31.87				
	OW-202U	799.47	786.65	12.82				
	OW-202L	776.79	787.43	-10.64				
	OW-423U	762.28	791.42	-29.14				
Run 22	OW-417U	749.18	752.24	-3.06	OW-415U	767.22	791.66	-24.44
	OW-417L	752.28	753.23	-0.95	OW-101U	795.74	796.75	-1.01
	OW-418U	757.14	764.57	-7.43				
	OW-418L	753.03	765.89	-12.86				
	OW-202U	799.47	789.59	9.88				
	OW-202L	776.79	786.62	-9.83				
	OW-423U	762.28	784.27	-21.99				
Run 23	OW-417U	749.18	769.80	-20.62	OW-415U	767.22	800.42	-33.20
	OW-417L	752.28	771.25	-18.97	OW-101U	795.74	801.86	-6.12
	OW-418U	757.14	782.06	-24.92				
	OW-418L	753.03	782.74	-29.71				
	OW-202U	799.47	799.75	-0.28				
	OW-202L	776.79	797.95	-21.16				
	OW-423U	762.28	803.39	-41.11				

Note: NC -Run 18 was not conducted for Profile C

Table 2.4.12C-9
Groundwater Budget

Profile A (Run 18)			Profile C (Run 1)		
	IN (ft^3/day)	OUT (ft^3/day)		IN (ft^3/day)	OUT (ft^3/day)
Constant Head	0.00	136.13	**Constant Head**	0.00	99.29
Recharge	620.01	487.21	**Recharge**	480.00	380.44
Percent Discrepancy	-0.54		**Percent Discrepancy**	0.06	

Table 2.4.12C-10
Groundwater Flow Across Each Layer in the Profile Models

Profile A (Run 18)		Profile C (Run 1)	
Layers	ft^3/day	Layers	ft^3/day
1	295.8	1	152.9
2	272.2	2	106.6
3	252.4	3	101.9
4	140.7	4	79.9
5	37.3	5	51.0
6	13.6	6	20.0

Table 2.4.12C-11 (Sheet 1 of 2)
Post-Construction Groundwater Heads: Profile A

Deep Foundation Embedment			Shallow Foundation Embedment		
Hydraulic Conductivity of Construction Fill Material (ft/day)	Location	Hydraulic Head (ft, NAVD88)	Hydraulic Conductivity of Construction Fill Material (ft/day)	Location	Hydraulic Head (ft, NAVD88)
28.35	A	803.0	28.35	A	803.9
28.35	B	803.9	28.35	B	804.6
28.35	C	804.7	28.35	C	805.2
28.35	D	805.5	28.35	D	805.8
28.35	E	806.4	28.35	E	806.5
28.35	F	807.2	28.35	F	807.1
28.35	G	808.1	28.35	G	807.7
28.35	H	810.2	28.35	H	808.4
28.35	I	810.3	28.35	I	809.2
28.35	1	800.7	28.35	1	802.4
28.35	2	800.7	28.35	2	802.4
28.35	3	800.7	28.35	3	802.6
28.35	4	800.8	28.35	4	810.9
28.35	5	801.1	28.35	5	811.1
28.35	6	812.0	28.35	6	811.1
28.35	7	812.2			
28.35	8	812.2			
28.35	9	812.2			
2.835	A	805.1	2.835	A	805.9
2.835	B	805.7	2.835	B	806.4
2.835	C	806.3	2.835	C	806.9
2.835	D	806.9	2.835	D	807.3
2.835	E	807.6	2.835	E	807.8
2.835	F	808.2	2.835	F	808.3
2.835	G	808.8	2.835	G	808.8
2.835	H	810.4	2.835	H	809.3
2.835	I	810.5	2.835	I	809.9
2.835	1	803.6	2.835	1	804.8
2.835	2	803.6	2.835	2	804.8
2.835	3	803.6	2.835	3	804.9
2.835	4	803.6	2.835	4	811.3
2.835	5	803.7	2.835	5	811.4
2.835	6	812.0	2.835	6	811.4
2.835	7	812.2			
2.835	8	812.3			
2.835	9	812.3			

Table 2.4.12C-11 (Sheet 2 of 2)
Post-Construction Groundwater Heads: Profile A

Deep Foundation Embedment			Shallow Foundation Embedment		
Hydraulic Conductivity of Construction Fill Material (ft/day)	Location	Hydraulic Head (ft, NAVD88)	Hydraulic Conductivity of Construction Fill Material (ft/day)	Location	Hydraulic Head (ft, NAVD88)
283.5	A	**802.3**	283.5	A	803.3
283.5	B	803.3	283.5	B	804.1
283.5	C	804.3	283.5	C	804.8
283.5	D	805.3	283.5	D	805.5
283.5	E	806.3	283.5	E	806.3
283.5	F	807.3	283.5	F	807.0
283.5	G	808.3	283.5	G	807.8
283.5	H	810.8	283.5	H	808.6
283.5	I	**810.9**	283.5	I	809.4
283.5	1	799.5	283.5	1	801.4
283.5	2	799.5	283.5	2	801.4
283.5	3	799.5	283.5	3	801.6
283.5	4	799.5	283.5	4	811.4
283.5	5	799.9	283.5	5	811.6
283.5	6	812.6	283.5	6	811.6
283.5	7	812.8			
283.5	8	812.8			
283.5	9	812.8			

Notes:

Bold highlighted color in **green** and **blue** indicates minimum and maximum hydraulic heads, respectively, underneath the structures (A to I).

Table 2.4.12C-12 (Sheet 1 of 2)
Post-Construction Groundwater Heads: Profile C

Deep Foundation Embedment			Shallow Foundation Embedment		
Hydraulic Conductivity of Construction Fill Material (ft/day)	**Location**	**Hydraulic Head (ft, NAVD88)**	**Hydraulic Conductivity of Construction Fill Material (ft/day)**	**Location**	**Hydraulic Head (ft, NAVD88)**
28.35	A	808.2	28.35	A	809.1
28.35	B	808.7	28.35	B	809.4
28.35	C	809.3	28.35	C	809.7
28.35	D	809.8	28.35	D	810.0
28.35	E	810.4	28.35	E	810.3
28.35	F	810.9	28.35	F	810.6
28.35	G	811.5	28.35	G	810.9
28.35	H	812.8	28.35	H	811.3
28.35	I	812.8	28.35	I	811.7
28.35	1	808.2	28.35	1	809.0
28.35	2	807.9	28.35	2	808.8
28.35	3	807.6	28.35	3	808.7
28.35	4	807.5	28.35	4	812.5
28.35	5	807.1	28.35	5	812.6
28.35	6	813.5	28.35	6	812.6
28.35	7	813.6			
28.35	8	813.6			
28.35	9	813.6			
2.835	A	811.1	2.835	A	812.1
2.835	B	811.5	2.835	B	812.2
2.835	C	811.9	2.835	C	812.4
2.835	D	812.3	2.835	D	812.6
2.835	E	812.7	2.835	E	812.8
2.835	F	813.1	2.835	F	813.0
2.835	G	813.5	2.835	G	813.3
2.835	H	814.4	2.835	H	813.5
2.835	I	814.5	2.835	I	813.8
2.835	1	812.3	2.835	1	812.9
2.835	2	811.8	2.835	2	812.4
2.835	3	811.3	2.835	3	812.0
2.835	4	811.2	2.835	4	814.6
2.835	5	810.4	2.835	5	814.7
2.835	6	815.2	2.835	6	814.7
2.835	7	815.3			
2.835	8	815.4			
2.835	9	815.4			

Table 2.4.12C-12 (Sheet 2 of 2)
Post-Construction Groundwater Heads: Profile C

Deep Foundation Embedment			Shallow Foundation Embedment		
Hydraulic Conductivity of Construction Fill Material (ft/day)	**Location**	**Hydraulic Head (ft, NAVD88)**	**Hydraulic Conductivity of Construction Fill Material (ft/day)**	**Location**	**Hydraulic Head (ft, NAVD88)**
283.5	A	807.7	283.5	A	**807.3**
283.5	B	808.7	283.5	B	807.7
283.5	C	809.6	283.5	C	808.1
283.5	D	810.6	283.5	D	808.5
283.5	E	811.6	283.5	E	808.9
283.5	F	812.6	283.5	F	809.2
283.5	G	813.5	283.5	G	809.7
283.5	H	816.0	283.5	H	810.1
283.5	I	**816.1**	283.5	I	810.6
283.5	1	806.0	283.5	1	806.8
283.5	2	805.8	283.5	2	806.7
283.5	3	805.6	283.5	3	806.7
283.5	4	805.6	283.5	4	811.6
283.5	5	805.4	283.5	5	811.7
283.5	6	818.9	283.5	6	811.7
283.5	7	819.6			
283.5	8	820.0			
283.5	9	820.0			

Notes:

Bold highlighted color in **green** and **blue** indicates minimum and maximum hydraulic heads, respectively, underneath the structures (A to I).

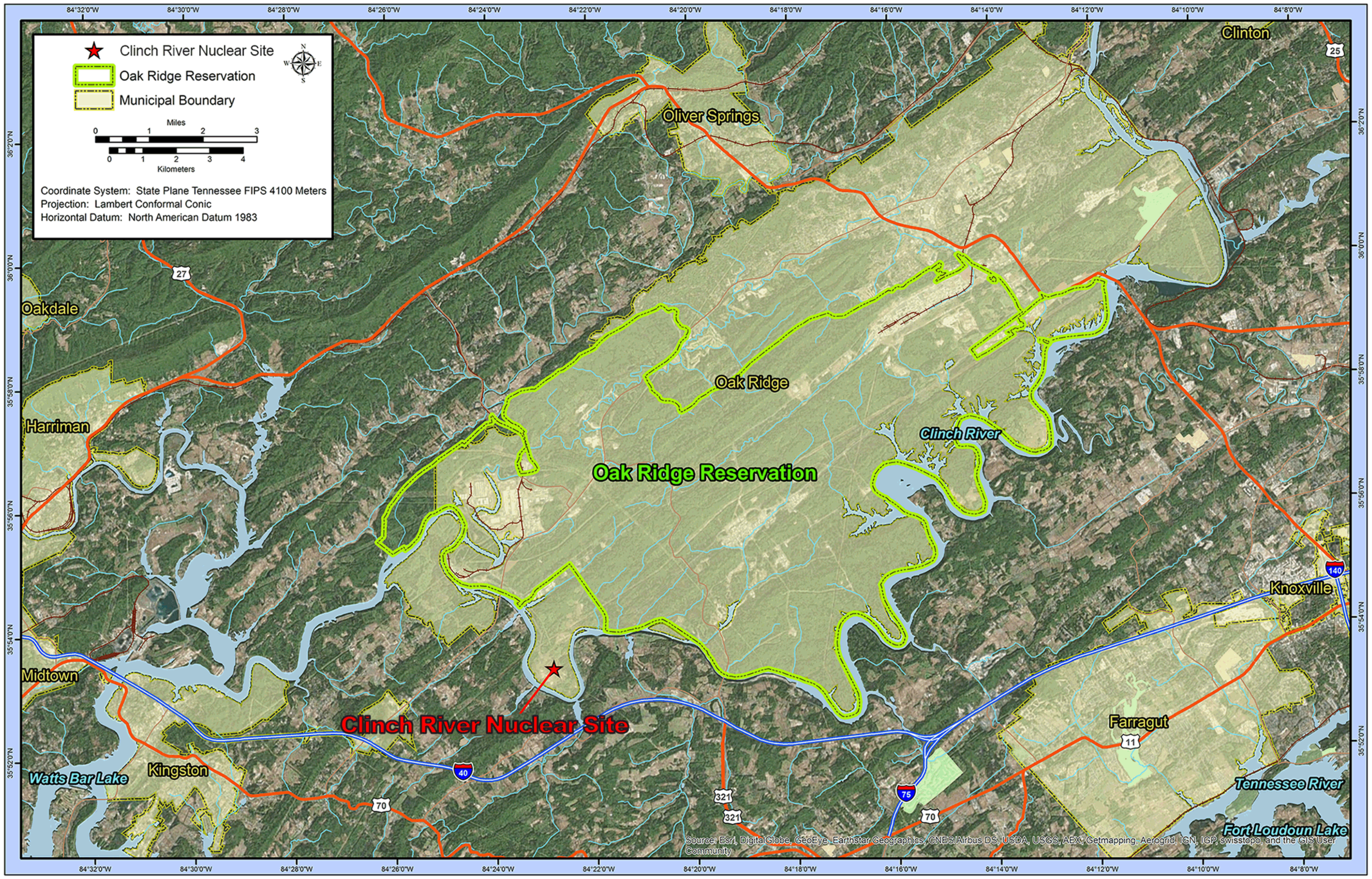

Figure 2.4.12C-1. (Sheet 1 of 2) Location Map—Oak Ridge Reservation and the Clinch River Nuclear Site

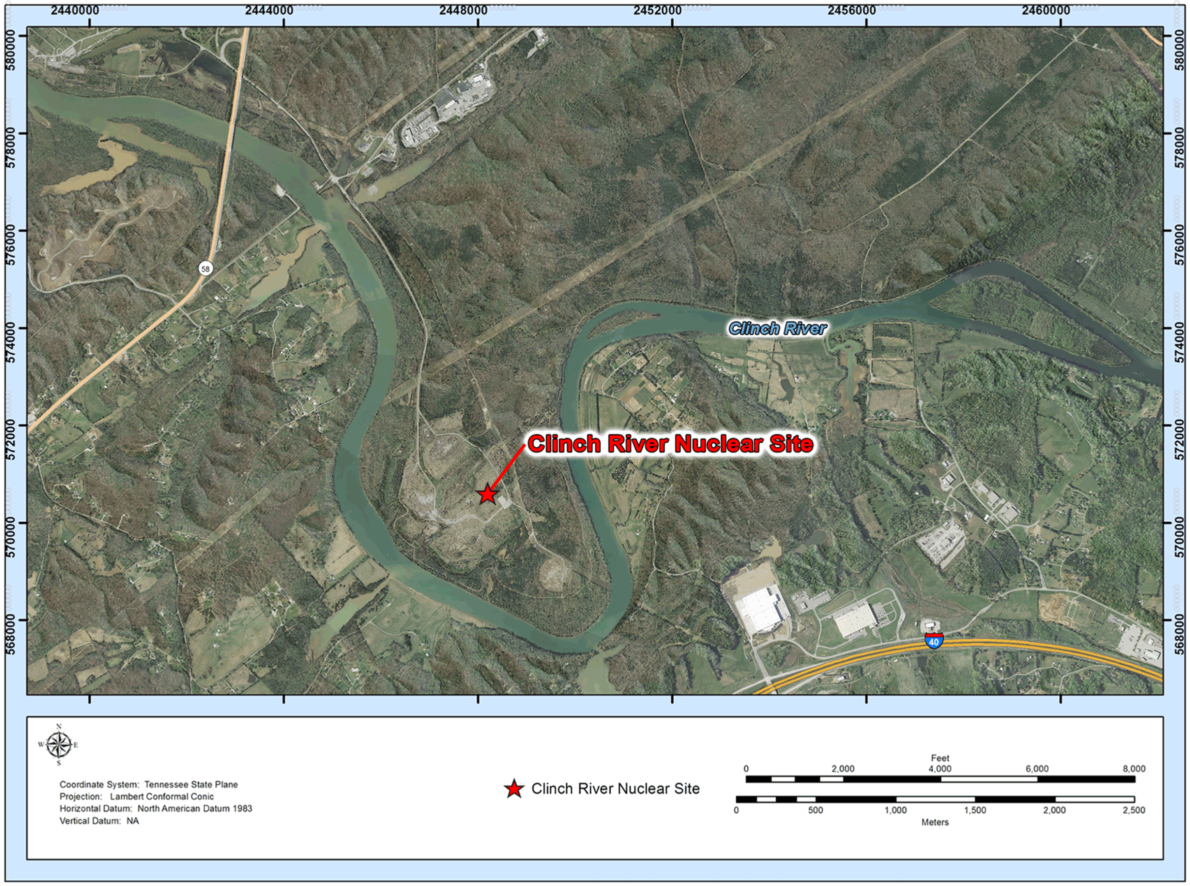

Figure 2.4.12C-1. (Sheet 2 of 2) Location Map—Clinch River Nuclear Site

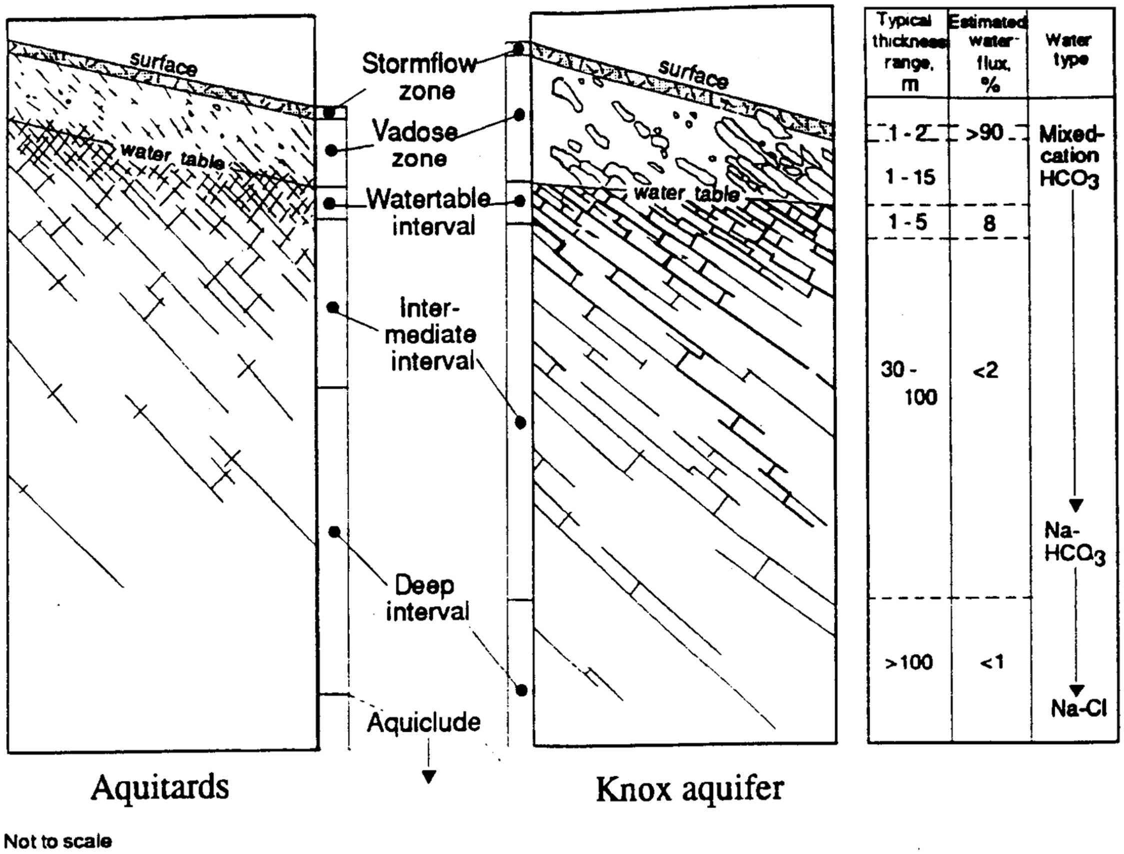

Source: Reference 2.4.12C-33

Figure 2.4.12C-2. Oak Ridge Reservation Vertical Flow Conceptualization

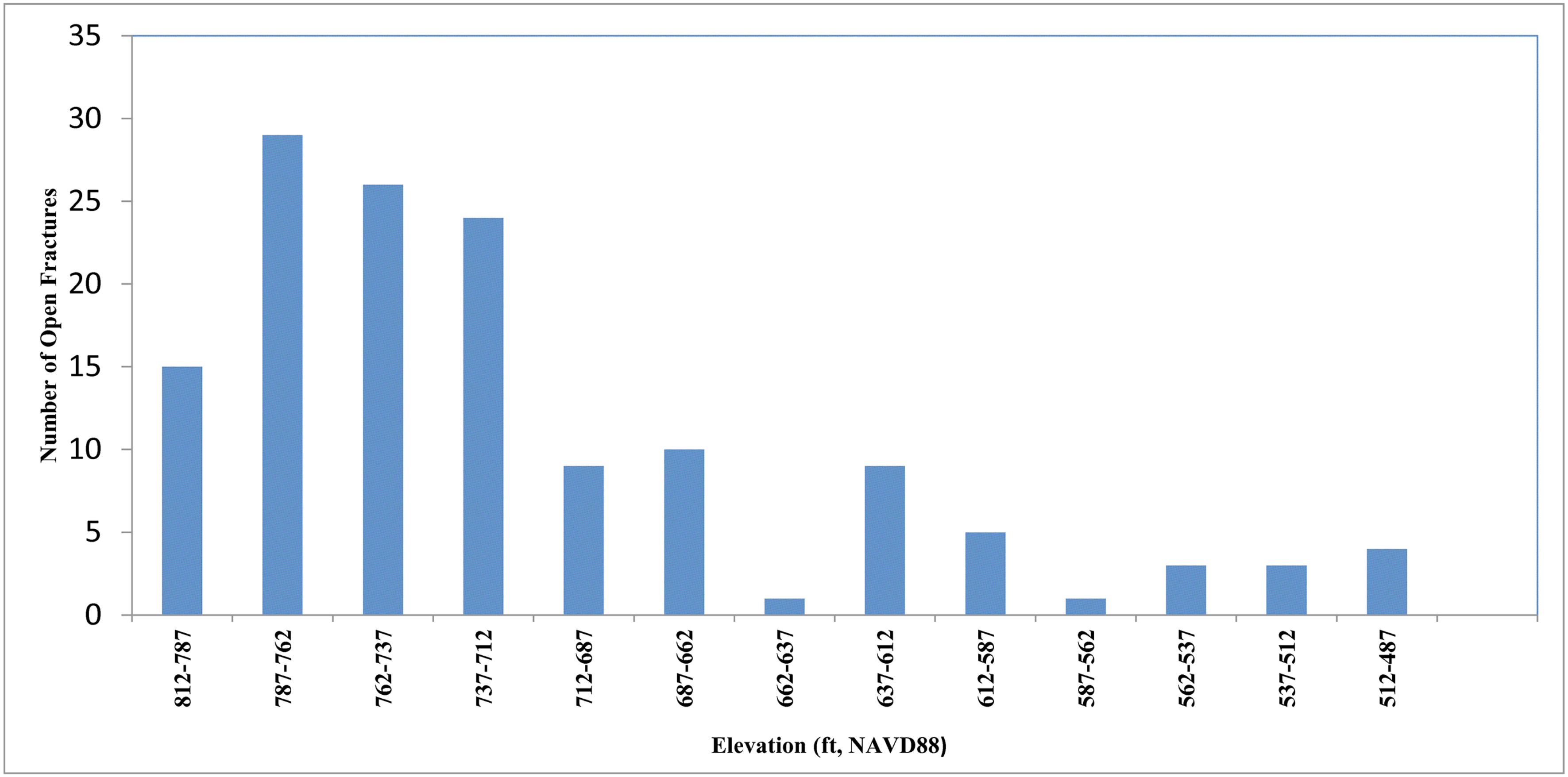

Figure 2.4.12C-3. Frequency Distribution of Open Fractures Versus Elevation

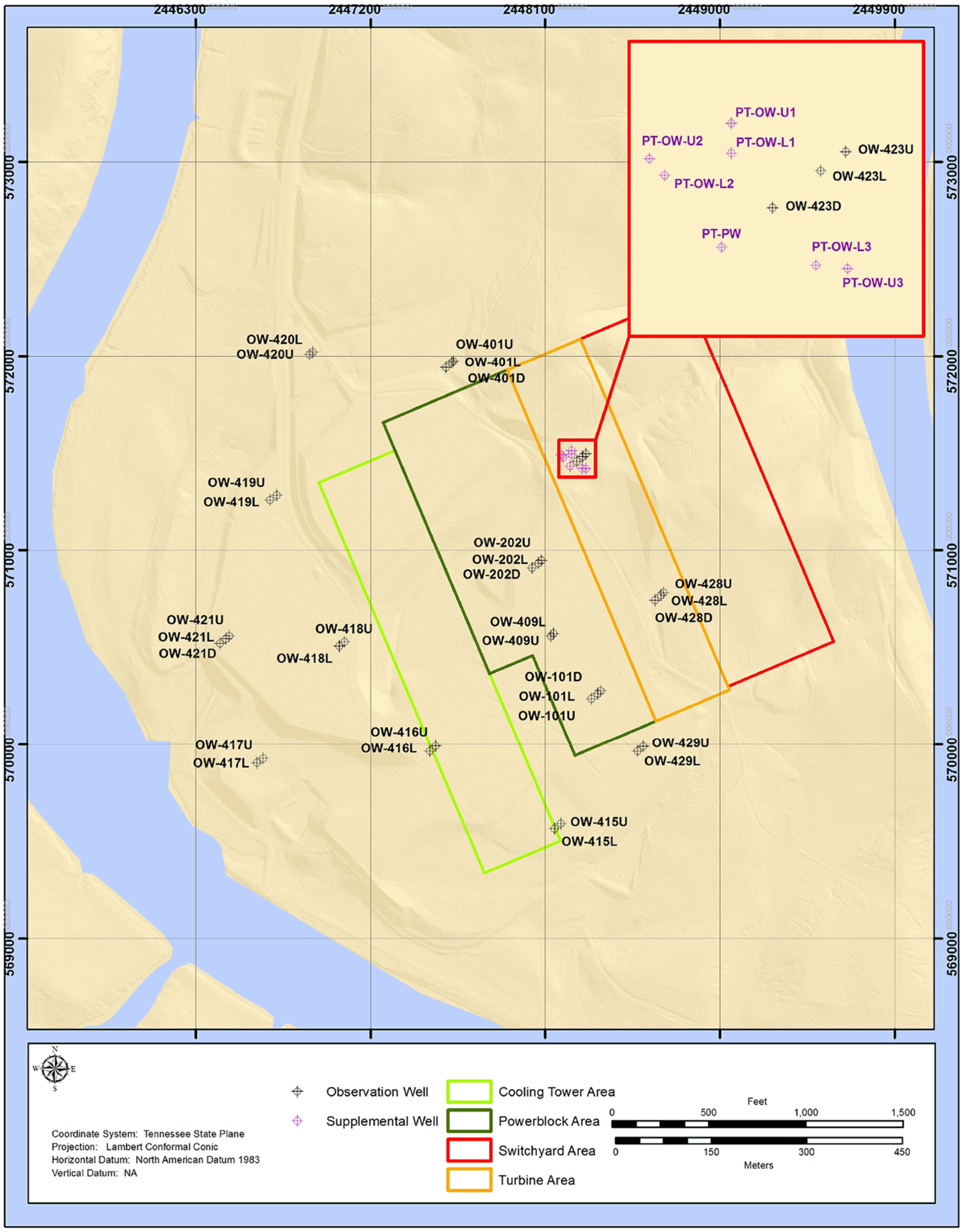

Figure 2.4.12C-4. Location of the Site Observation Wells

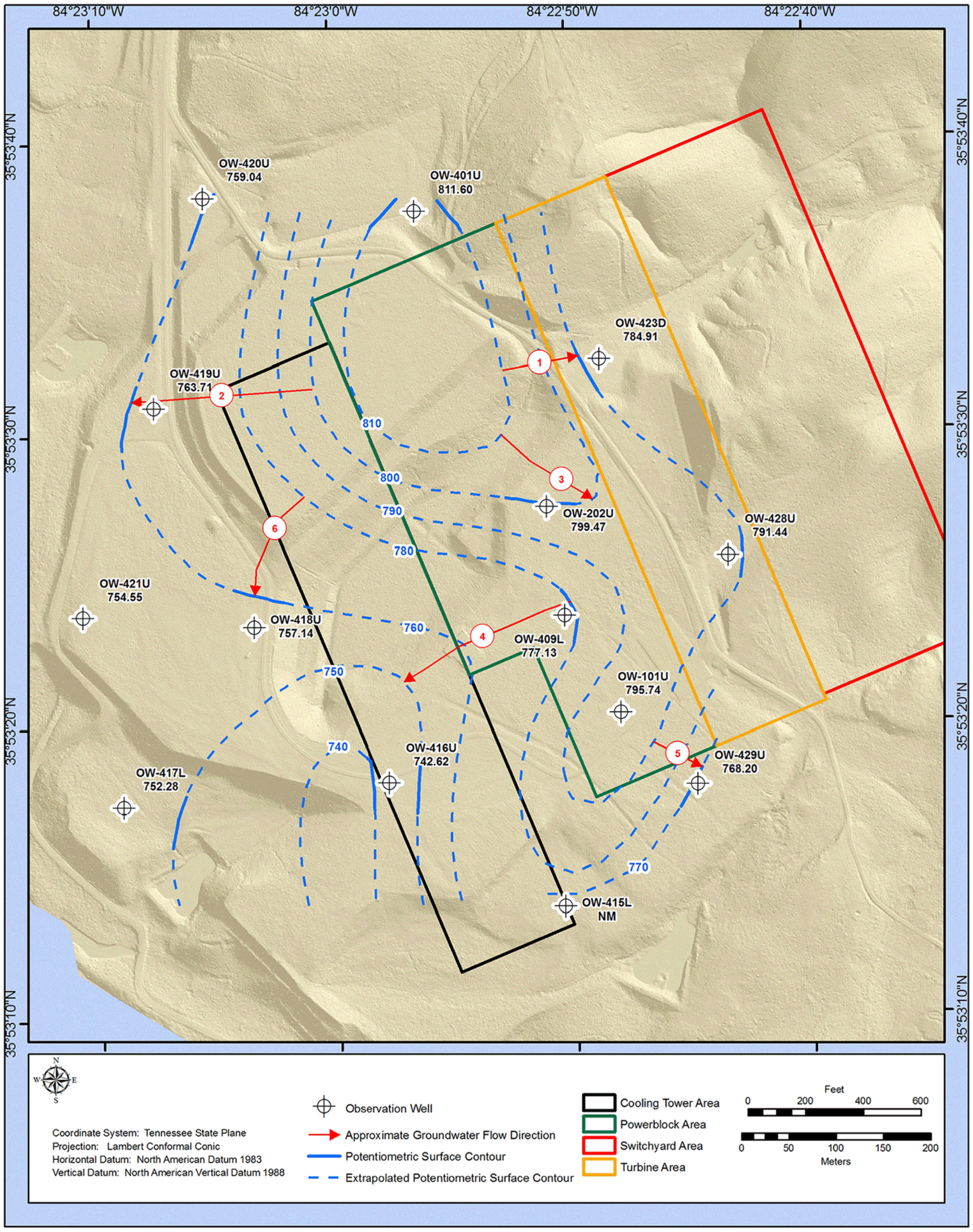

Figure 2.4.12C-5. Maximum Potentiometric Surface Map and Flow Direction for January 13, 2014

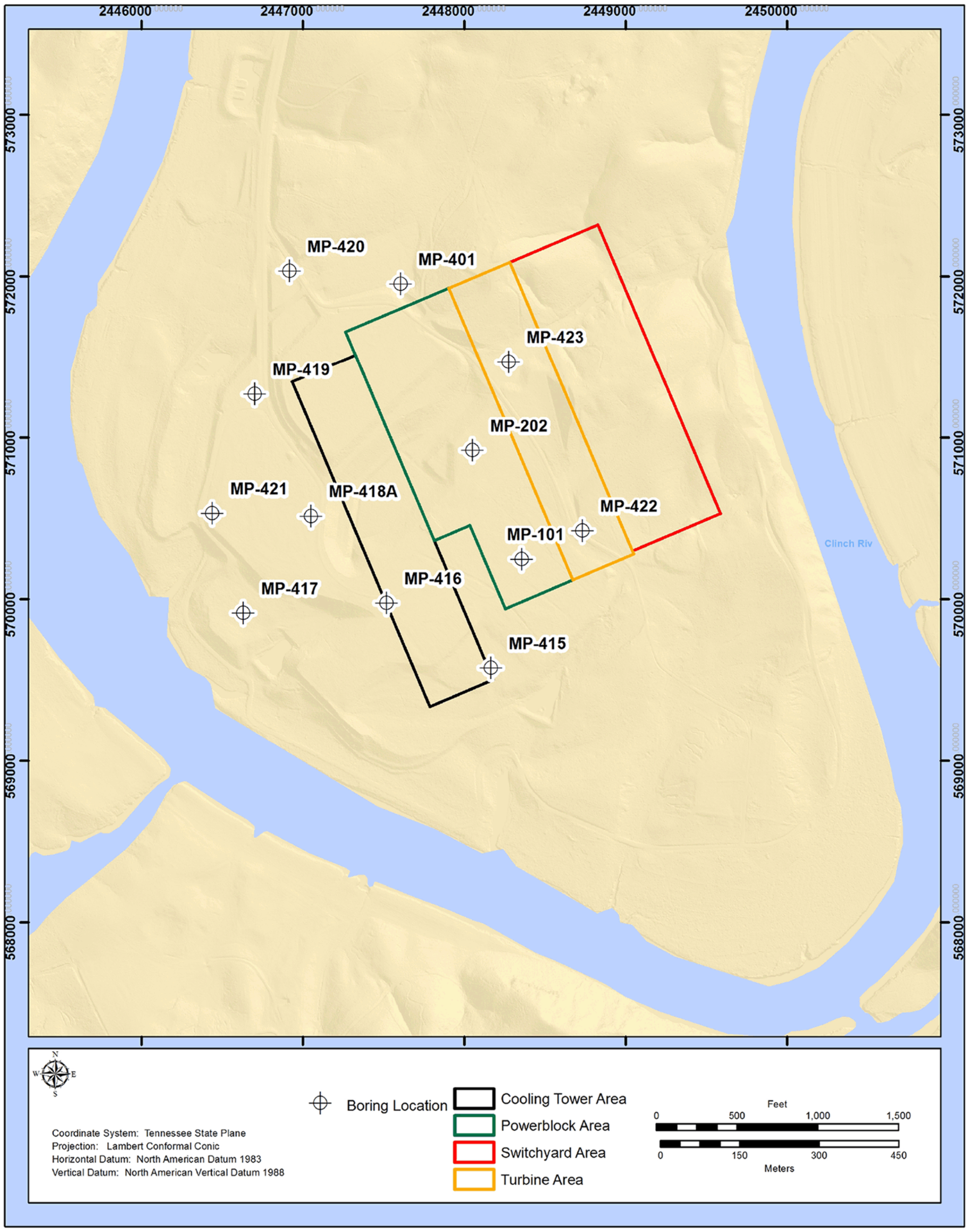

Figure 2.4.12C-6. Packer Test Locations

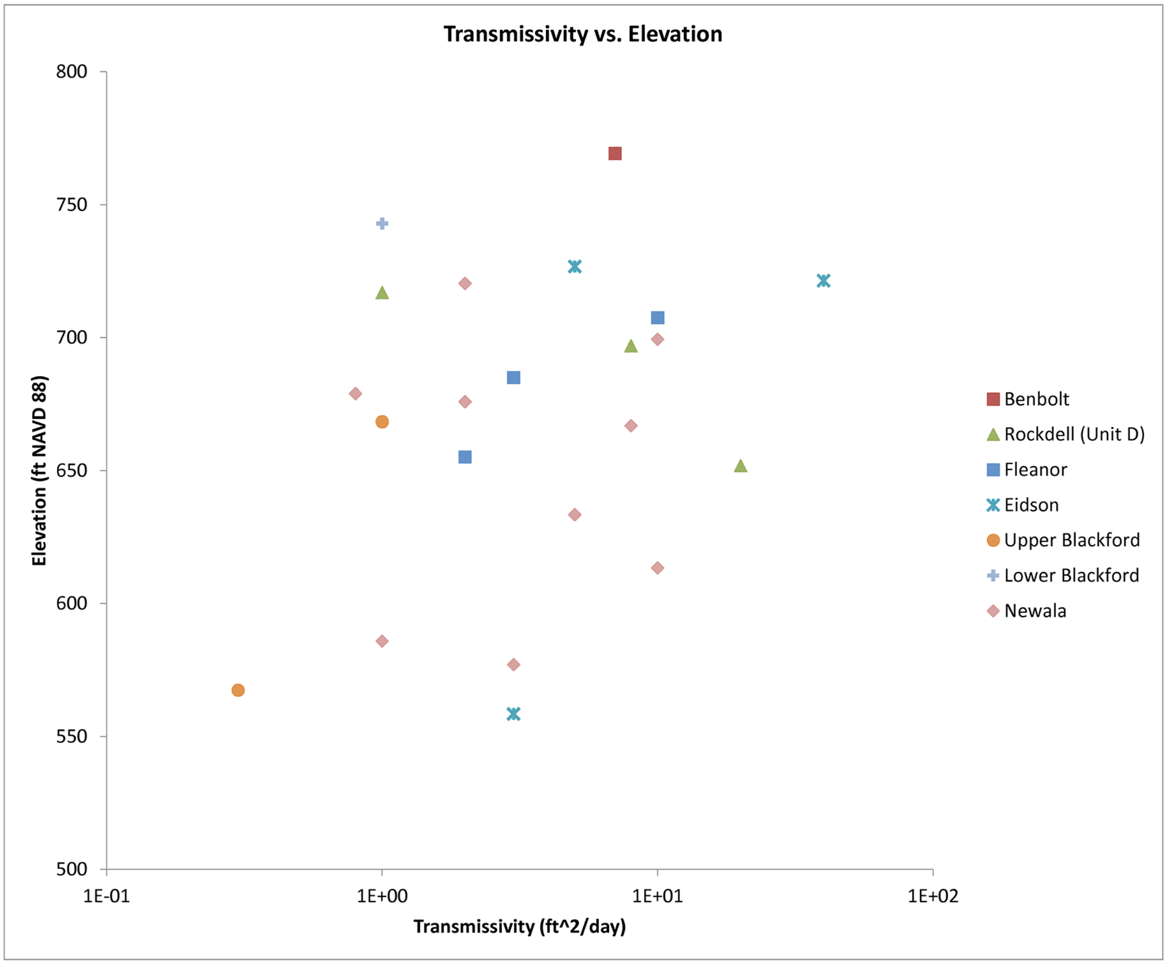

Note: Geologic units as determined from Table B.1.2 of Reference 2.4.12C-1.

Figure 2.4.12C-7. Transmissivity vs. Elevation—Packer Tests

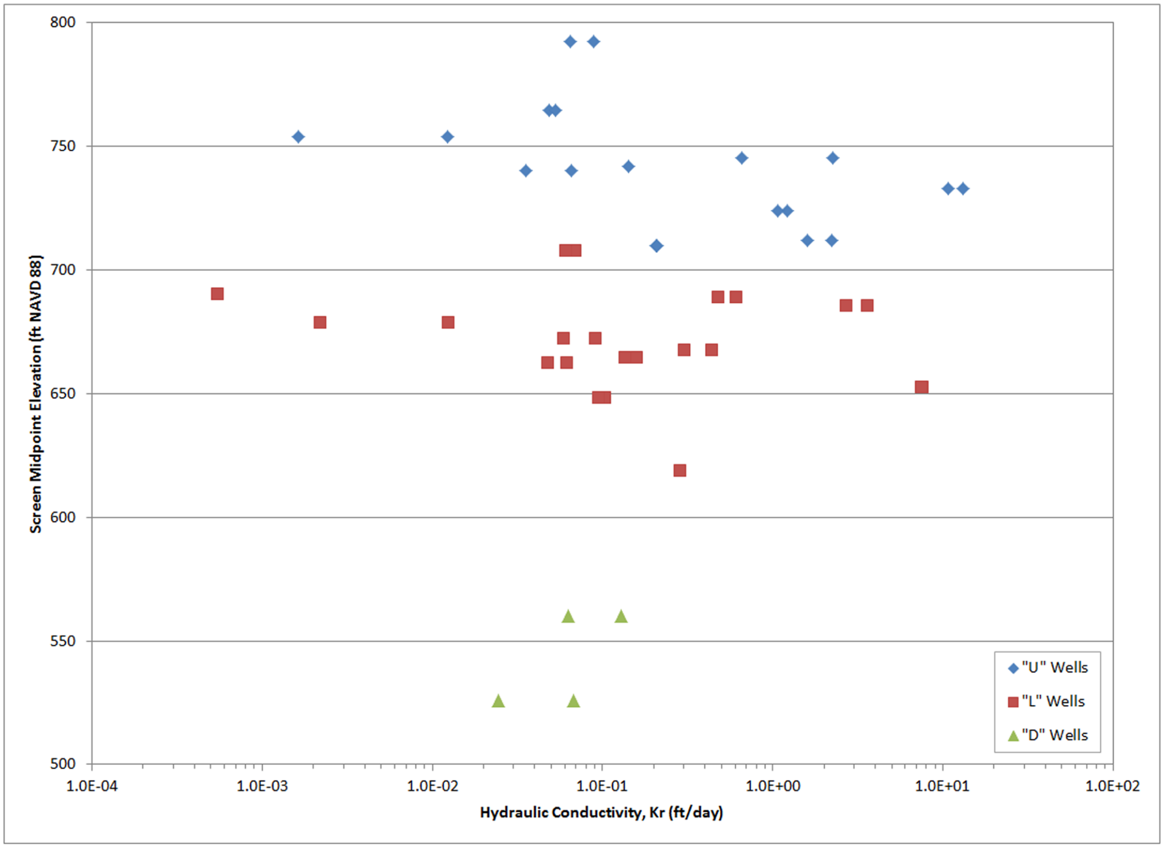

Figure 2.4.12C-8. Hydraulic Conductivity vs. Elevation—Slug Tests

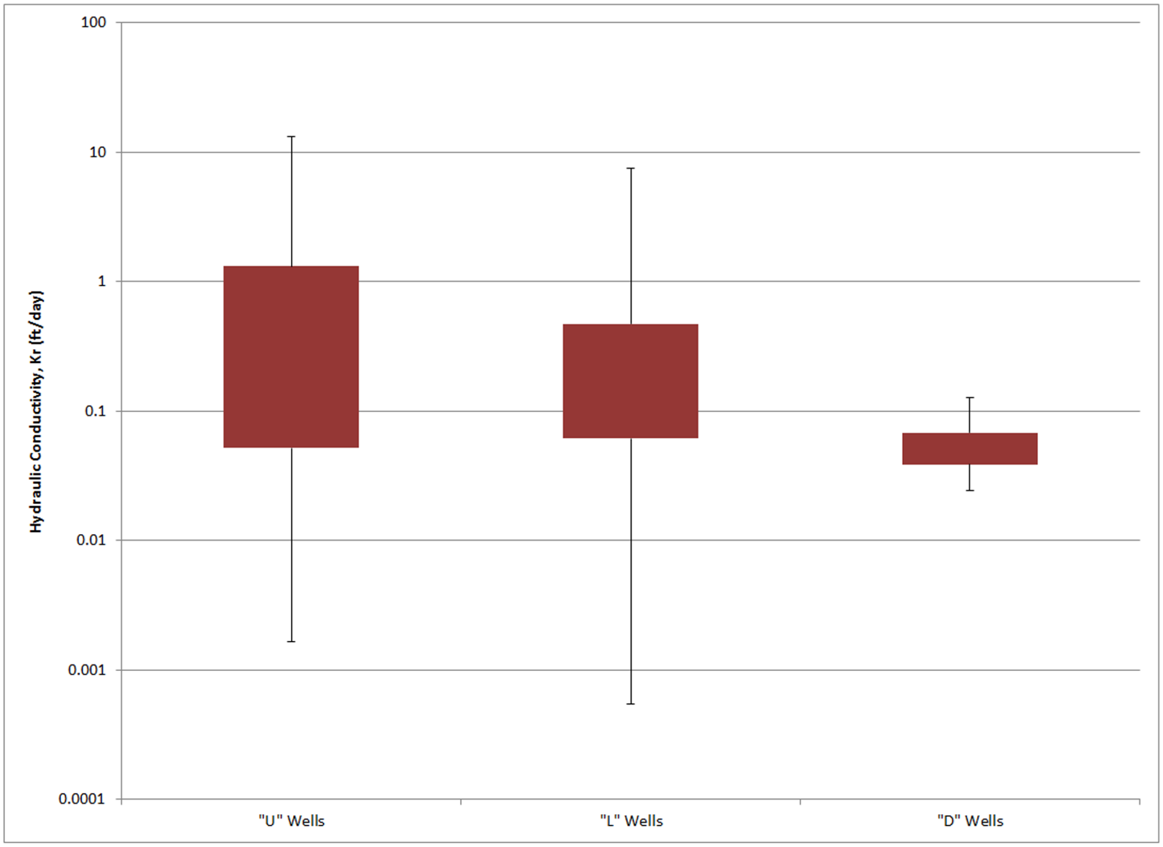

Note: Red bars indicate results within the 25th to 75th percentile; outer lines indicate minimum and maximum estimates.

Figure 2.4.12C-9. Hydraulic Conductivity for U, L, and D Wells—Slug Tests

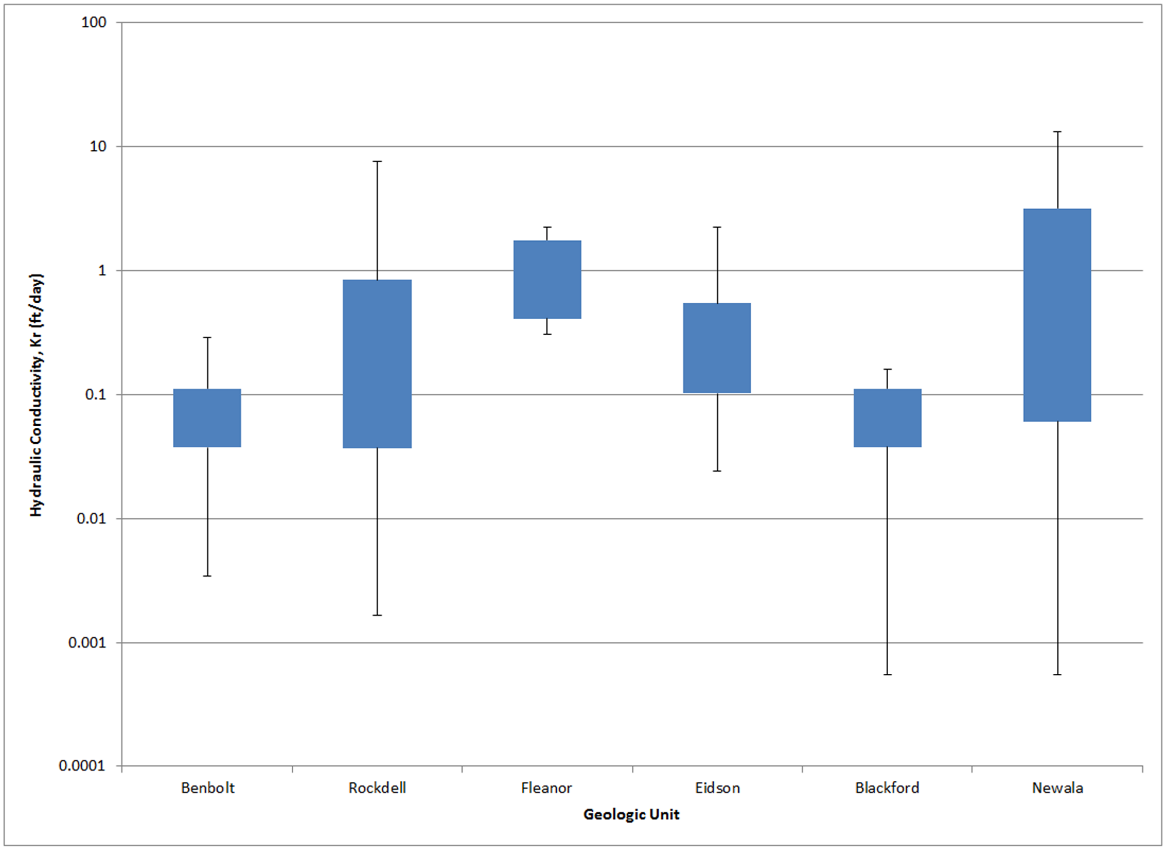

Notes:
Blue bars indicate results within the 25th to 75th percentile; outer lines indicate minimum and maximum estimates; geologic units determined from Table B.1.2 Reference 2.4.12C-1:

- Benbolt – 101U, 415L, 429U (also in contact with Bowen)
- Rockdell – 101D, 101L, 409L, 409U, 416L, 416U, 428L, 428U
- Fleanor – 417L, 417U
- Eidson – 202D, 418U, 423U
- Blackford – 418L, 421U, 421L (also in contact with Newala and included in its statistics), 423D, 423L
- Newala – 401L, 401U, 419L, 419U, 420L, 421L (also in contact with Blackford and included in its statistics)

Figure 2.4.12C-10. Hydraulic Conductivity vs. Geologic Unit—Slug Tests

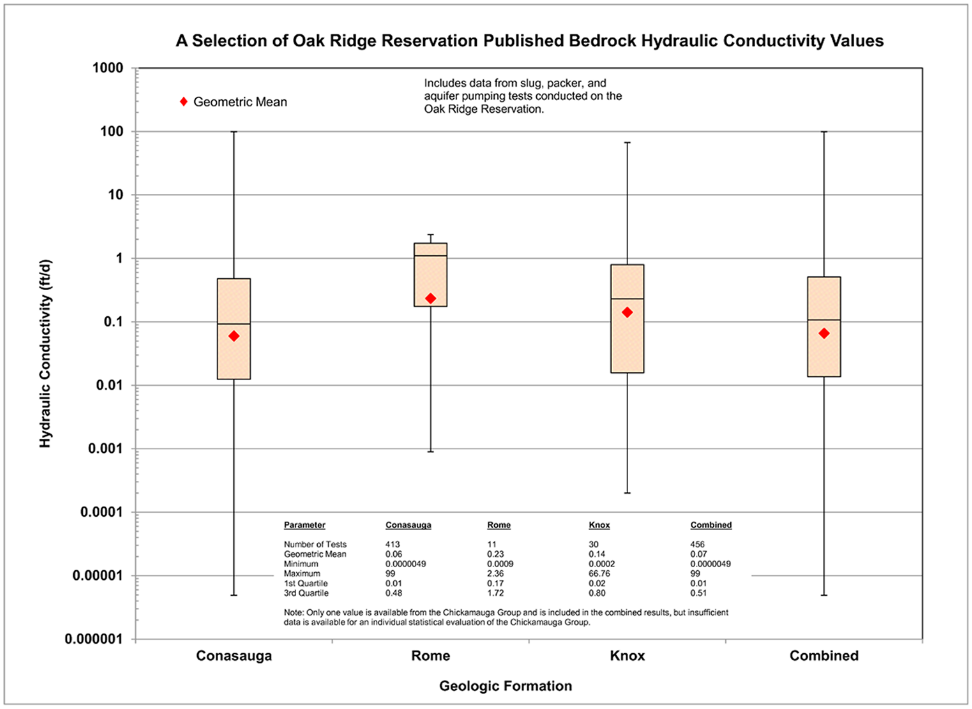

Parameter	Conasauga	Rome	Knox	Combined
Number of Tests	413	11	30	456
Geometric Mean	0.06	0.23	0.14	0.07
Minimum	0.0000049	0.0009	0.0002	0.0000049
Maximum	99	2.36	66.76	99
1st Quartile	0.01	0.17	0.02	0.01
3rd Quartile	0.48	1.72	0.80	0.51

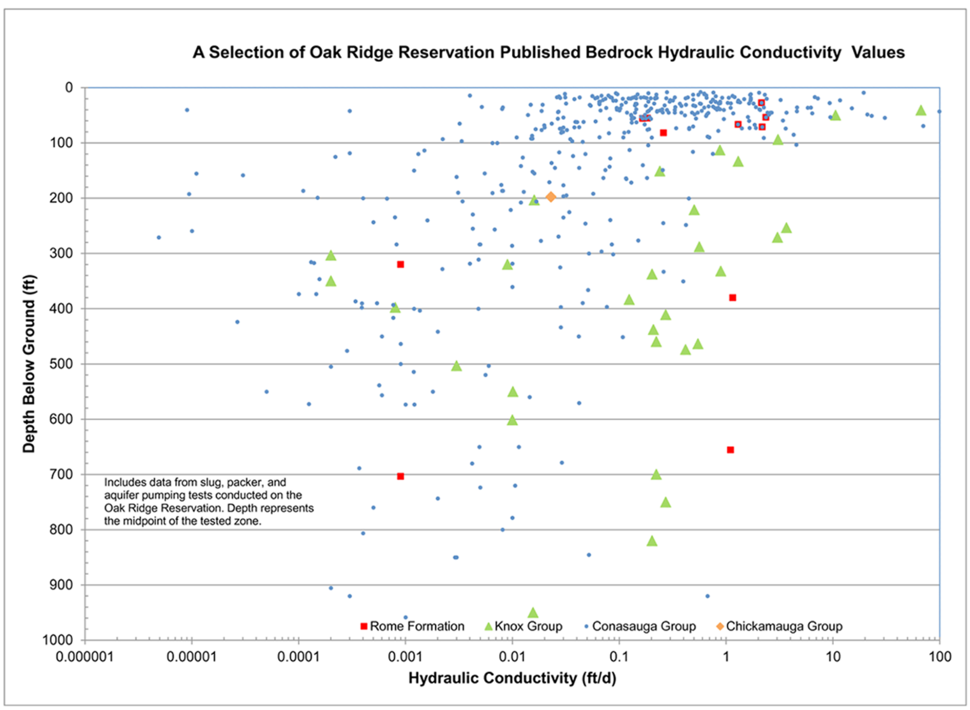

Source: References 2.4.12C-16, 2.4.12C-4, 2.4.12C-7, 2.4.12C-9, 2.4.12C-12, 2.4.12C-21, 2.4.12C-27, 2.4.12C-29, 2.4.12C-30, 2.4.12C-35, 2.4.12C-36, and 2.4.12C-37.

Figure 2.4.12C-11. ORR Historic Bedrock Hydraulic Conductivity Test Data—Literature Information

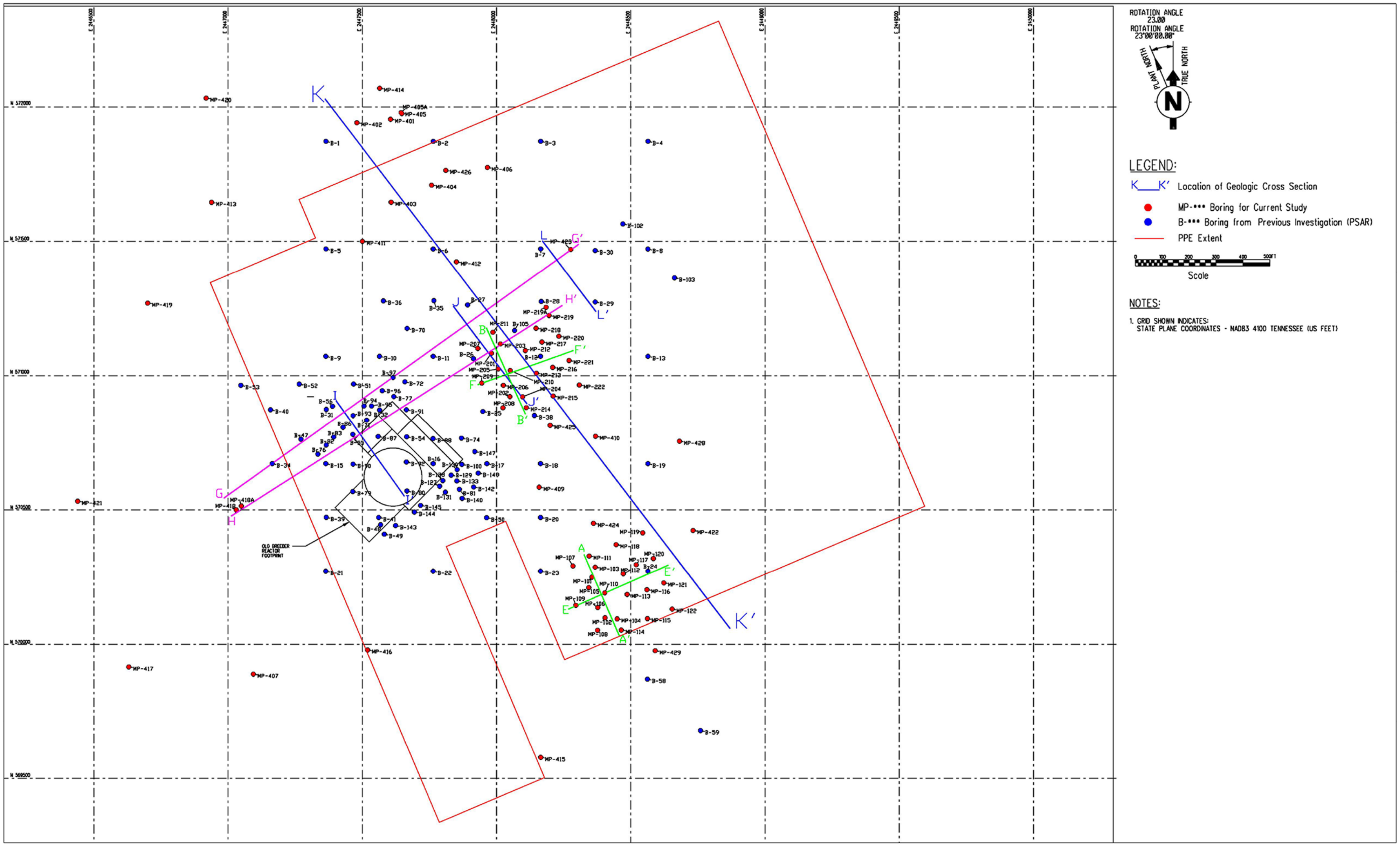

Figure 2.4.12C-12. (Sheet 1 of 11) Geologic Cross-Section Location Plan

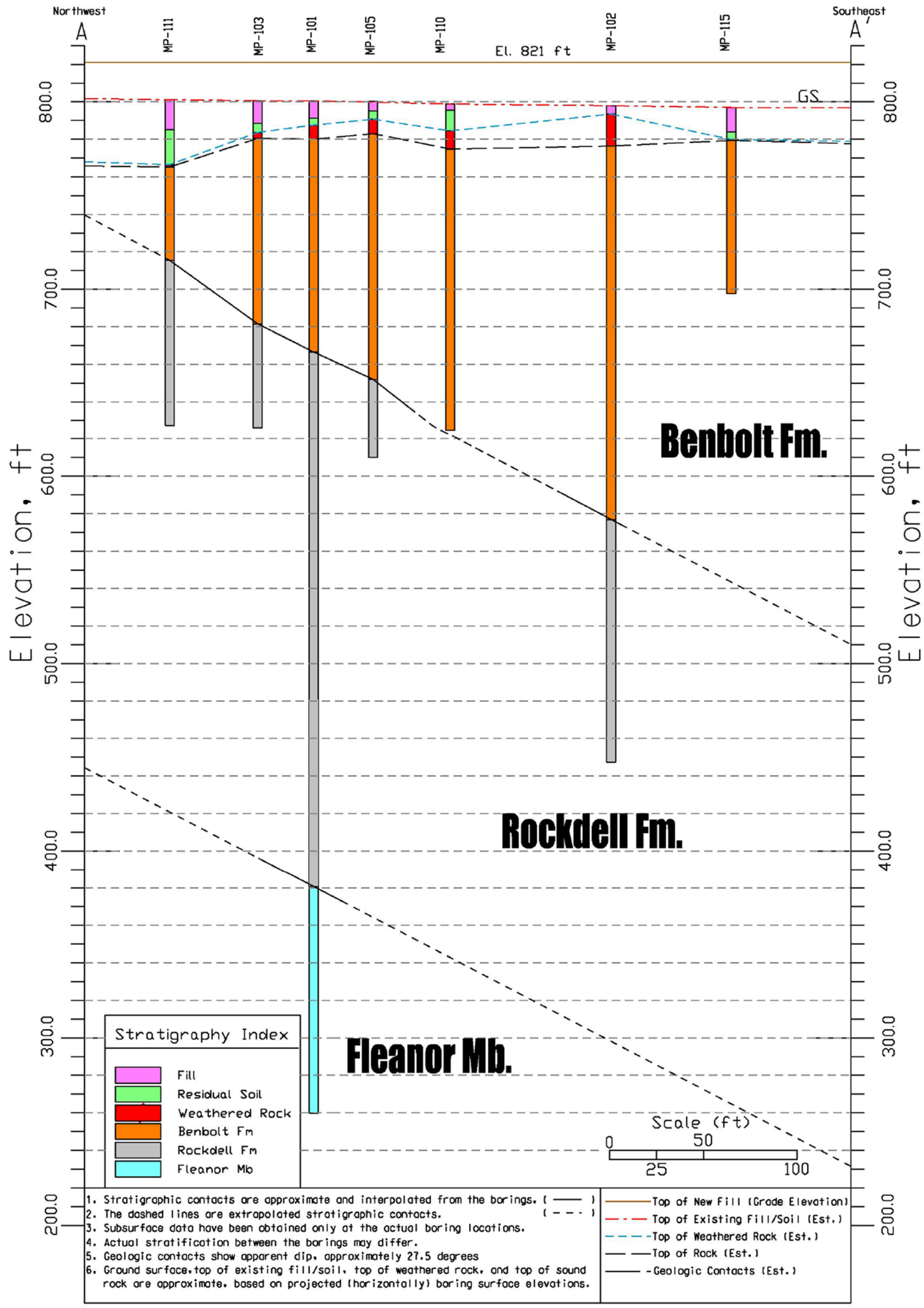

Figure 2.4.12C-12. (Sheet 2 of 11) Geologic Cross-Section A–A'

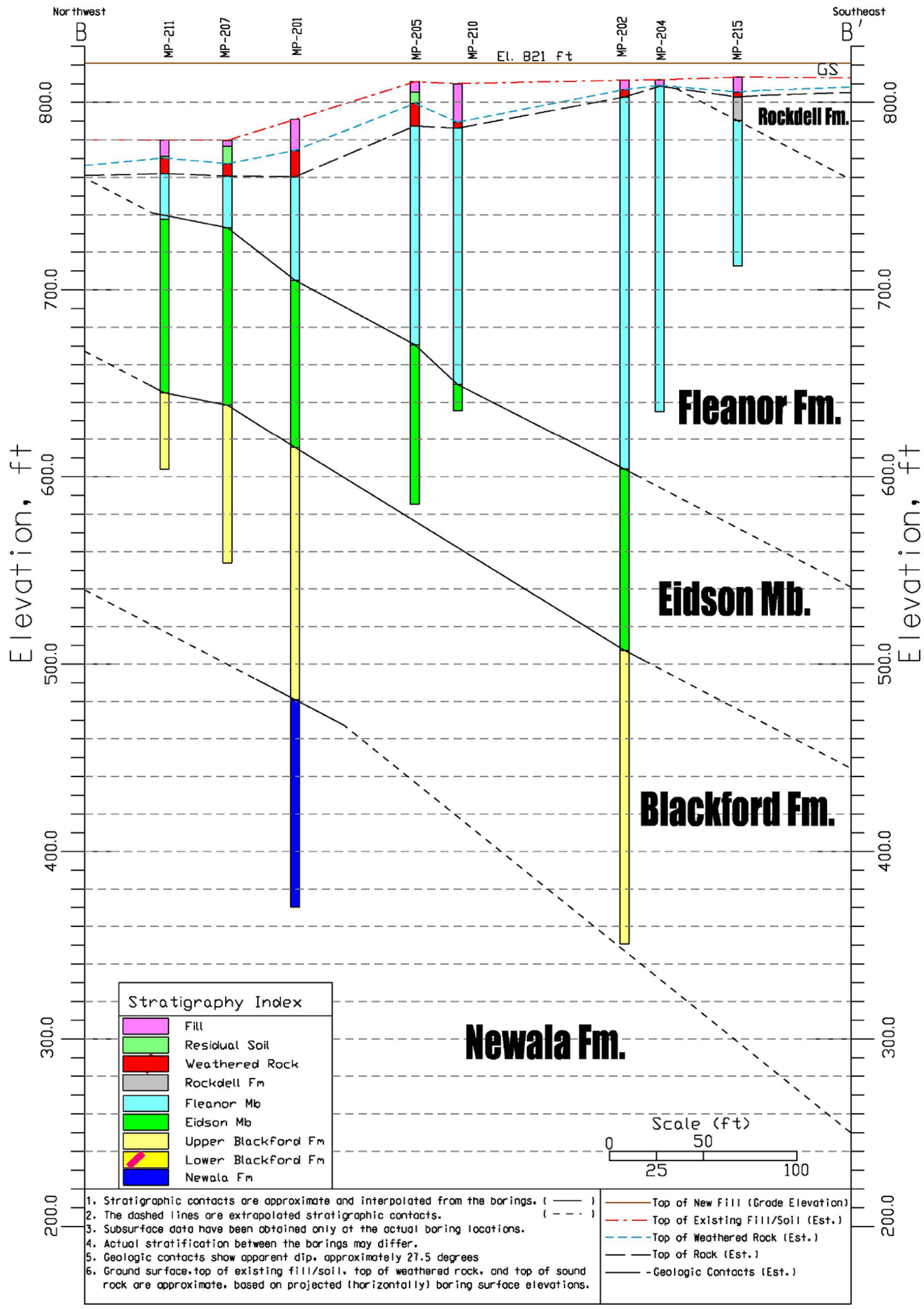

Figure 2.4.12C-12. (Sheet 3 of 11) Geologic Cross-Section B–B'

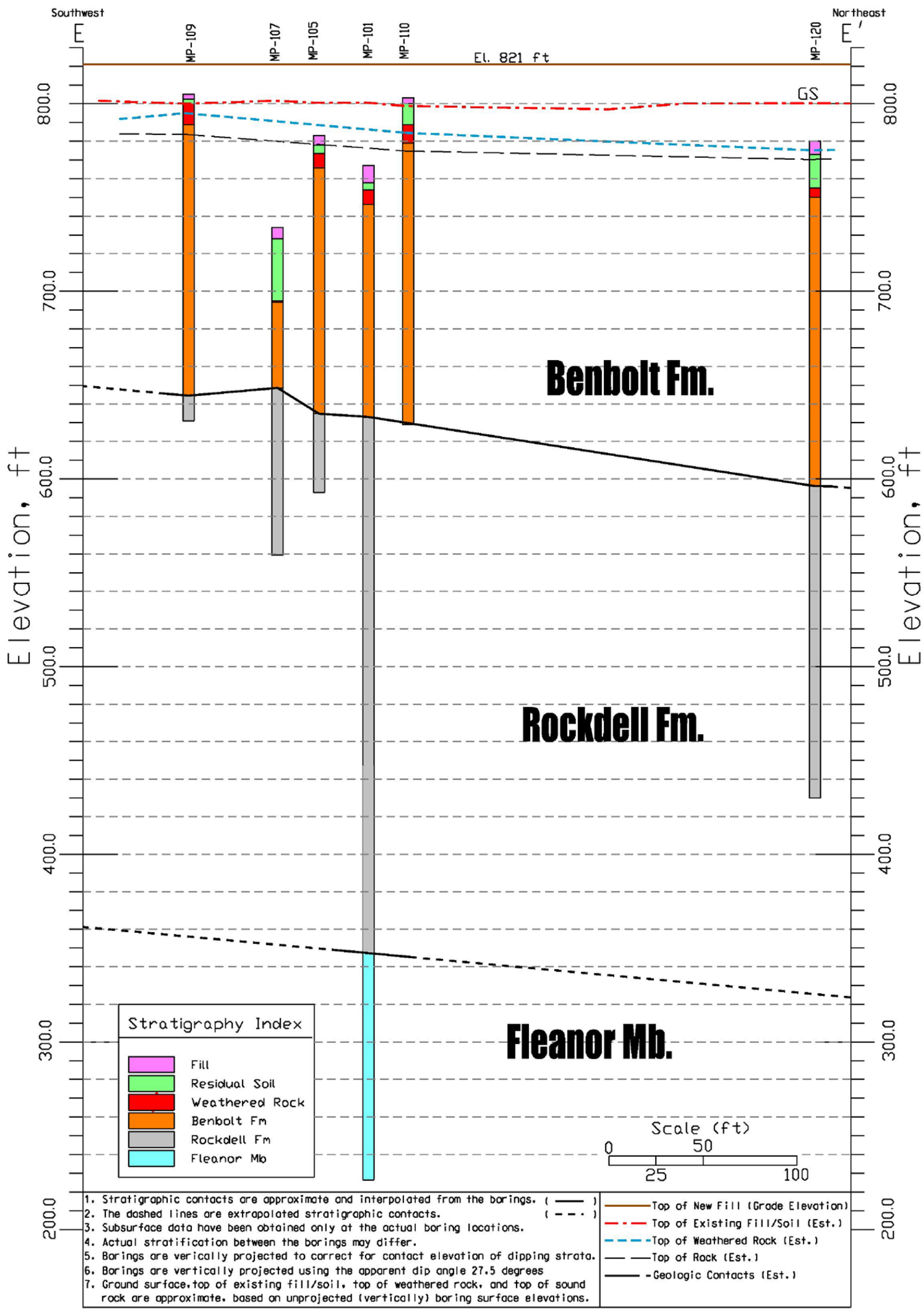

Figure 2.4.12C-12. (Sheet 4 of 11) Geologic Cross-Section E–E'

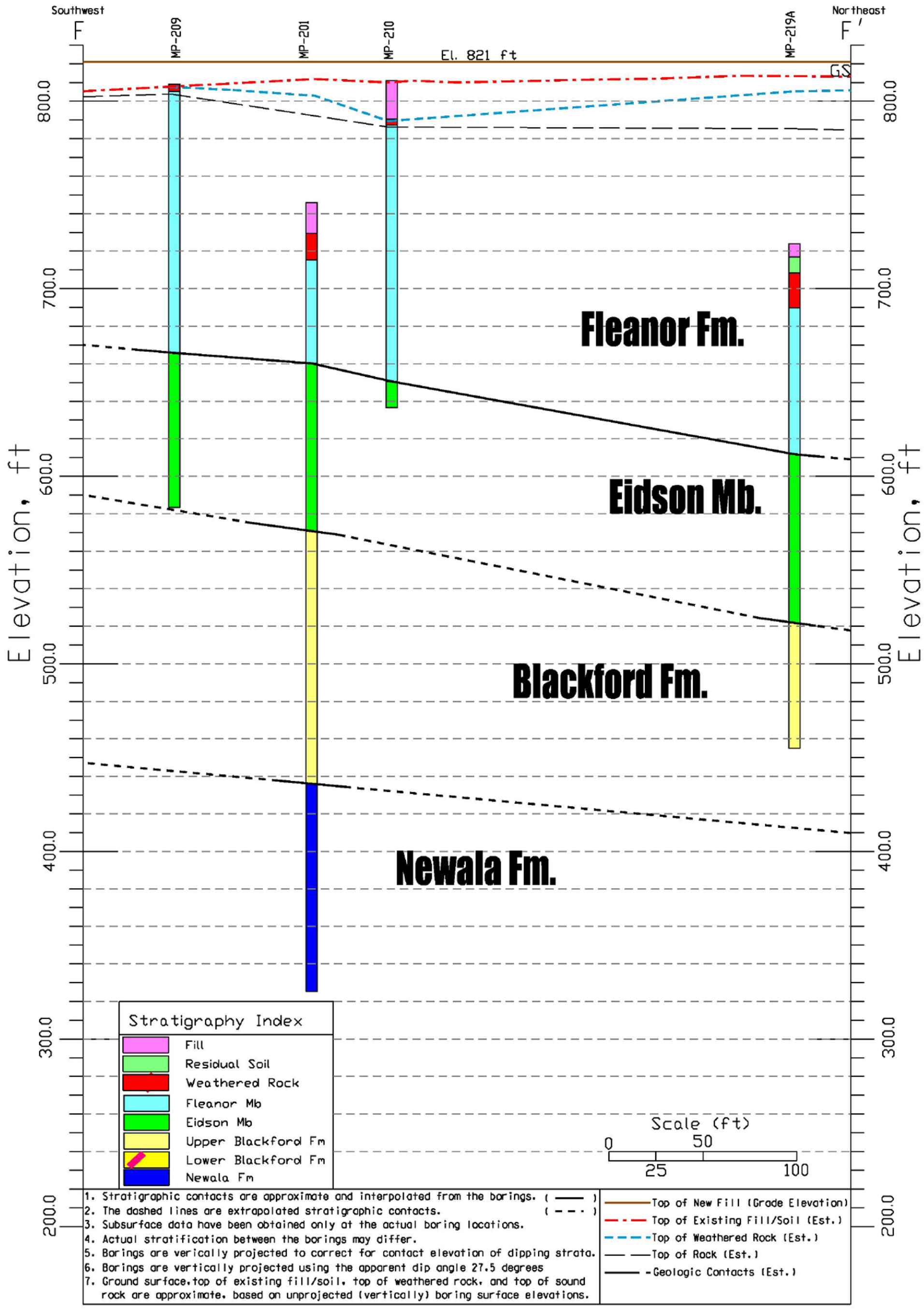

Figure 2.4.12C-12. (Sheet 5 of 11) Geologic Cross-Section F–F'

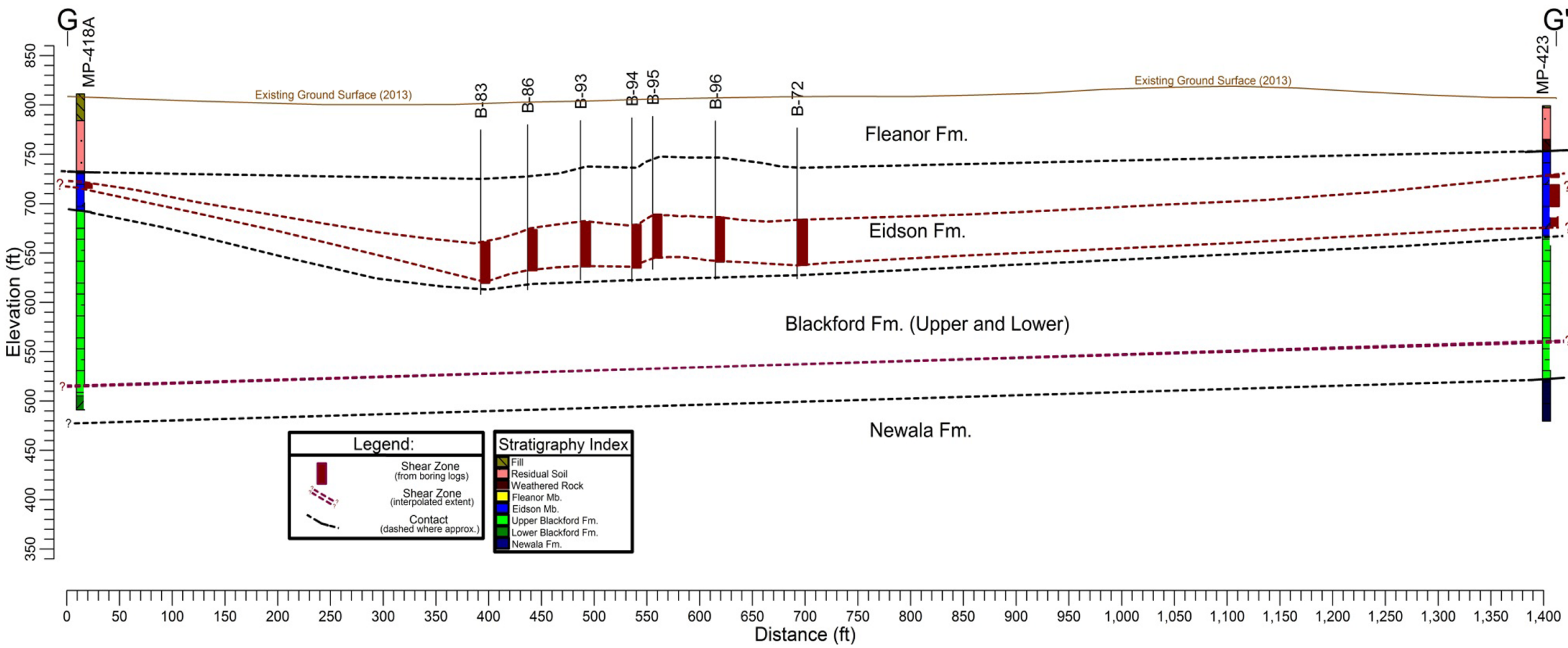

Figure 2.4.12C-12. (Sheet 6 of 11) Geologic Cross-Section G–G' (Shear Zone)

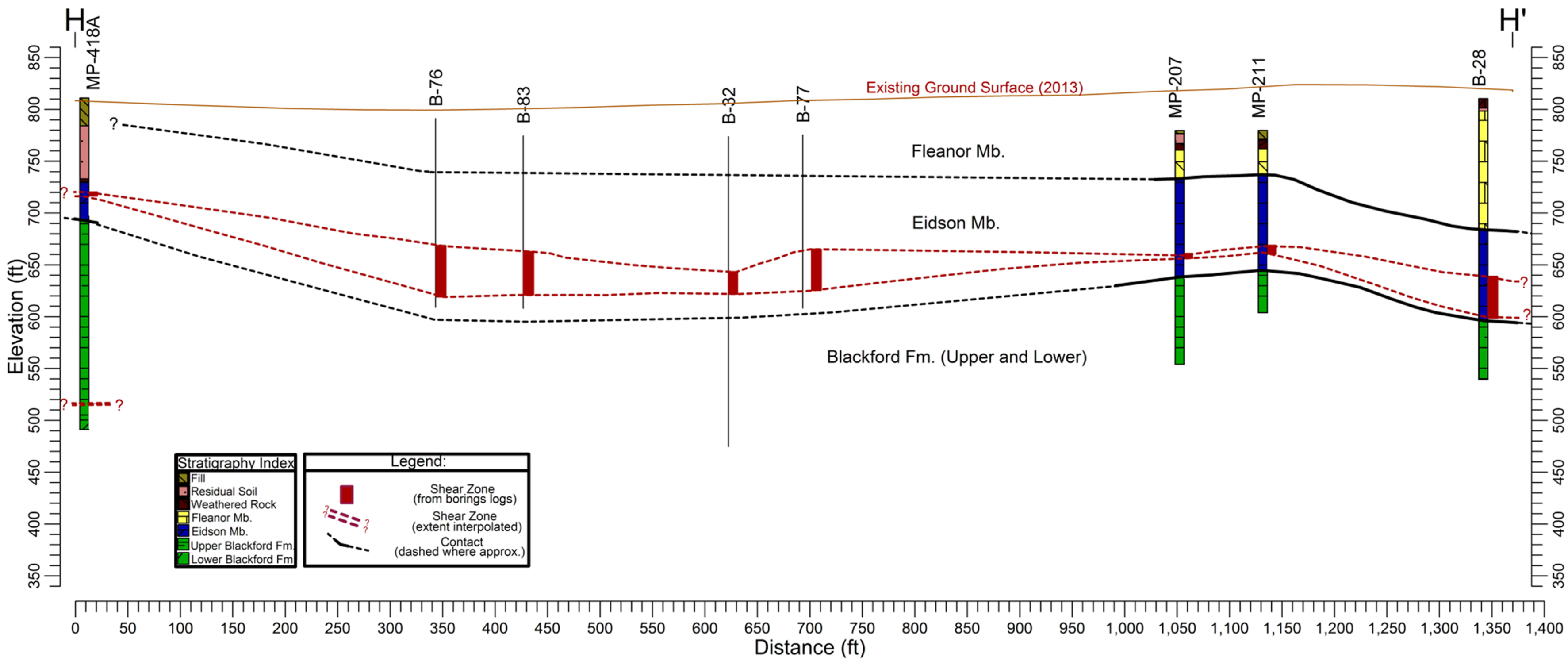

Figure 2.4.12C-12. (Sheet 7 of 11) Geologic Cross-Section H–H' (Shear Zone)

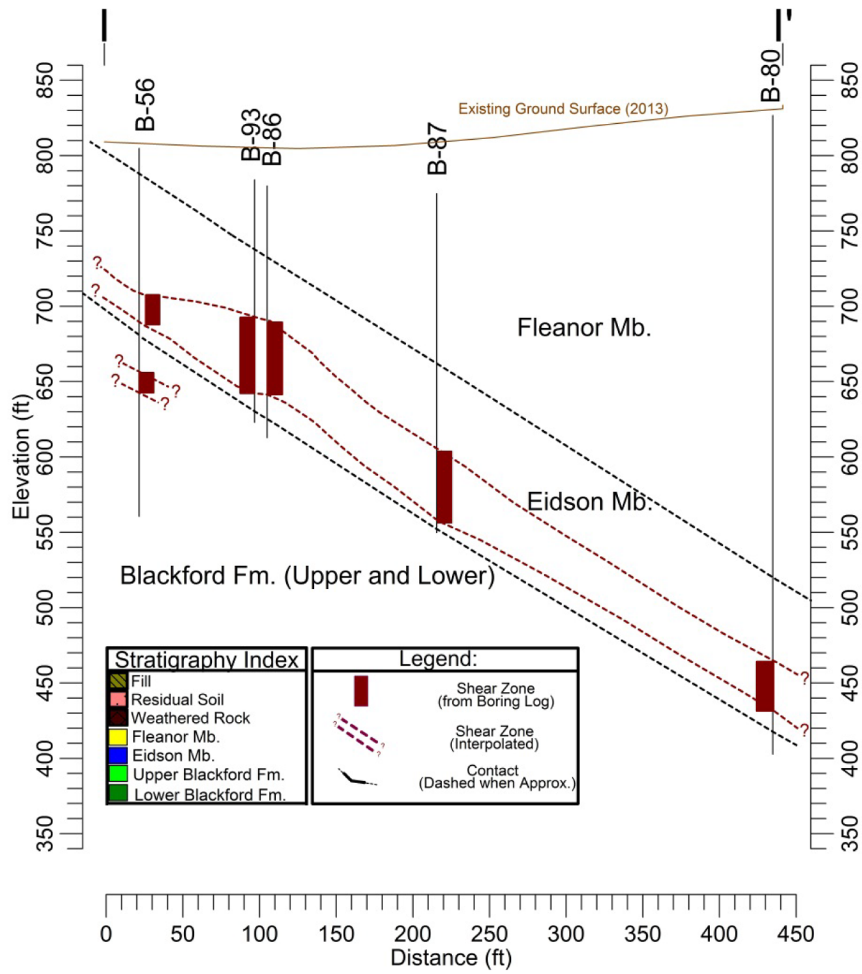

Figure 2.4.12C-12. (Sheet 8 of 11) Geologic Cross-Section I–I' (Shear Zone)

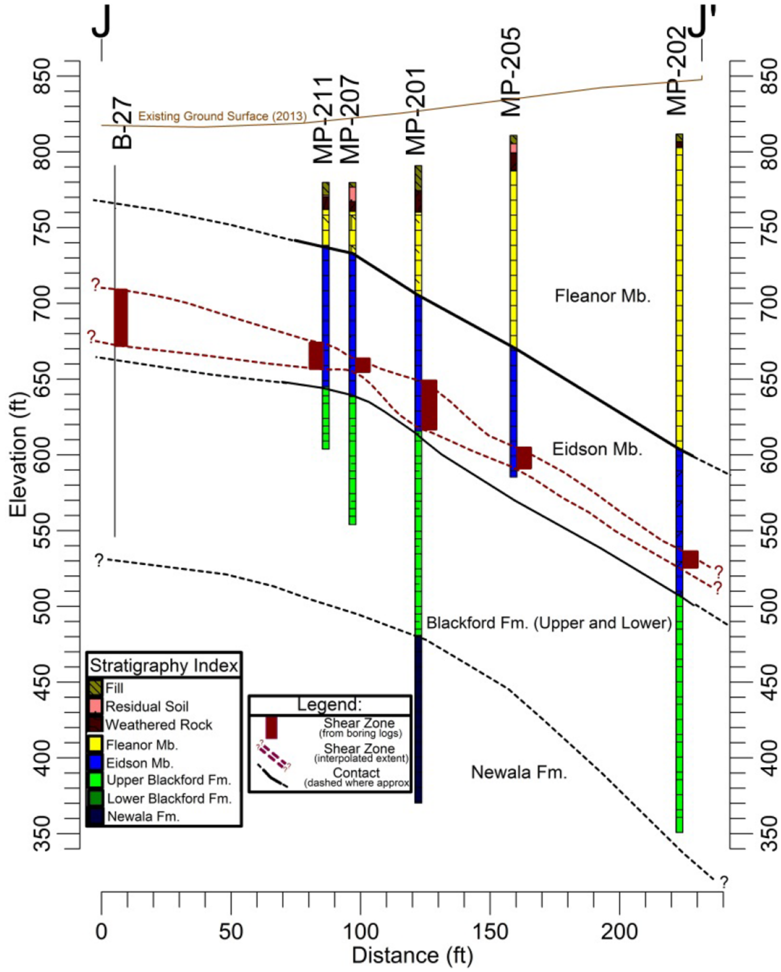

Figure 2.4.12C-12. (Sheet 9 of 11) Geologic Cross-Section J–J' (Shear Zone)

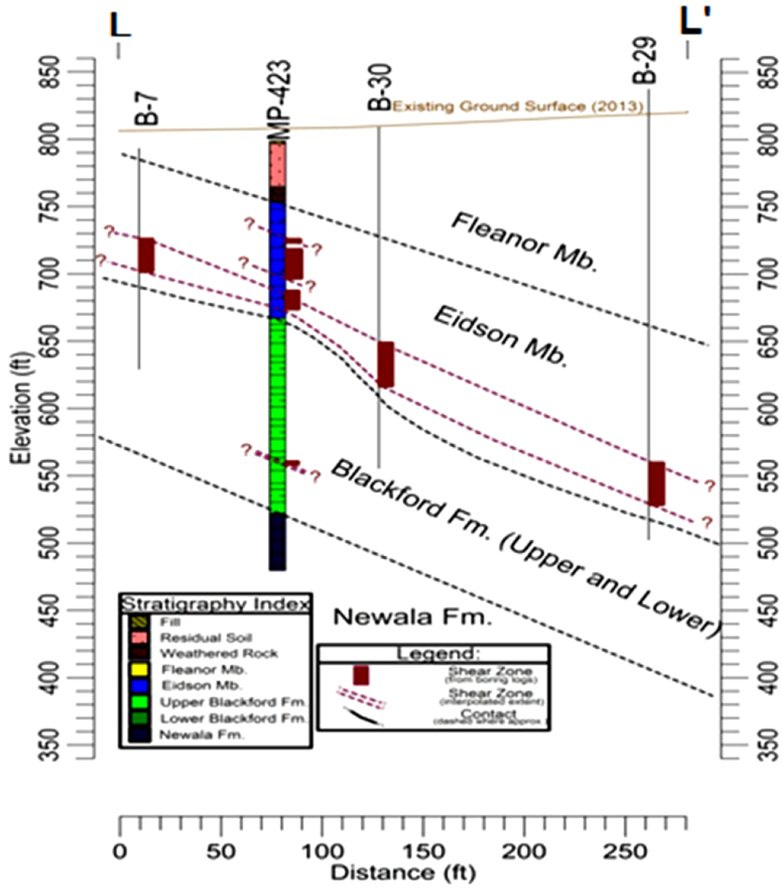

Figure 2.4.12C-12. (Sheet 10 of 11) Geologic Cross-Section L–L' (Shear Zone)

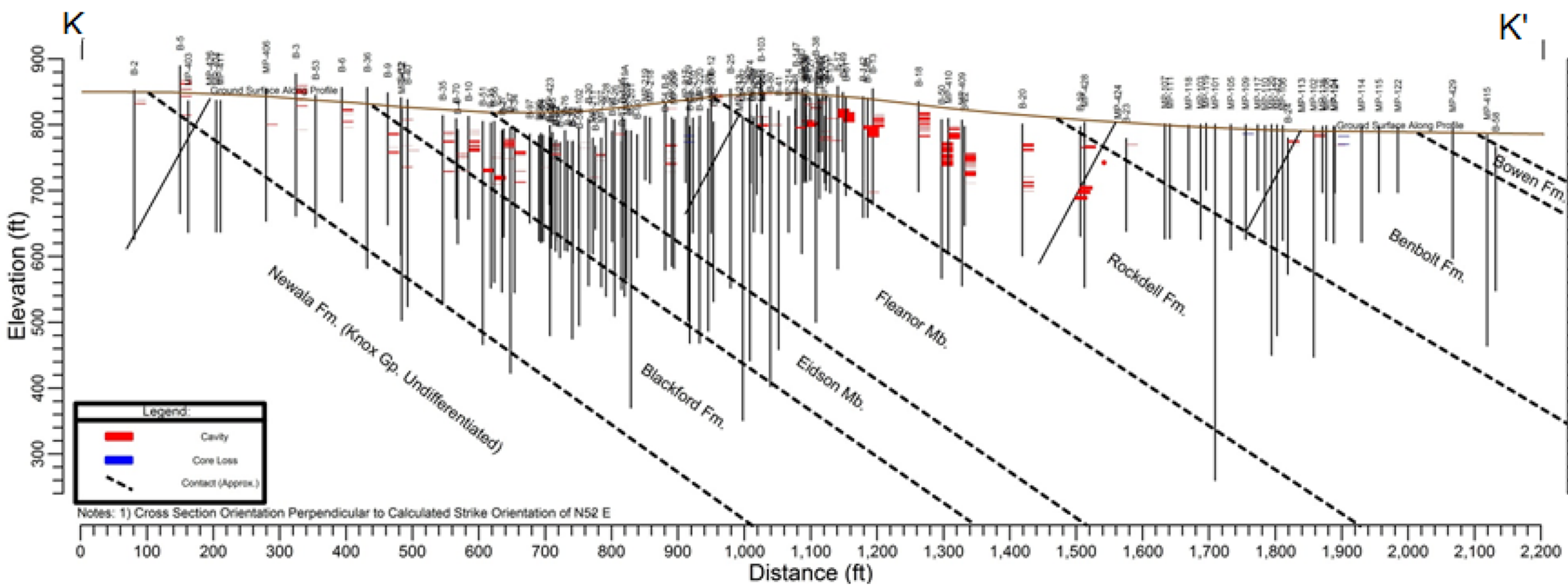

Figure 2.4.12C-12. (Sheet 11 of 11) Geologic Cross-Section K–K' (Karst Cavities)

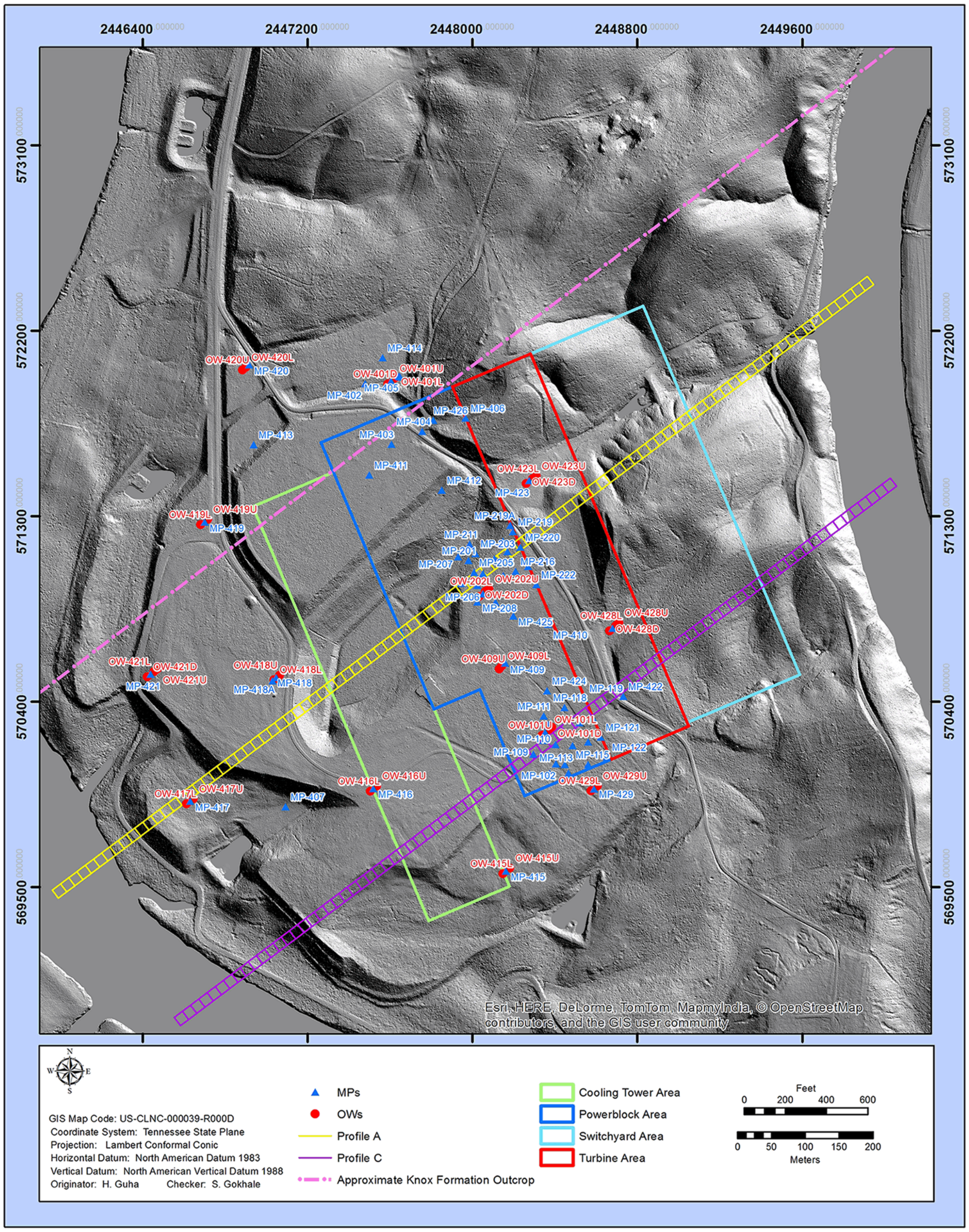

Figure 2.4.12C-13. Plan View of the Profile Model with Grids

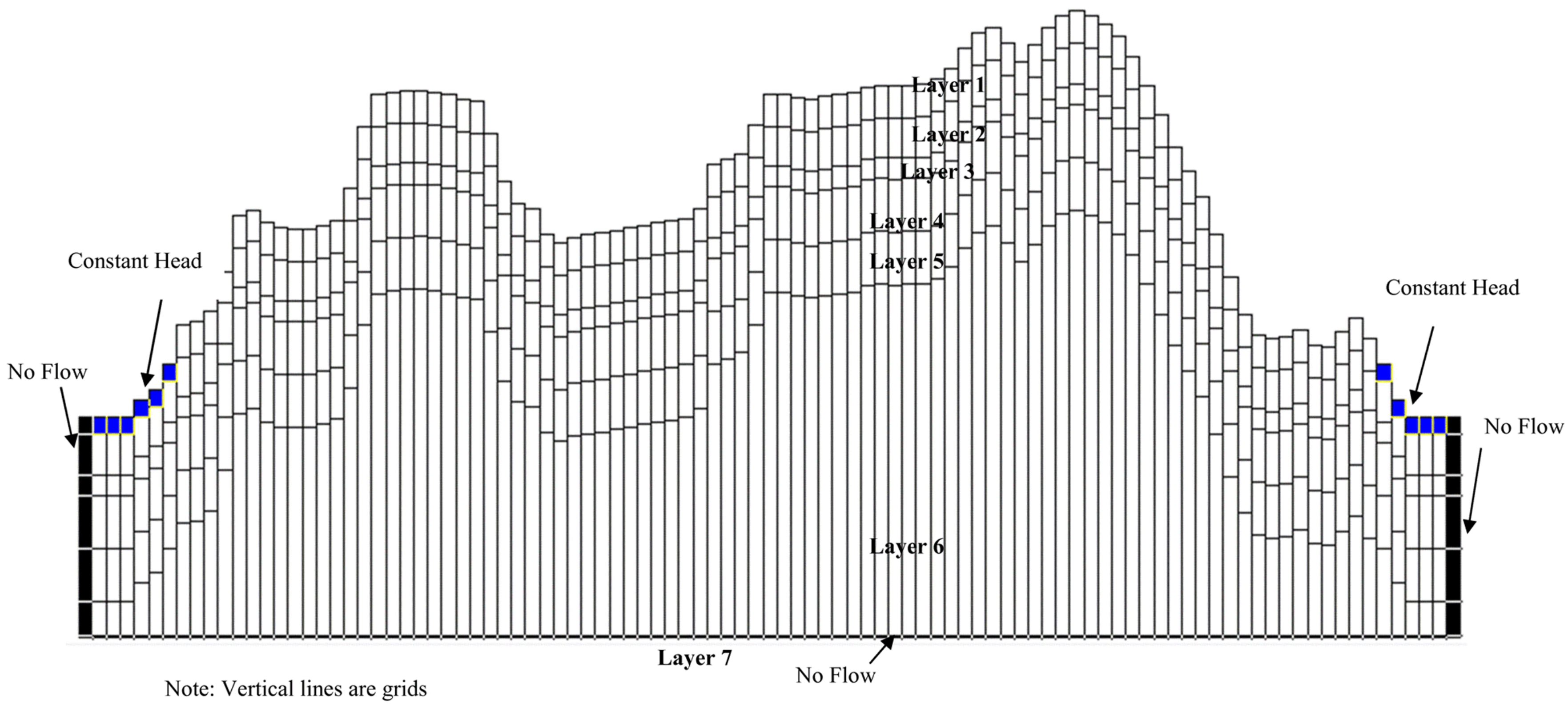

Figure 2.4.12C-14. Boundary Conditions Along Profile A

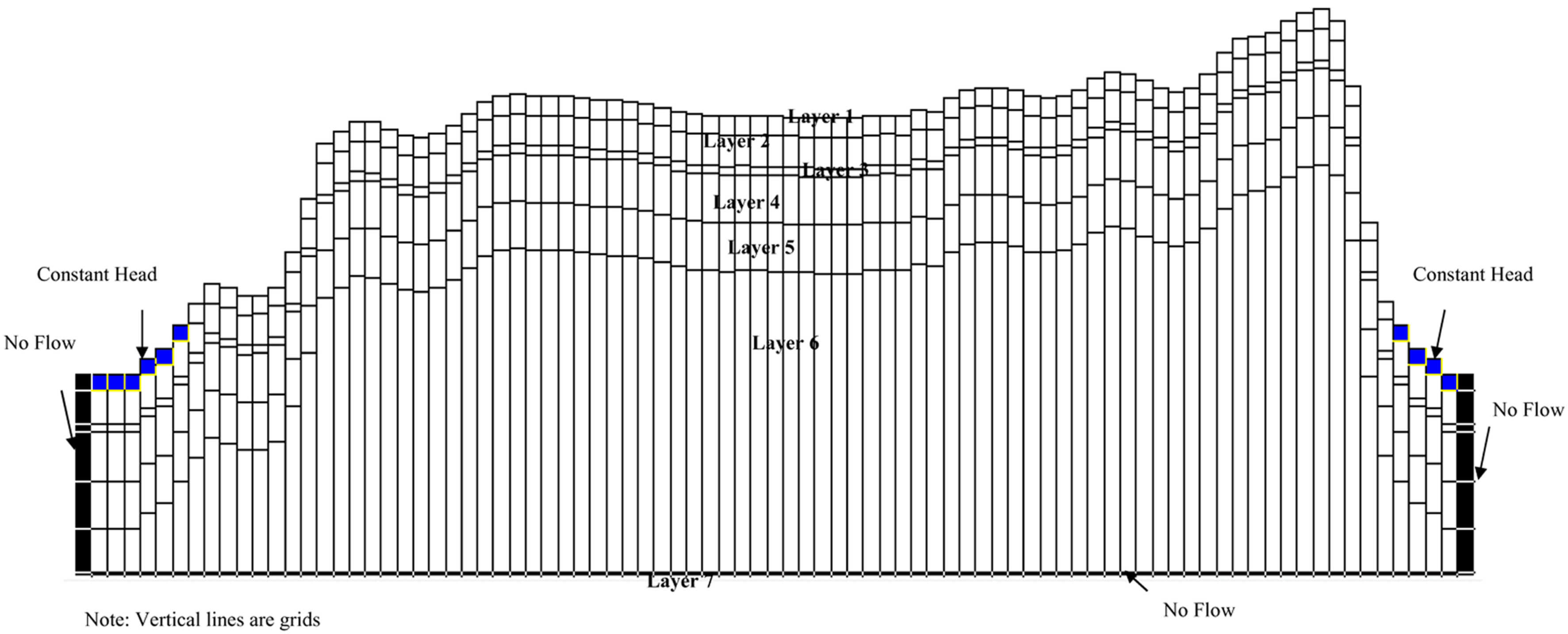

Figure 2.4.12C-15. Boundary Conditions Along Profile C

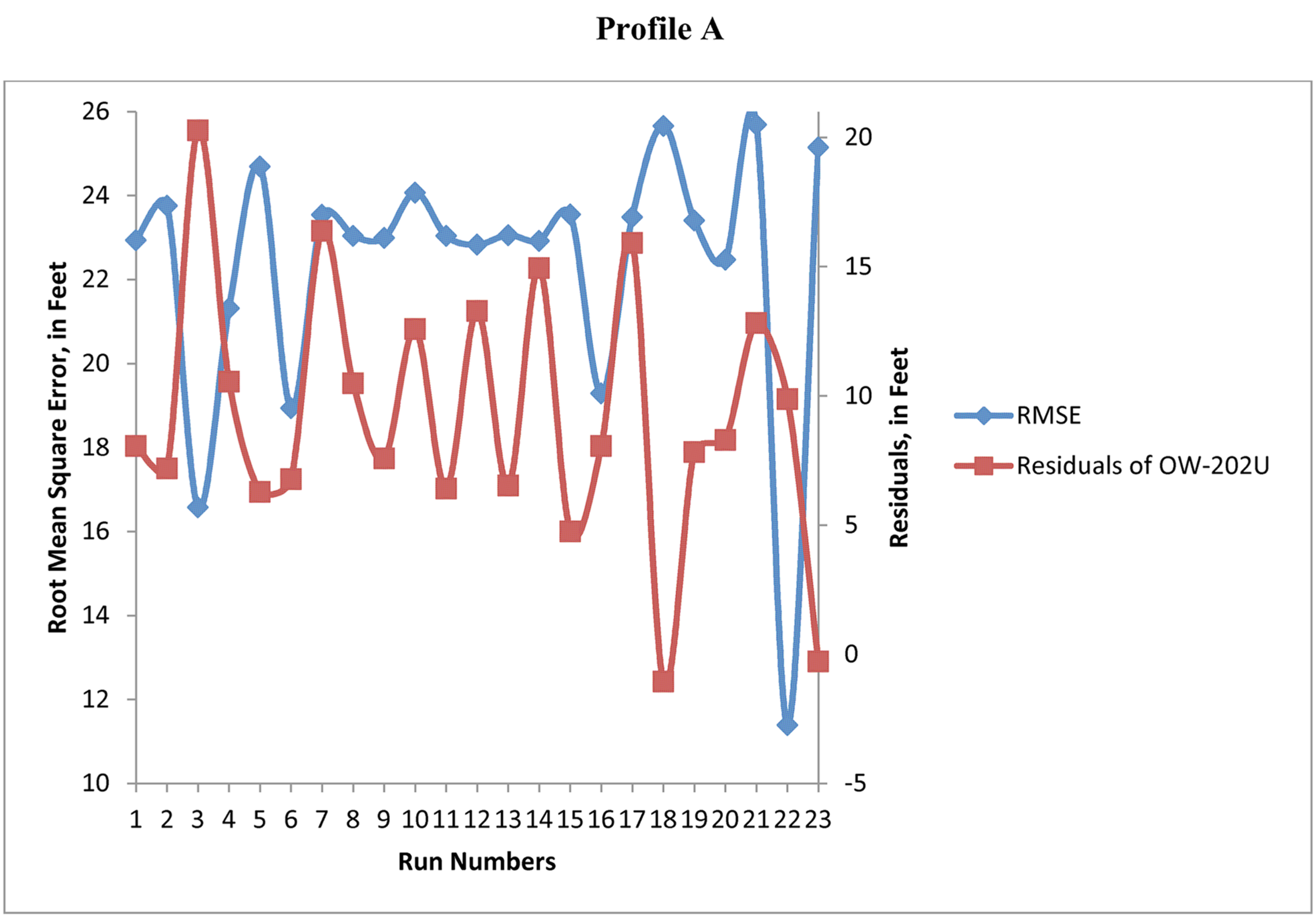

Note: The description of the model runs are provided in Table 2.4.12C-7.

Figure 2.4.12C-16. Sensitivity of the Profile A Model to Adjustment of Different Parameters

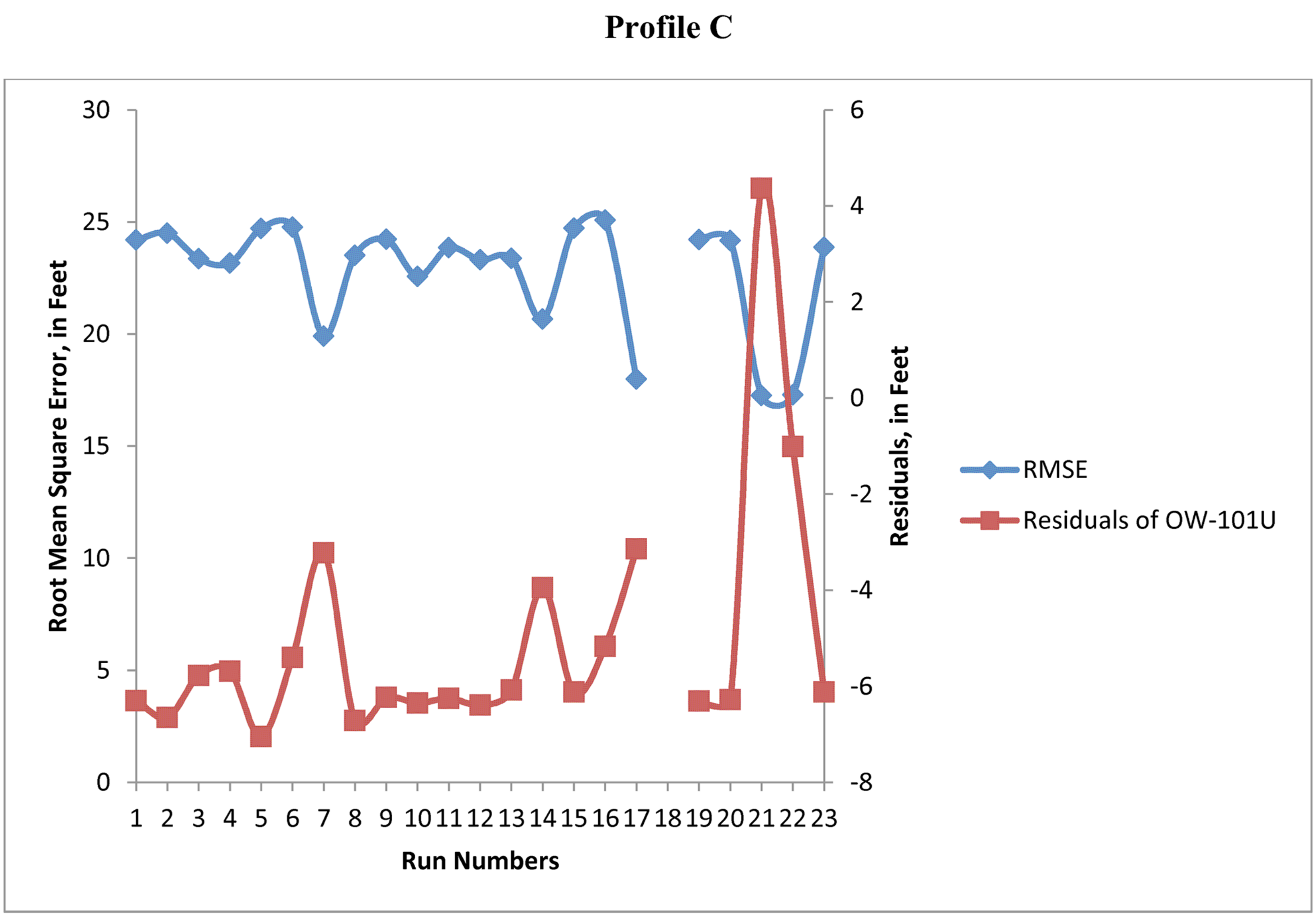

Note: The description of the model runs are provided in Table 2.4.12C-7.

Figure 2.4.12C-17. Sensitivity of the Profile C Model to Adjustment of Different Parameters

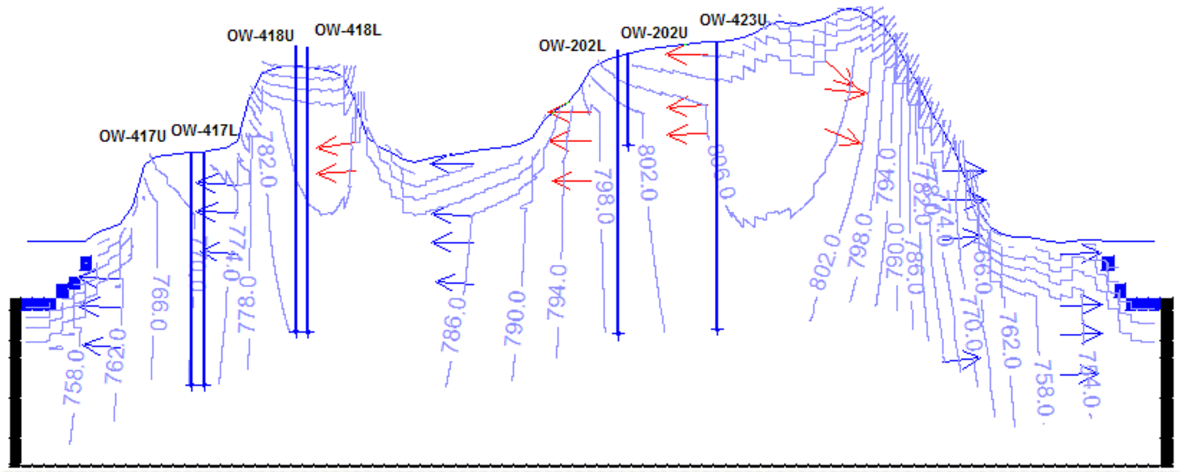

Note: Red arrow indicates downward groundwater flow directions and blue arrow upward groundwater flow directions.

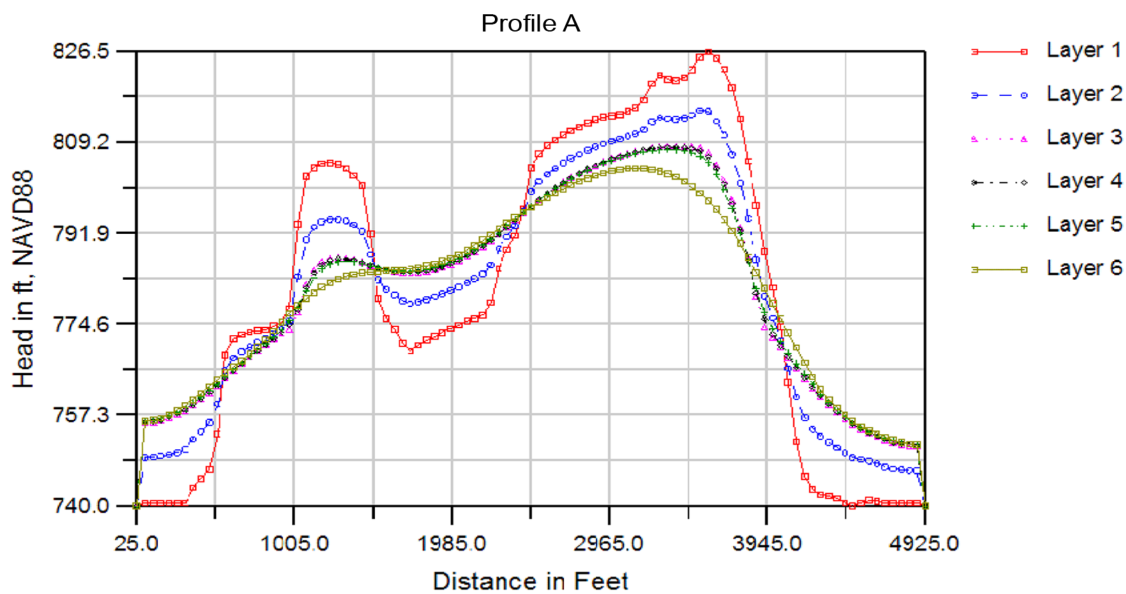

Figure 2.4.12C-18. Profile A—Run 18 a) Groundwater Heads and Flow Directions and b) Groundwater Heads Within Layers

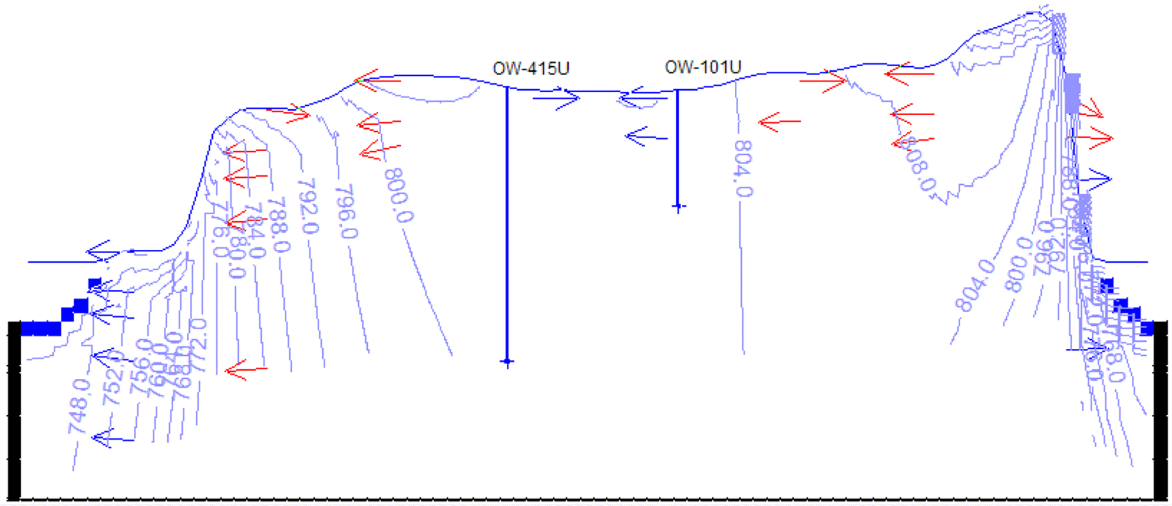

Note: Red arrow indicates downward groundwater flow directions and blue arrow upward groundwater flow directions.

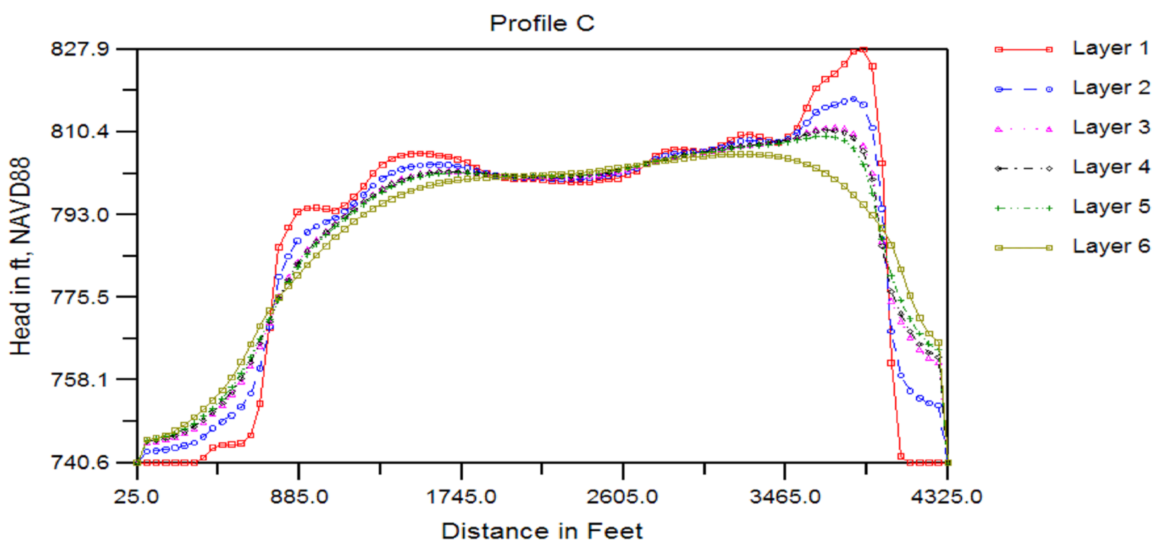

Figure 2.4.12C-19. Profile C—Run 1 a) Groundwater Heads and Flow Directions and b) Groundwater Heads Within Layers

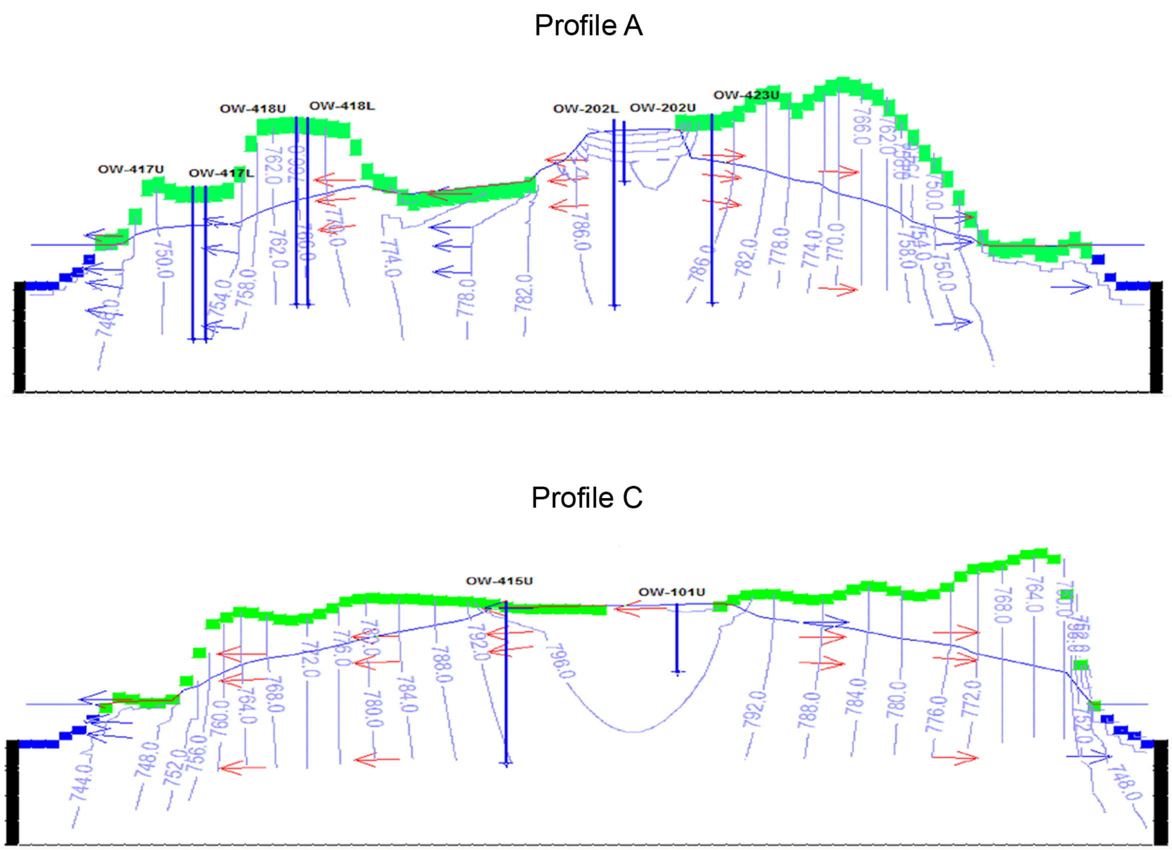

Note: Green color depicts zone of 0 inches/year of recharge and white color depicts zone of 8.76 in./yr for Profiles A and C.

Figure 2.4.12C-20. Depiction of Recharge in Alternate Conceptual Model (Run 22)

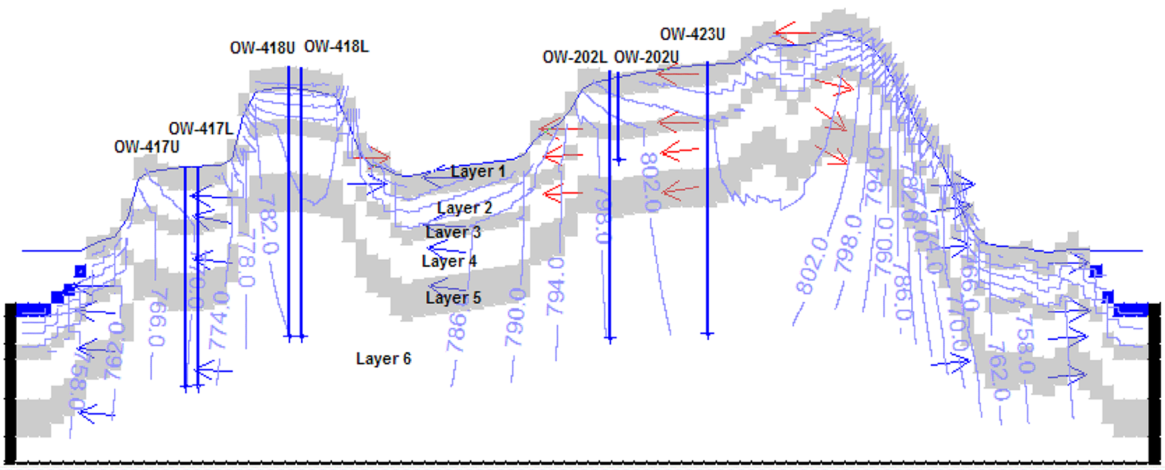

Note: Red arrow indicates downward groundwater flow directions and blue arrow upward groundwater flow directions.

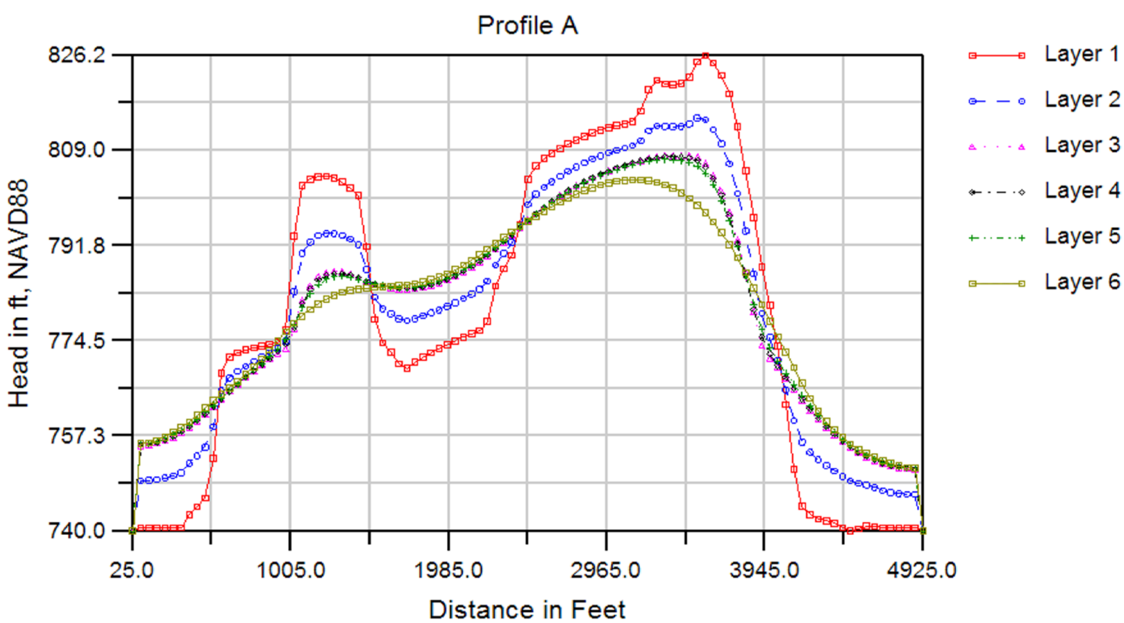

Figure 2.4.12C-21. Profile A—Run 23 a) Groundwater Heads and Flow Directions and b) Groundwater Heads Within Layers

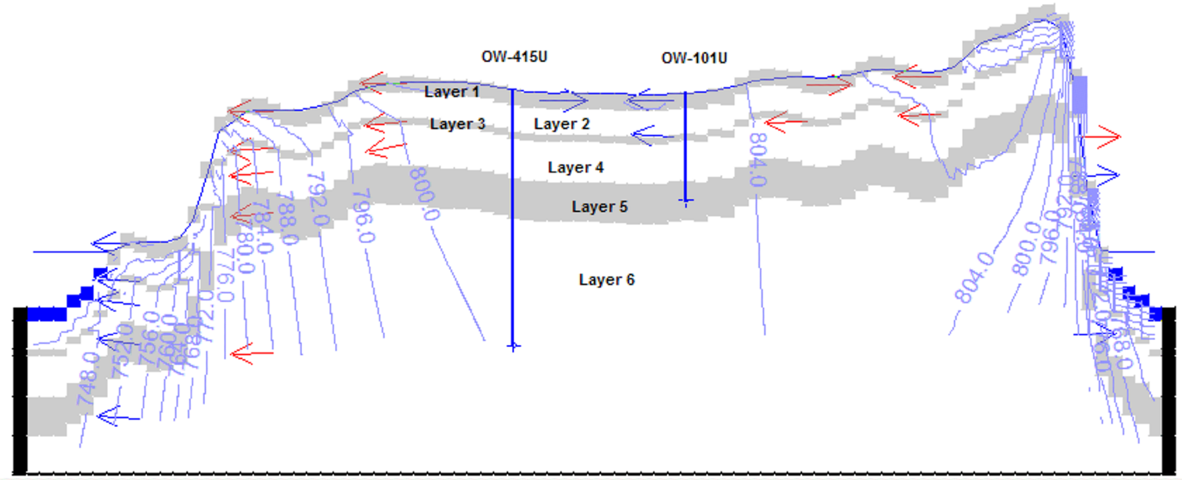

Note: Red arrow indicates downward groundwater flow directions and blue arrow upward groundwater flow directions.

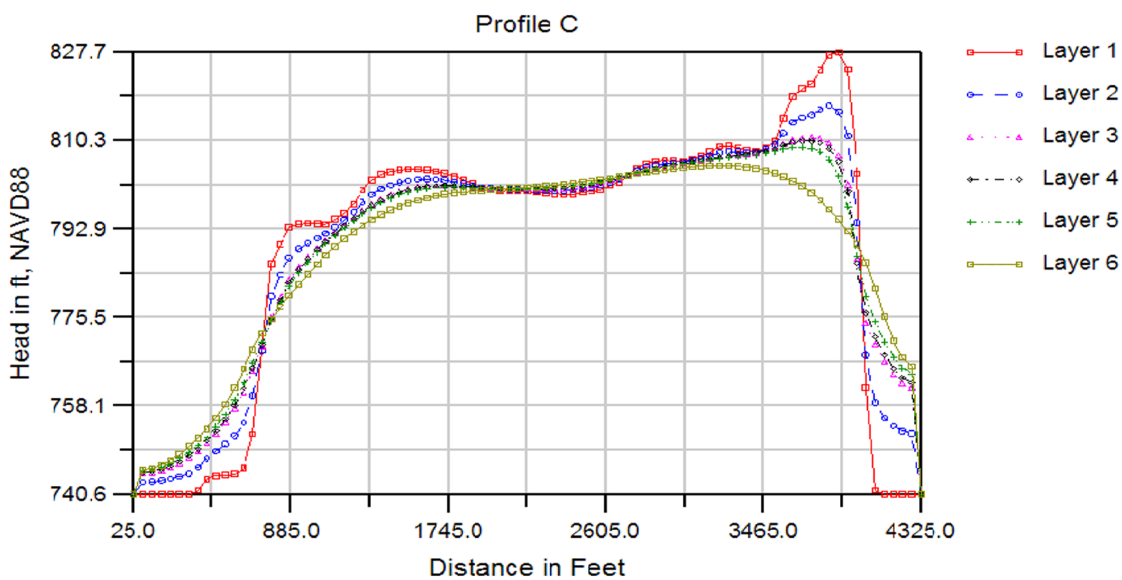

Figure 2.4.12C-22. Profile C—Run 23 a) Groundwater Heads and Flow Directions and b) Groundwater Heads Within Layers

Profile A

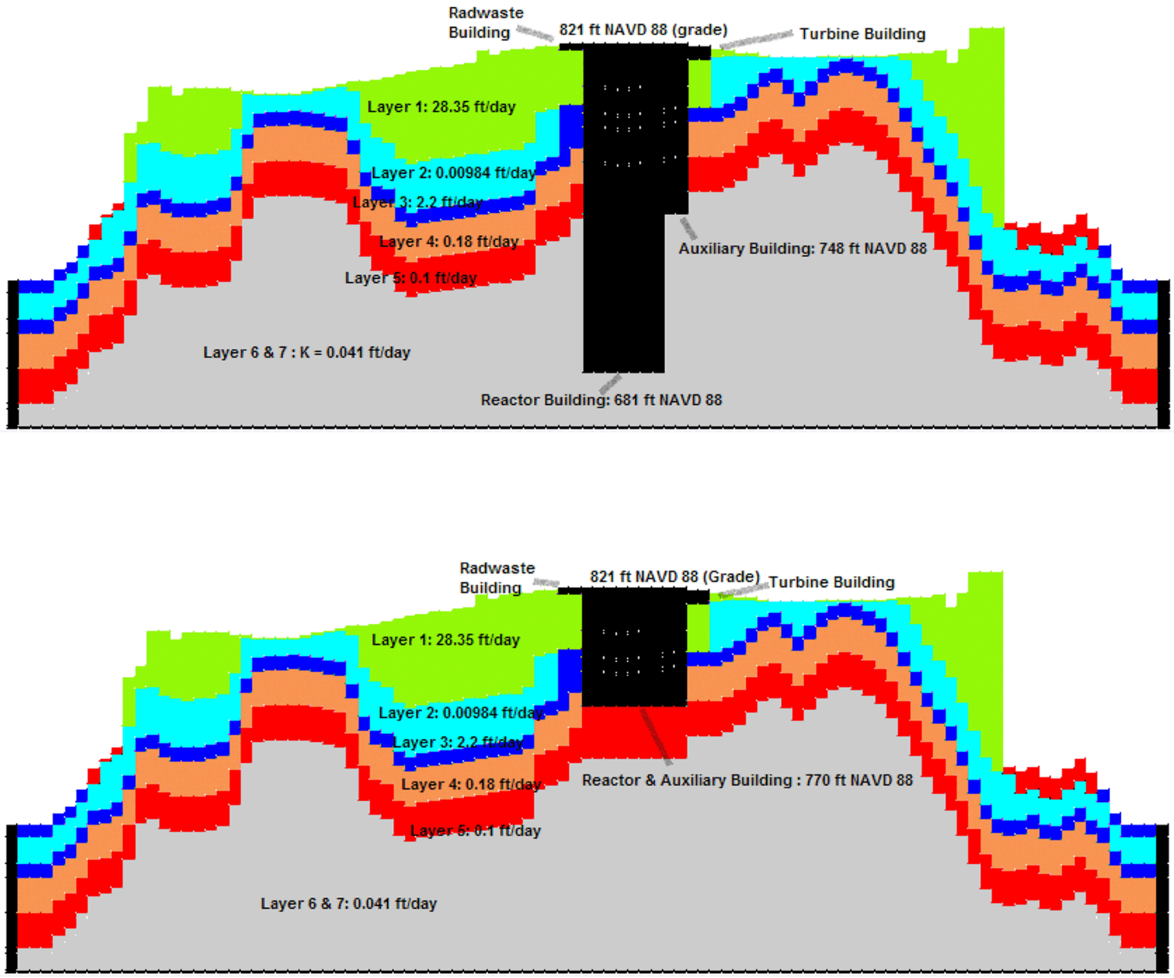

Figure 2.4.12C-23. Hydraulic Conductivity Distribution in Profile A for a) Deep Foundation Embedment and b) Shallow Foundation Embedment

Profile C

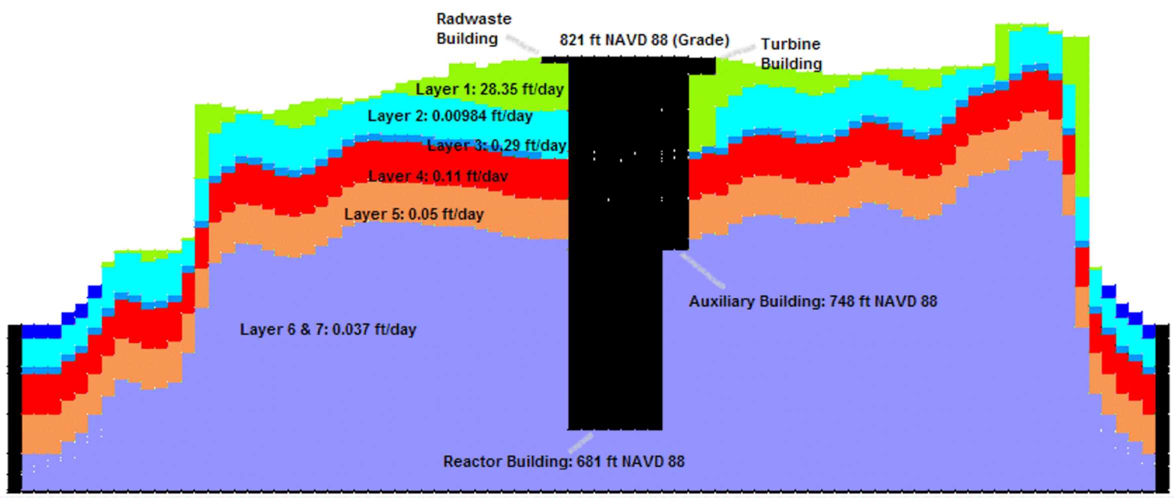

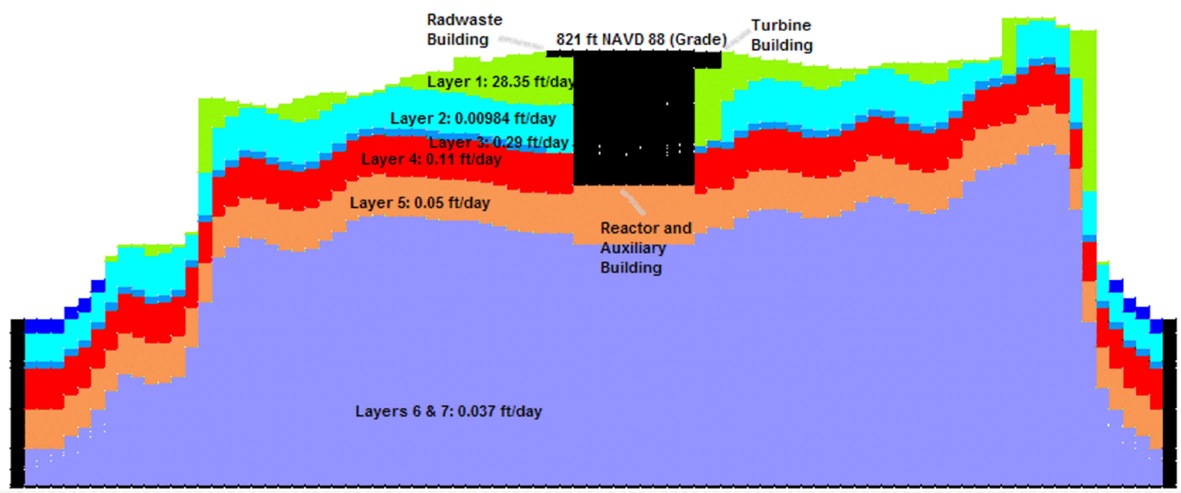

Figure 2.4.12C-24. Hydraulic Conductivity Distribution in Profile C for a) Deep Foundation Embedment and b) Shallow Foundation Embedment

Profile A

Deep Foundation Embedment	Shallow Foundation Embedment
Cross-Section Profile 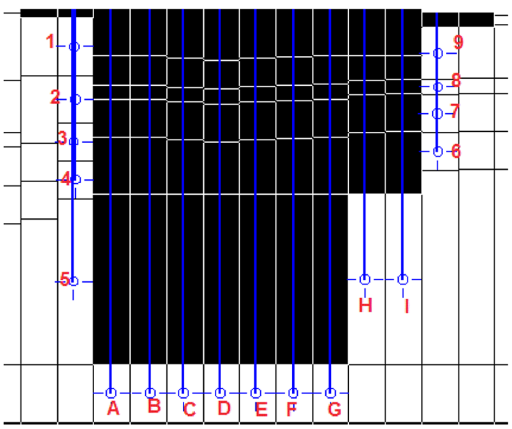	Cross-Section Profile 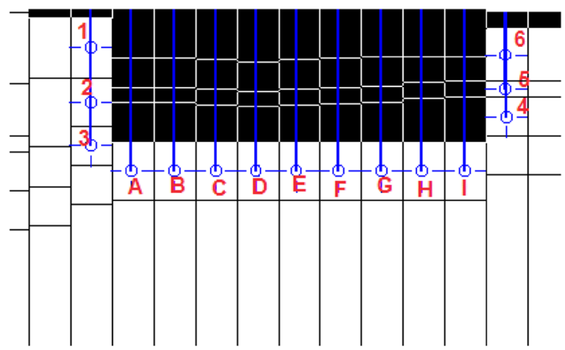
Plan View – Layer 2 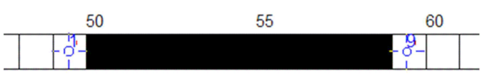	Plan View – Layer 2 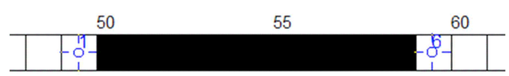
Plan View – Layer 3 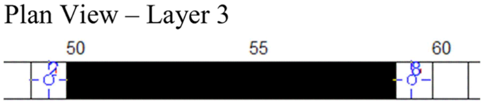	Plan View – Layer 3 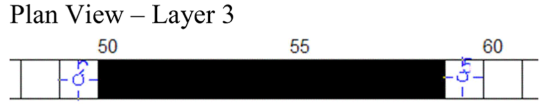

Figure 2.4.12C-25. (Sheet 1 of 2) Locations of Simulated Groundwater Heads in Profile A Post-Construction Model

Note: The numbers outside the grid represents column numbers. The circle represents location of the simulated groundwater head. Numbers and letters besides the circle are the names of the simulated groundwater head locations.

Figure 2.4.12C-25. (Sheet 2 of 2) Locations of Simulated Groundwater Heads in Profile A Post-Construction Model

Profile C

Deep Foundation Embedment	Shallow Foundation Embedment
Cross-Section Profile 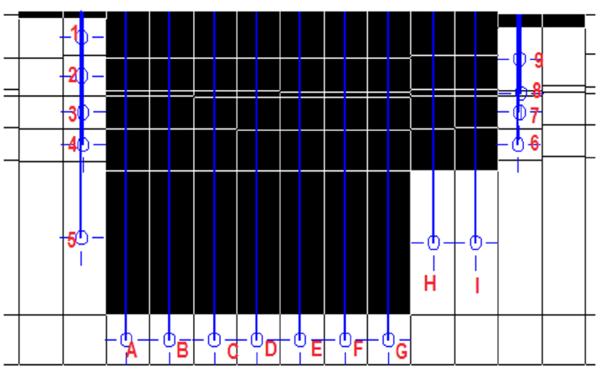	Cross-Section Profile 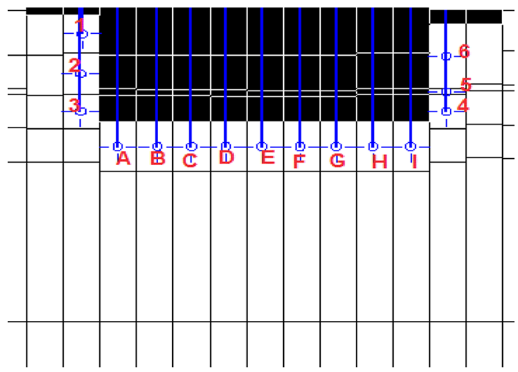
Plan View – Layer 2 	Plan View – Layer 2 
Plan View – Layer 3 	Plan View – Layer 3 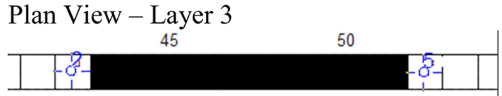
Plan View – Layer 4 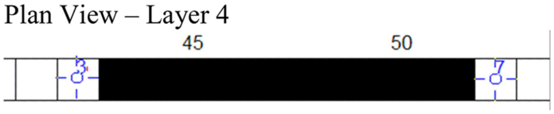	Plan View – Layer 4 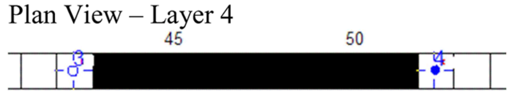

Figure 2.4.12C-26. (Sheet 1 of 2) Locations of Simulated Groundwater Heads in Profile C Post-Construction Model

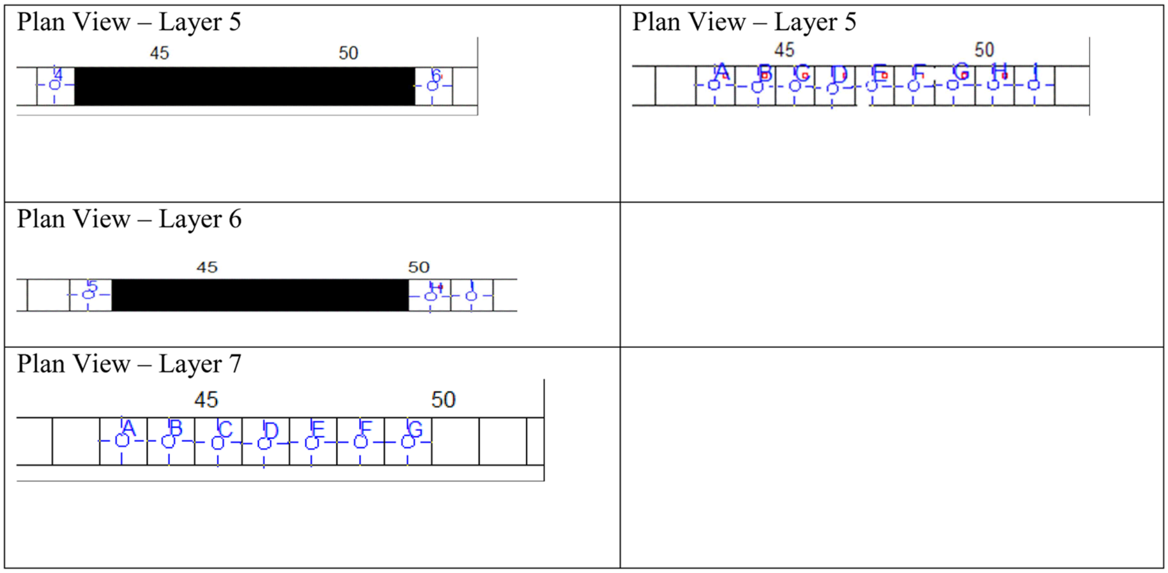

Note: The numbers outside the grid represents column numbers. The circle represents location of the simulated groundwater head. Numbers and letters besides the circle are the names of the simulated groundwater head locations.

Figure 2.4.12C-26. (Sheet 2 of 2) Locations of Simulated Groundwater Heads in Profile C Post-Construction Model

Profile A

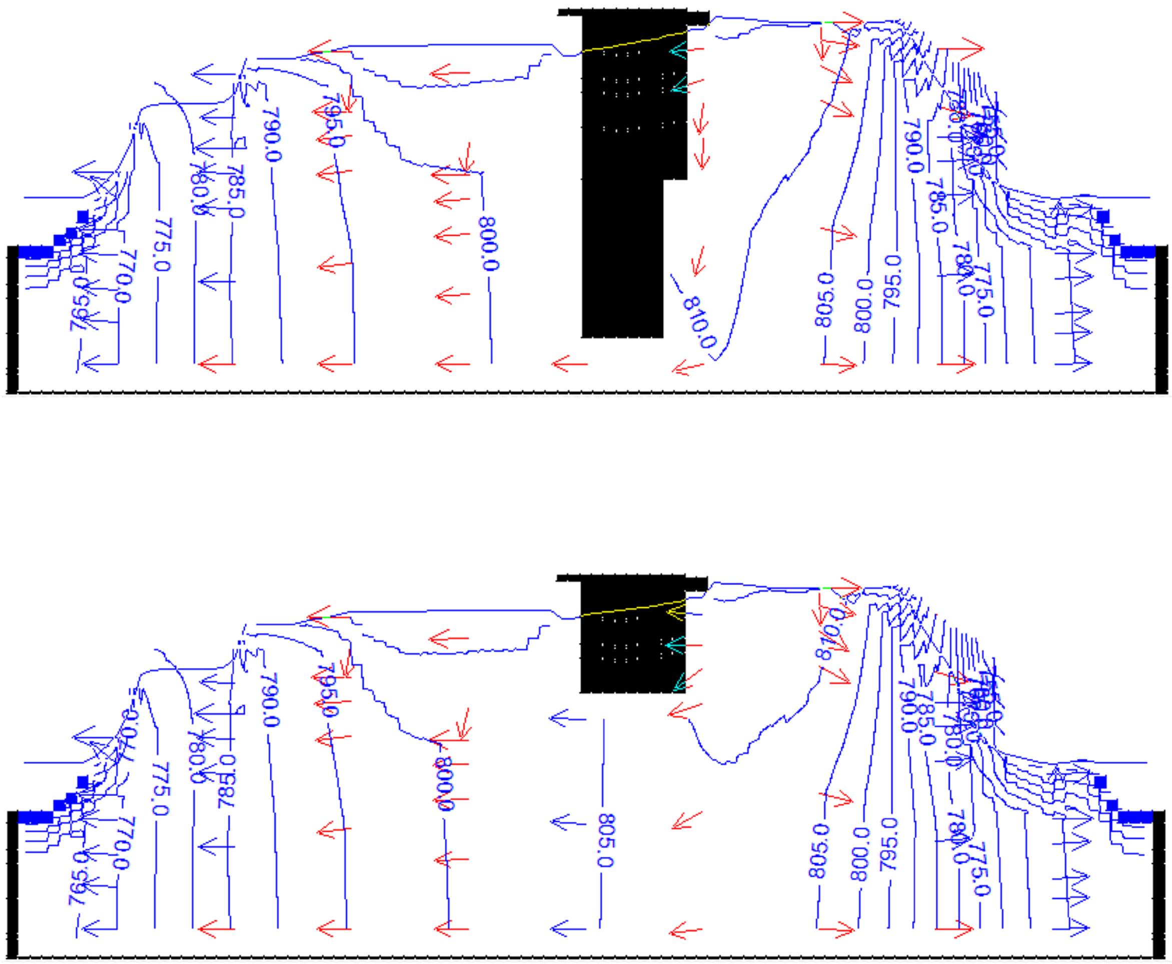

Note: Red arrow indicates downward flow and blue arrow indicates upward flow; blue lines with numbers indicates groundwater contours; deep blue blocks represent constant head of Clinch River; and black blocks represents no flow cells.

Figure 2.4.12C-27. Groundwater Heads—Granular Backfill Hydraulic Conductivity of 10^{-2} cm/s in Profile A Model: a) Deep Foundation Embedment and b) Shallow Foundation Embedment

Profile A

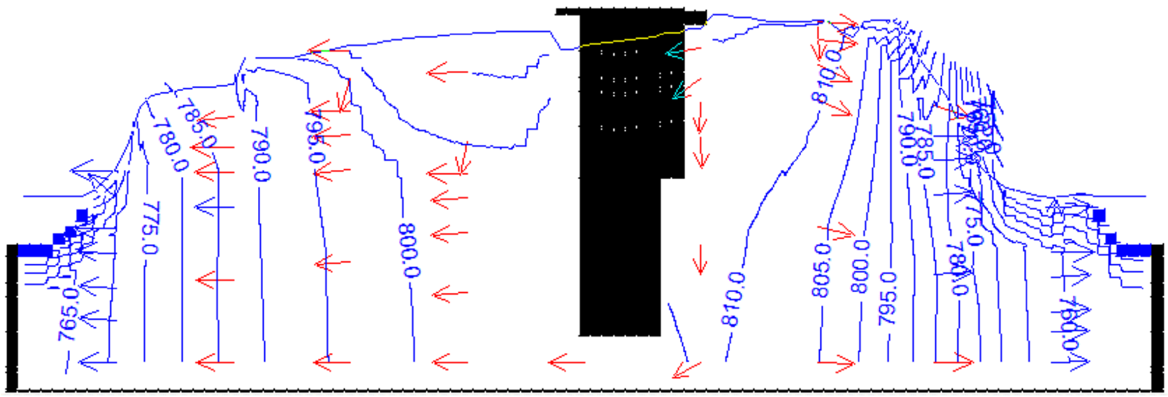

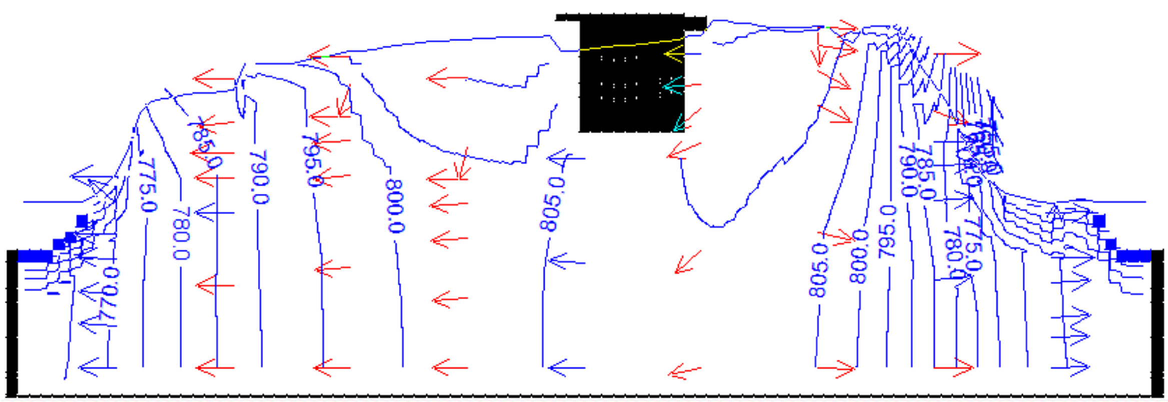

Note: Red arrow indicates downward flow and blue arrow indicates upward flow; blue lines with numbers indicates groundwater contours; deep blue blocks represent constant head of Clinch River; and black blocks represents no flow cells.

Figure 2.4.12C-28. Groundwater Heads—Granular Backfill Hydraulic Conductivity of 10^{-3} cm/s in Profile A Model: a) Deep Foundation Embedment and b) Shallow Foundation Embedment

Profile A

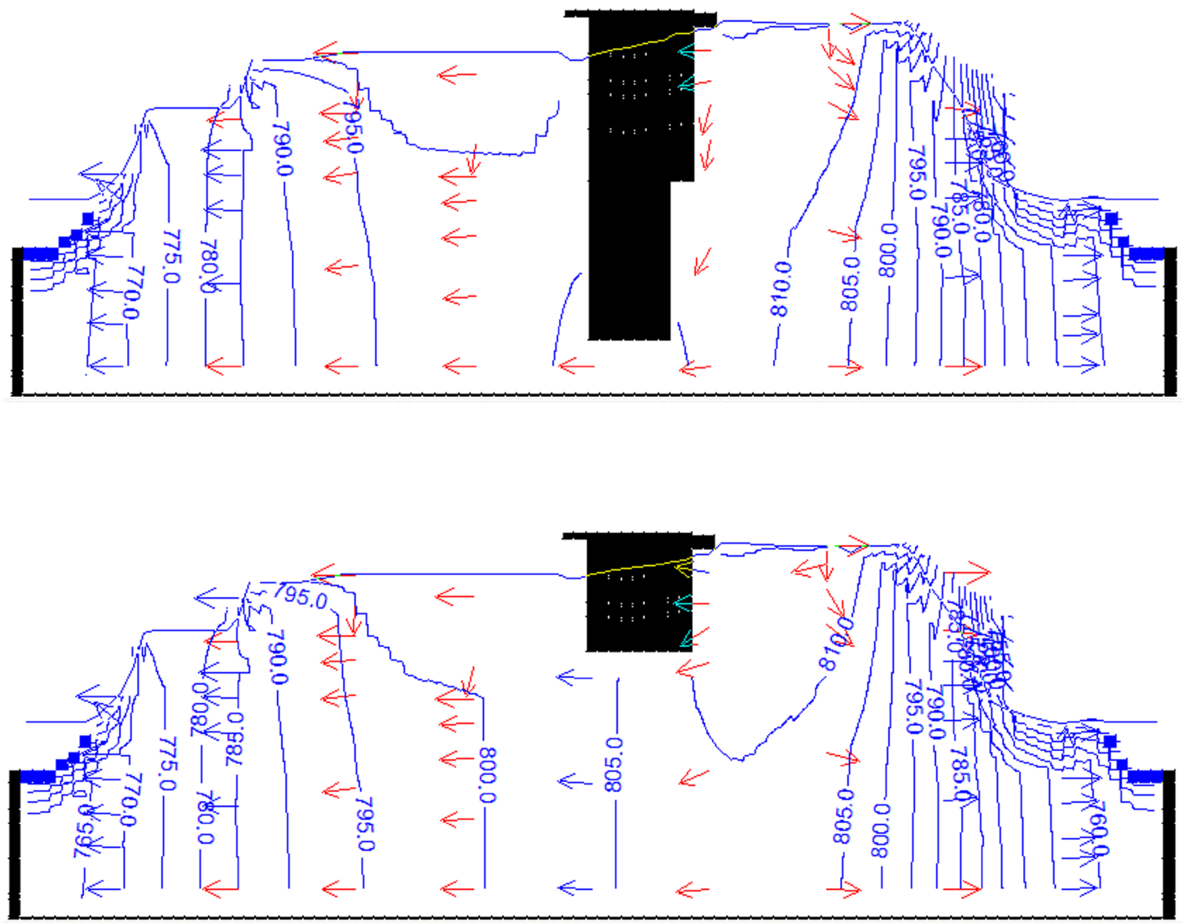

Note: Red arrow indicates downward flow and blue arrow indicates upward flow; blue lines with numbers indicates groundwater contours; deep blue blocks represent constant head of Clinch River; and black blocks represents no flow cells.

Figure 2.4.12C-29. Groundwater Heads—Granular Backfill Hydraulic Conductivity of 10^{-1} cm/s in Profile A Model: a) Deep Foundation Embedment and b) Shallow Foundation Embedment

Profile C

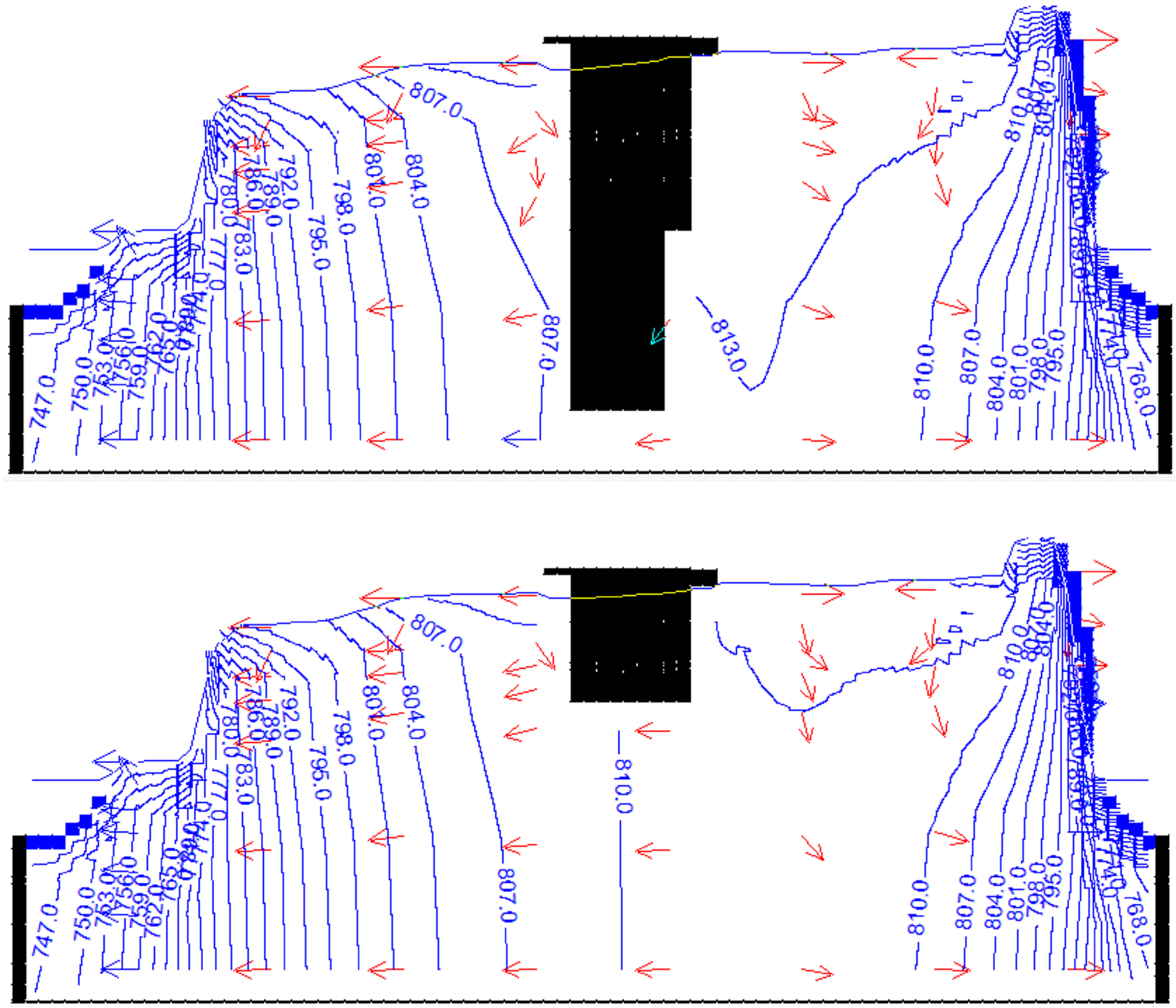

Note: Red arrow indicates downward flow and blue arrow indicates upward flow; blue lines with numbers indicates groundwater contours; deep blue blocks represent constant head of Clinch River; and black blocks represents no flow cells.

Figure 2.4.12C-30. Groundwater Heads—Granular Backfill Hydraulic Conductivity of 10^{-2} cm/s in Profile C Model: a) Deep Foundation Embedment and b) Shallow Foundation Embedment

Profile C

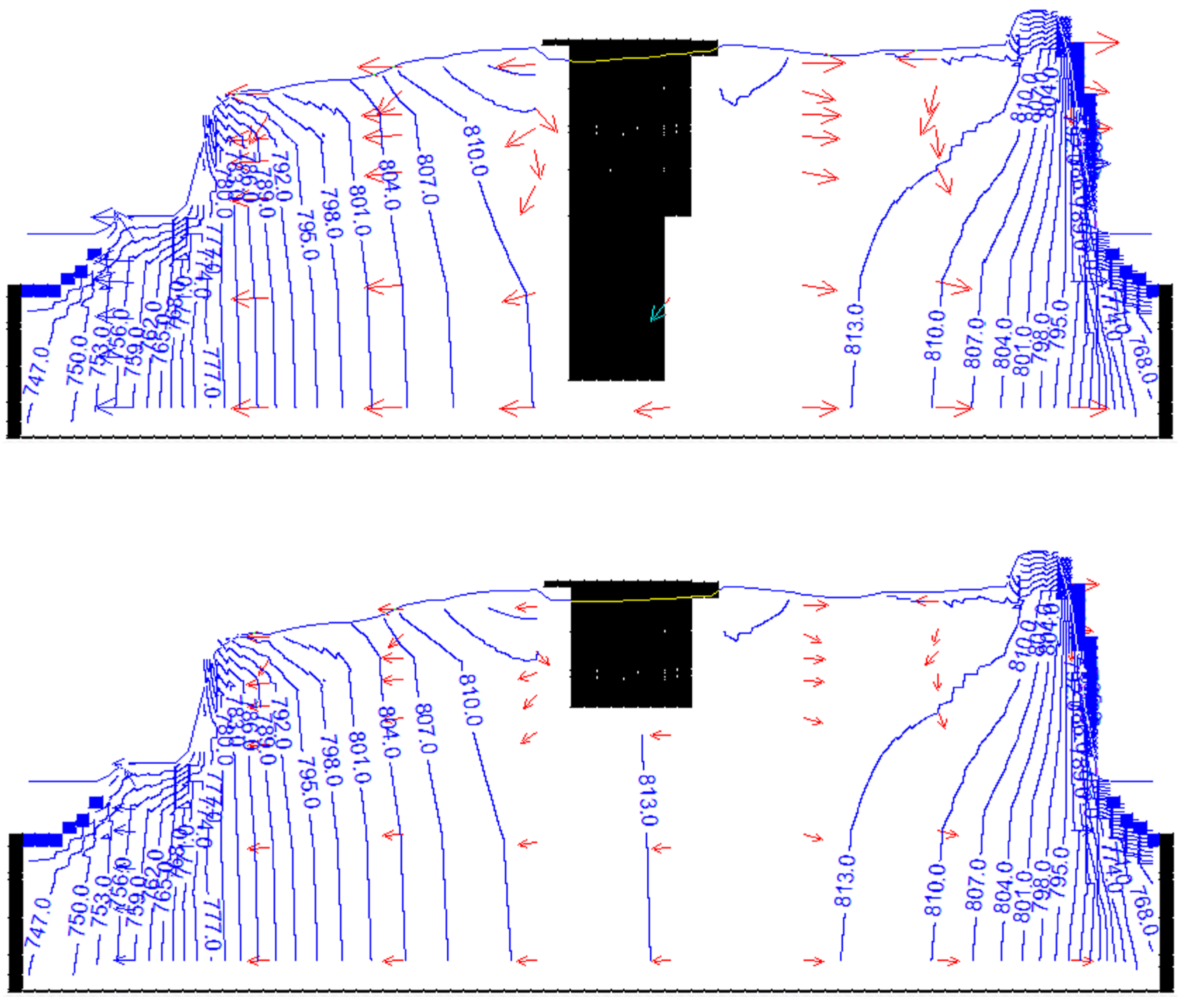

Note: Red arrow indicates downward flow and blue arrow indicates upward flow; blue lines with numbers indicates groundwater contours; deep blue blocks represent constant head of Clinch River; and black blocks represents no flow cells.

Figure 2.4.12C-31. Groundwater Heads—Granular Backfill Hydraulic Conductivity of 10^{-3} cm/s in Profile C Model: a) Deep Foundation Embedment and b) Shallow Foundation Embedment

Profile C

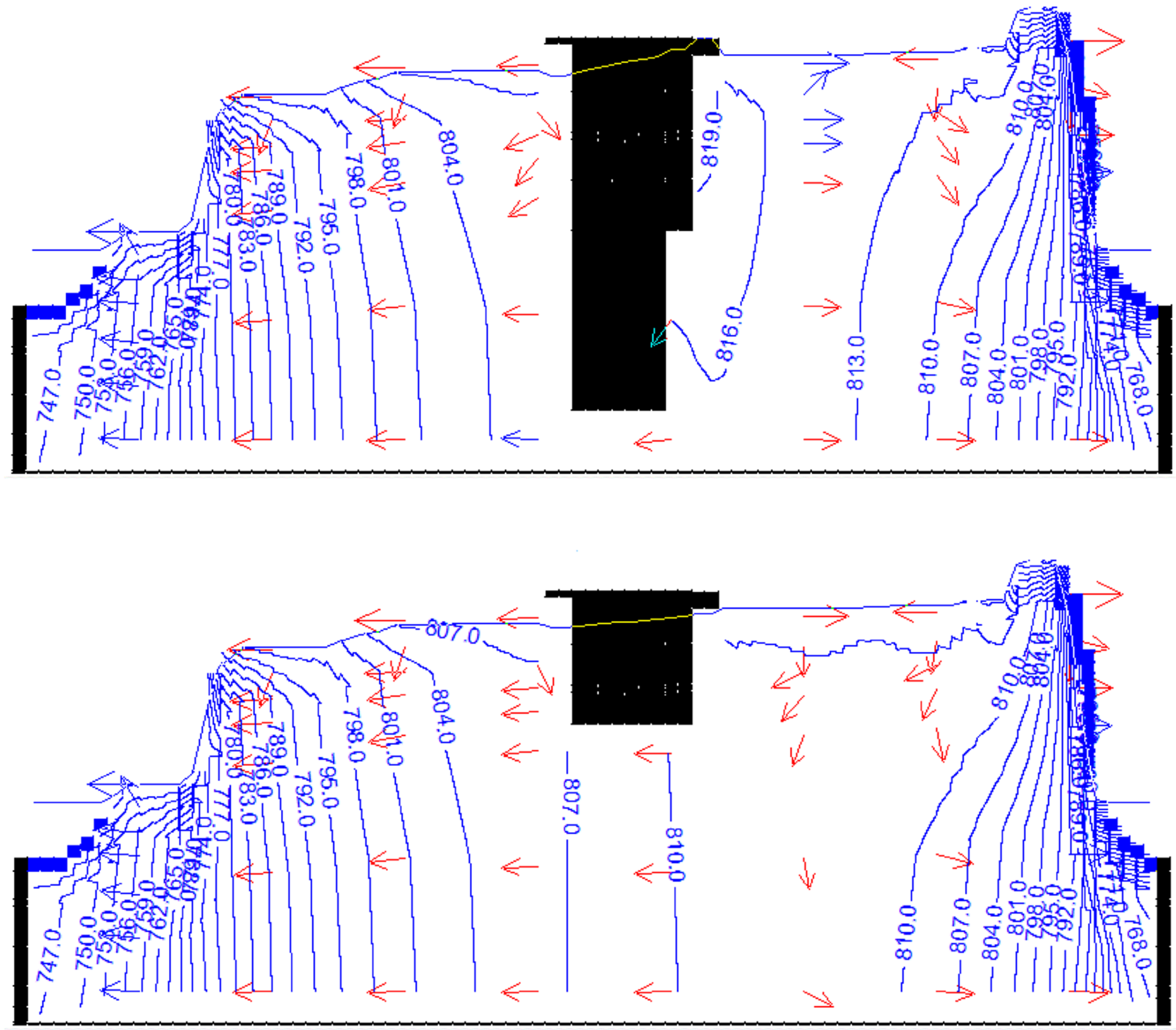

Note: Red arrow indicates downward flow and blue arrow indicates upward flow; blue lines with numbers indicates groundwater contours; deep blue blocks represent constant head of Clinch River; and black blocks represents no flow cells.

Figure 2.4.12C-32. Groundwater Heads—Granular Backfill Hydraulic Conductivity of 10^{-1} cm/s in Profile C Model: a) Deep Foundation Embedment and b) Shallow Foundation Embedment